International Telecommunication Union

ITU-R

Radiocommunication Sector of ITU

Report ITU-R RS.2313-0
(09/2014)

Sharing analyses of wideband Earth exploration-satellite service (active) transmissions with stations in the radio determination service operating in the frequency bands 8 700-9 300 MHz and 9 900-10 500 MHz

RS Series

Remote sensing systems

150 1865-2015

International Telecommunication Union

Foreword

The role of the Radiocommunication Sector is to ensure the rational, equitable, efficient and economical use of the radio-frequency spectrum by all radiocommunication services, including satellite services, and carry out studies without limit of frequency range on the basis of which Recommendations are adopted.

The regulatory and policy functions of the Radiocommunication Sector are performed by World and Regional Radiocommunication Conferences and Radiocommunication Assemblies supported by Study Groups.

Policy on Intellectual Property Right (IPR)

ITU-R policy on IPR is described in the Common Patent Policy for ITU-T/ITU-R/ISO/IEC referenced in Annex 1 of Resolution ITU-R 1. Forms to be used for the submission of patent statements and licensing declarations by patent holders are available from http://www.itu.int/ITU-R/go/patents/en where the Guidelines for Implementation of the Common Patent Policy for ITU-T/ITU-R/ISO/IEC and the ITU-R patent information database can also be found.

Series of ITU-R Reports

(Also available online at http://www.itu.int/publ/R-REP/en)

Series	Title
BO	Satellite delivery
BR	Recording for production, archival and play-out; film for television
BS	Broadcasting service (sound)
BT	Broadcasting service (television)
F	Fixed service
M	Mobile, radiodetermination, amateur and related satellite services
P	Radiowave propagation
RA	Radio astronomy
RS	**Remote sensing systems**
S	Fixed-satellite service
SA	Space applications and meteorology
SF	Frequency sharing and coordination between fixed-satellite and fixed service systems
SM	Spectrum management

***Note**: This ITU-R Report was approved in English by the Study Group under the procedure detailed in Resolution ITU-R 1.*

Electronic Publication
Geneva, 2015

REPORT ITU-R RS.2313-0

Sharing analyses of wideband Earth exploration-satellite service (active) transmissions with stations in the radio determination service operating in the frequency bands 8 700-9 300 MHz and 9 900-10 500 MHz[1]

(2014)

TABLE OF CONTENTS

Page

1 Introduction 2

2 Characteristics of EESS (active) synthetic aperture radar operating at 9 GHz 2

3 Comparison of sharing conditions of SAR-4 with previous synthetic aperture radars .. 5

3.1 Characteristics of synthetic aperture radar systems used for the comparison 5

3.2 Comparison of interference conditions under peak *I*/*N* 7

3.3 Comparison of interference conditions under averaged *I*/*N* 9

3.4 Comparison of pulse width at IF output of radar receiver 11

3.5 Comparison of duty cycle at the IF output of radar receiver 12

3.6 Comparison of SAR-4 with the EESS waveforms tested in Report ITU-R M.2081 13

4 Sharing studies 14

4.1 Sharing with the radio navigation service in the band 8 700-9 300 MHz 14

5 Summary 104

6 Supporting documents 105

Annex A – List of acronyms and abbreviations 106

[1] The Administration of the Islamic Republic of Iran in considering this Report expressed its serious concerns regarding the scope and objectives of synthetic aperture radar systems which assumes the bandwidth larger than 600 MHz due to the fact that it may contradict the purpose and objectives of Resolution 174 (Guadalajara 2010) "Risk of illicit use of information and communication technology".

1 Introduction

This Report comprises results from sharing studies between Earth exploration-satellite service (EESS (active)) and the radio determination service (RDS) in the frequency ranges 8 700-9 300 MHz and 9.9-10.5 GHz.

– Section 2 provides the assumed characteristics of EESS synthetic aperture radars (SARs) operating at 9 GHz as given by Recommendation ITU-R RS.2043.
– Section 3 provides a comparison study of the new SAR-4 system with previous SARs.

Sharing studies are provided in:

– Section 4.1 regarding the sharing of EESS (active) with the radio navigation service (RNS) in the frequency band 8 700-9 300 MHz.
– Section 4.2 regarding the sharing of EESS (active) with the radio location service (RLS) in the frequency band 8 700-9 300 MHz.
– Section 4.3 regarding the sharing of EESS (active) with the RLS in the frequency band 10.0-10.5 GHz.

Acronyms and abbreviations used in this Report are listed in Annex A.

2 Characteristics of EESS (active) synthetic aperture radar operating at 9 GHz

Table 1 provides the characteristics of the currently operated SAR-1, SAR-2 and SAR-3 systems as well as SAR-4 which were taken from Recommendation ITU-R RS.2043. SAR-4 represents a new generation of SAR systems intending to provide high resolution performance of less than 25 cm while using transmission chirp bandwidth of up to 1 200 MHz. Figure 1 shows the typical operating modes of SAR systems in Table 1.

TABLE 1

Technical characteristics of EESS SAR systems

Parameter	SAR-1	SAR-2	SAR-3	SAR-4
Orbital altitude (km)	400	619	506	510
Orbital inclination (°)	57	98	98	98
RF center frequency (GHz)	9.6	9.6	9.6	9.3-9.9(*)
Peak radiated power (W)	1 500	5 000	25 000	7 000
Pulse modulation	Linear FM chirp	Linear FM chirp	Linear FM chirp	Linear FM chirp
Chirp bandwidth (MHz)	10	400	450	1200
Pulse duration (μs)	33.8	10-80	1-10	50
Pulse repetition rate (pps)	1 736	2 000-4 500	410-515	6000
Duty cycle (%)	5.9	2.0-28.0	0.04-0.5	30
Range compression ratio	338	< 12 000	450-4 500	60 000

TABLE 1 (*end*)

Parameter	SAR-1	SAR-2	SAR-3	SAR-4
Antenna type	Slotted waveguide	Planar array	Planar phased array	Planar array
Antenna peak gain (dBi)	44.0	44.0-46.0	39.5-42.5	47.0
e.i.r.p. (dBW)	75.8	83.0	83.5-88.5	85.5
Antenna orientation from Nadir	20˚ to 55˚	34˚	20˚ to 44˚	18.5° to 49.3°
Antenna beamwidth	5.5 (El) 0.14˚ (Az)	1.6-2.3˚ (El) 0.3˚ (Az)	1.1-2.3˚ (El) 1.15˚ (Az)	1.13° (El) 0.53° (Az)
Antenna polarization	Linear vertical	Linear HH or VV	Linear horizontal/ vertical	Linear horizontal/ vertical
System noise temperature (K)	551	500	600	500

* Final value depends on the decision eventually taken under WRC-15 agenda item 1.12

It should be noted that only the technical characteristics of a SAR-4 system have been taken into account for the studies since only SAR-4 systems are assumed to transmit with the full chirp bandwidth of up to 1 200 MHz, unless mentioned otherwise in the report.

Table 2 provides the pattern of a SAR-4 antenna. The antenna patterns of SAR-1 to SAR-3 systems are defined in Recommendation ITU-R RS.2043.

TABLE 2

SAR-4 average antenna gain pattern around 9 600 MHz

Pattern	Gain $G(\theta)$ (dBi) as function of off-axis angle θ	Angular range
Vertical (elevation) (°)	$G_v(\theta_v) = 47.0-9.91\ (\theta v)^2$ $G_v(\theta_v) = 35.189-1.944\theta v$ $G_v(\theta_v) = 21.043-0.468\theta v$ $G_v(\theta_v) = 12.562-0.185\theta v$ $Gv(\theta v) = 3.291$	$\theta_v < 1.149$ $1.149 \le \theta_v \le 9.587$ $9.587 \le \theta_v \le 29.976$ $29.976 \le \theta_v \le 50$ $50.0 \le \theta_v$
Horizontal (azimuth) (°)	$G_h(\theta_h) = 0-45.53(\theta_h)^2$ $G_h(\theta_h) = -11.210-4.022\theta_h$ $G_h(\theta_h) = -26.720-0.953\theta_h$ $G_h(\theta_h) = -35.031-0.388\theta_h$ $G_h(\theta_h) = -41.936-0.158\theta_h$ $G_h(\theta_h) = -51.387$	$\theta_h \le 0.542$ $0.542<\theta_h \le 5.053$ $5.053 <\theta_h \le 14.708$ $14.708 <\theta_h \le 30.00$ $30.00 <\theta_h \le 59.915$ $59.915 <\theta_h$
Beam pattern (°)	$G(\theta) = G_v(\theta_v) + G_h(\theta_h)$	

FIGURE 1

Typical modes of operation for SAR systems operating in the 9 GHz EESS (active) allocation

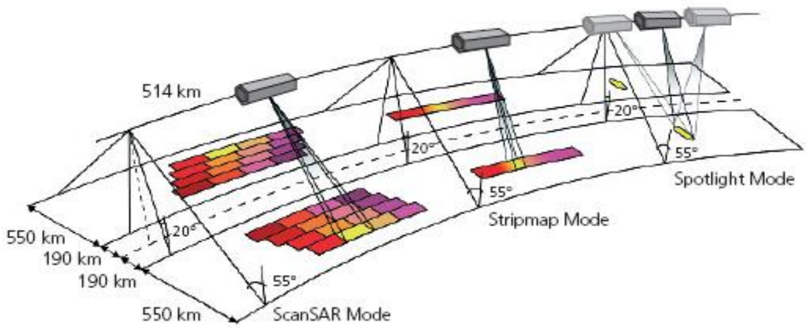

Figure 1 illustrates the different operating modes that can be provided by typical EESS SAR systems. Figure 2 provides definitions and terminologies of a SAR-4 type instrument operating in the wideband spotlight mode.

The maximum chirp bandwidth of up to 1 200 MHz is assumed for the spotlight mode of the SAR-4 system, when highest radar picture resolution is required as described in Report ITU-R RS.2274. This mode is estimated to occur for less than 30% of all images ("snapshots") taken by the SAR. For the other SAR modes, the bandwidth will be either 600 MHz or less, thus in full compliance with the existing allocation.

FIGURE 2

EESS SAR imaging geometry for high resolution spotlight mode (wideband with 1 200 MHz chirp bandwidth)

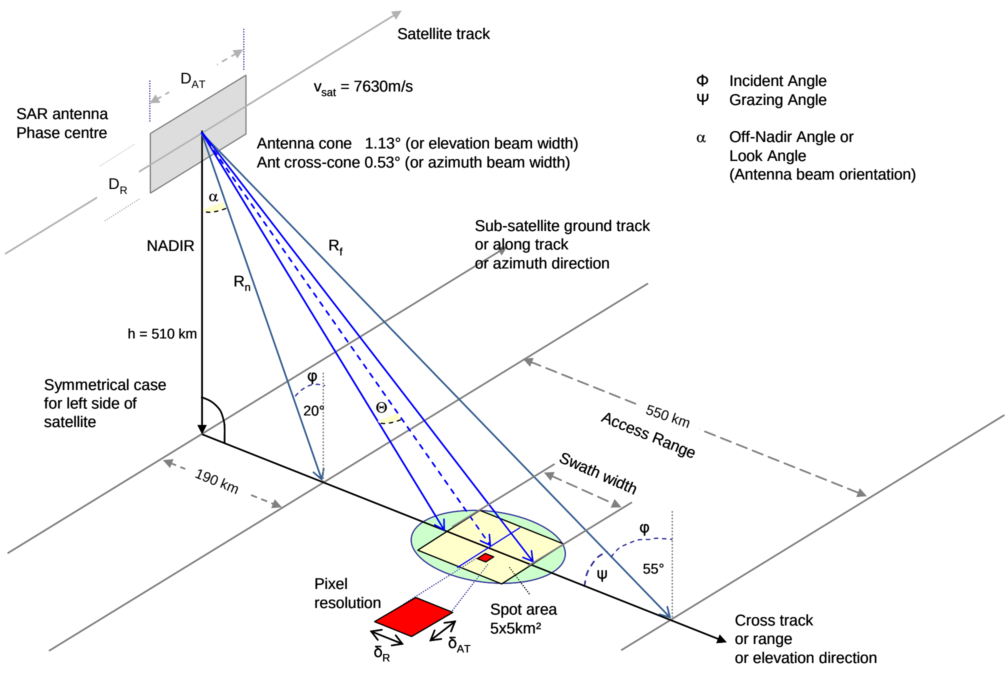

As shown in Fig. 2, in spotlight mode, the spot area can be tracked with incident angles of between 20° and 55° selectable on either or both sides of the satellite. When taking snapshots the azimuth angle (cross track) is within 90° ± 2.5°, thus reducing the effective exposure time.

3 Comparison of sharing conditions of SAR-4 with previous synthetic aperture radars

3.1 Characteristics of synthetic aperture radar systems used for the comparison

Several parameters essential for assessing the impact of synthetic aperture radar systems on terrestrial radar receivers have been compared.

– the peak and average interference signal power levels. Mainly used for assessing the impact of continuous interference type into radar receivers;

– the interference signal pulse width and duty cycle at the radar receiver IF output. More important for assessing the impact of pulsed interference.

Figures 3 and 4 provide the antenna pattern of SAR-1 to SAR-4. The antenna patterns of SAR-1 to SAR-3 are taken from Report ITU-R RS.2094.

FIGURE 3

Antenna pattern along track

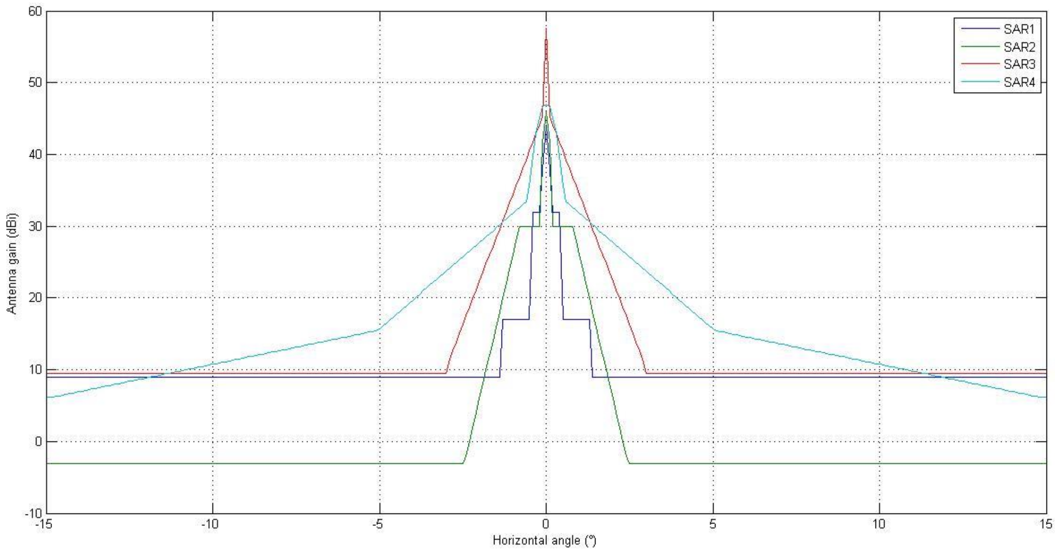

FIGURE 4

Antenna pattern cross track

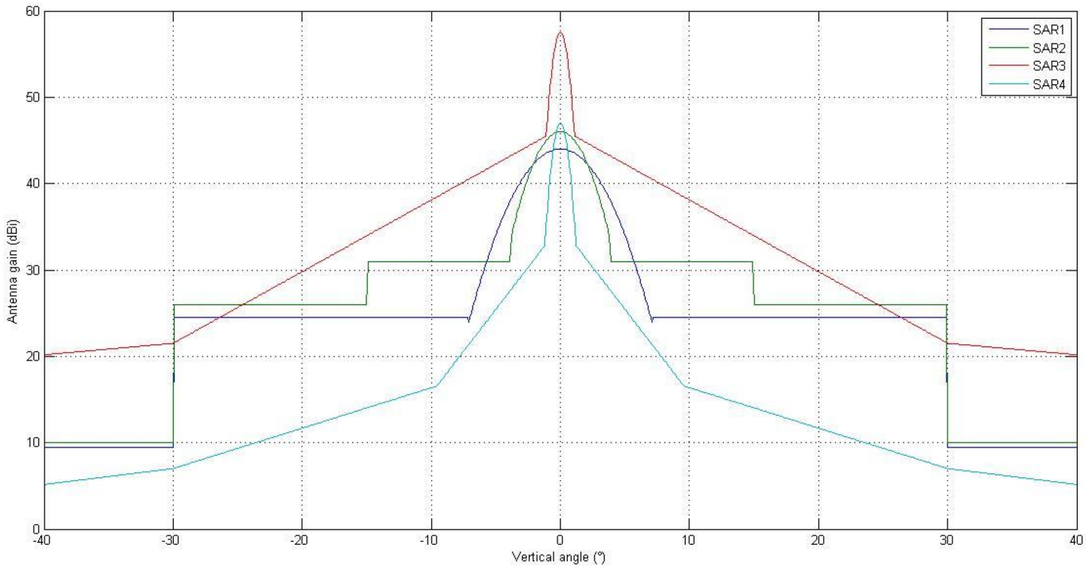

The characteristics of a SAR-4 instrument transmitting at different chirp bandwidths 700 MHz (SAR-4/700), 900 MHz (SAR-4/900), and 1 100 MHz (SAR-4/1100) are provided in Table 3.

TABLE 3

Technical characteristics of EESS SAR systems with bandwidth between 600 MHz and 1 200 MHz

Parameter	SAR-4/700	SAR-4/900	SAR-4/1100
Orbital altitude (km)	510	510	510
Orbital inclination (°)	98	98	98
RF center frequency (GHz)	(9.3-9.9)*	(9.3-9.9)*	(9.3-9.9)*
Peak radiated power (W)	7 000	7 000	7 000
Pulse modulation	Linear FM chirp	Linear FM chirp	Linear FM chirp
Chirp bandwidth (MHz)	700	900	1100
Pulse duration (μs)	50	50	50
Pulse repetition rate (pps)	6000	6000	6000
Duty cycle (%)	30	30	30
Range compression ratio	60 000	60 000	60 000
Antenna type	Planar array	Planar array	Planar array
Antenna peak gain (dBi)	47.0	47.0	47.0
e.i.r.p. (dBW)	85.5	85.5	85.5
Antenna orientation from Nadir	18.5° to 49.3°	18.5° to 49.3°	18.5° to 49.3°
Antenna beamwidth	1.13° (El) 0.53° (Az)	1.13° (El) 0.53° (Az)	1.13° (El) 0.53° (Az)

TABLE 3 (*end*)

Parameter	**SAR-4/700**	**SAR-4/900**	**SAR-4/1100**
Antenna polarization	Linear horizontal/vertical	Linear horizontal/vertical	Linear horizontal/vertical
System noise temperature (K)	500	500	500

* Final value depends on the decision eventually taken under WRC-15 agenda item 1.12

3.2 Comparison of interference conditions under peak I/N

The peak interference signal power level received by terrestrial radar from a spaceborne SAR is calculated with equations 1, 4a and 4b given in Recommendation ITU-R RS.1280.

$$\frac{I_{peak}}{N} = 10 \cdot \log(P_t) + G_t + G_r - (32.44 + 20 \cdot \log(f \cdot R)) + OTR - PG - N$$

where:

P_t: peak spaceborne sensor transmitter power (W)

G_t: spaceborne sensor antenna gain towards terrestrial radar (dB)

G_r: terrestrial radar antenna gain towards spaceborne sensor (dBi)

F: frequency (MHz)

R: slant range between sensor and radar (km)

OTR: radar receiver on-tune rejection (dB)

P_G: processing gain (dB), rejection of unwanted signals due to radar receiver signal processing (assumed to be zero if not known)

N: receiver inherent noise level (dBW).

$N = –204$ dBW + 10 log (B_r) + NF

where:

B_r: receiver IF bandwidth (Hz)

NF: receiver noise figure (dB).

The on-tune rejection term is calculated as:

$OTR = 0$ for $B_c / (B_r^2 T) \leq 1$

$OTR = 10 \cdot \log (B_r^2 T / B_c)$ for $B_c / (B_r^2 T) > 1$

where:

T: spaceborne sensor pulse width before the terrestrial radar receiver IF filter bandwidth (50µs for SAR-4)

B_c: chirp bandwidth of the spaceborne sensor (1 200 MHz for SAR-4)

B_r: terrestrial radar IF bandwidth.

For all SAR systems in Table 4, the shorter slant ranges (see Fig. 1) are used as worst cases.

TABLE 4

Slant ranges

	Nadir (°)	Elevation angle (°)	Altitude (km)	Slant range *R* (km)
SAR-1	18.5	69.96	400	427.45
SAR-2	20	68.34	619	763.92
SAR-3	34	51.16	506	541.33
SAR-4	20	68.69	510	540.22
SAR-4/700	20	68.69	510	540.22
SAR-4/900	20	68.69	510	540.22
SAR-4/1100	20	68.69	510	540.22

In addition, the values provided in Table 5 are used as typical system parameters.

TABLE 5

Typical radar parameters

F (MHz)	9 600
NF (dB)	5
B_r (MHz)	from 0.1 to 60
G_r (dB)	0

Figures 5 and 6 provide the peak interference power level I_{peak} produced by each of the SAR systems versus the radar receiver IF bandwidth B_r.

FIGURE 5

SAR systems maximum *I*/*N* peak over radar IF bandwidth up to 60 MHz

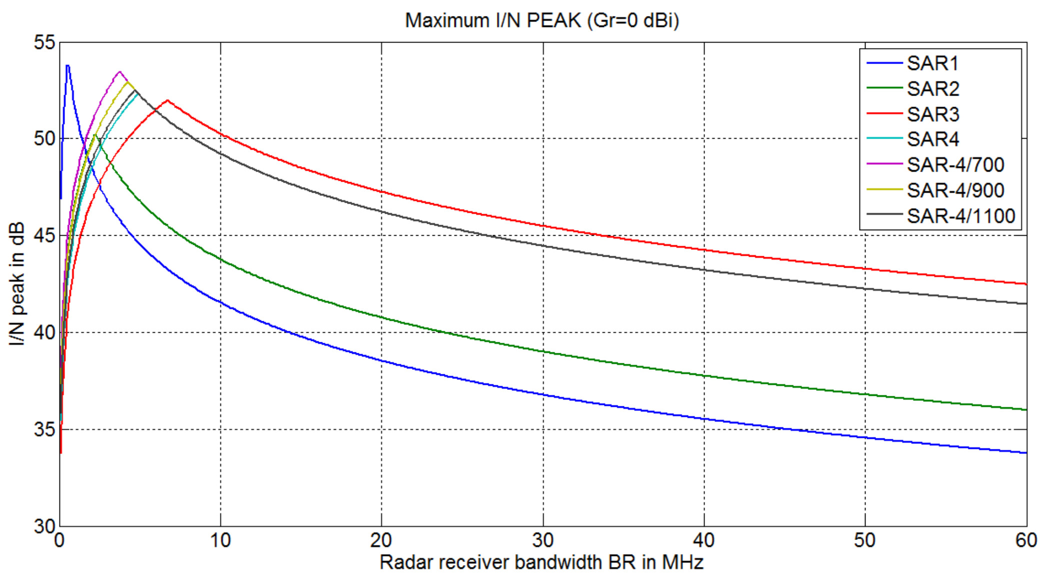

FIGURE 6

SAR systems maximum *I*/*N* peak for radar bandwidth up to 10 MHz

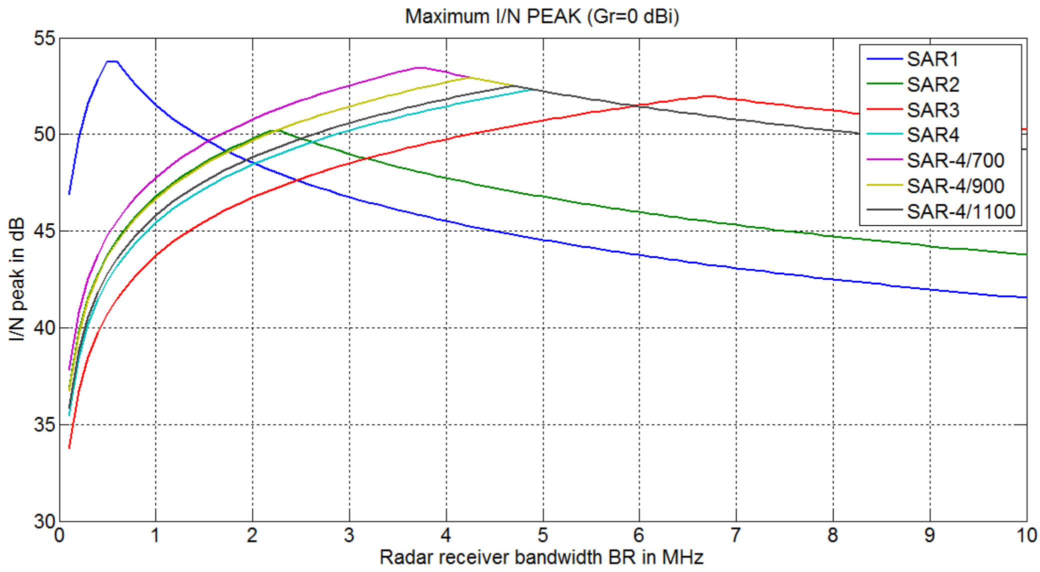

The curves in Figs 5 and 6 show that the potential impact of SAR-4 and SAR-4/700, SAR-4/900 and SAR-4/1100 emissions are

– lower than SAR-1 impact for a B_r between 0 and 1.5 MHz;

– closer than SAR-2 impact for a B_r between 0 and 2 MHz;

– close to a SAR-3 impact for a B_r of larger than 2 MHz.

Therefore, in conclusion, SAR-4 and SAR-4/700, SAR-4/900 and SAR-4/1100 emissions can be considered as similar to those SAR-1, SAR-2, and SAR-3 system characteristics that were used in the calculations in § 3.

3.3 Comparison of interference conditions under averaged *I*/*N*

To calculate the average interfering signal power levels, the following formula is used, which is similar to the Recommendation ITU-R RS.1280 equations 1, 2a and 2b:

$$\frac{I_{av}}{N} = 10 \cdot \log(P_t) + 10\log(\tau \cdot PRF) + G_t + G_r - (32.44 + 20 \cdot \log(f \cdot R)) + OTR - N$$

where:

τ : spaceborne sensor pulse width at the IF output (s)

PRF: spaceborne sensor pulse repetition frequency (Hz).

The spaceborne sensor pulse width at the IF output is calculated from:

$$\tau = \frac{B_r}{B_c} T \qquad \text{for } B_c / (B_r^2\, T) \le 1$$

$$\tau = \frac{1}{B_r} \qquad \text{for } B_c / (B_r^2\, T) > 1$$

where:

T: spaceborne sensor pulse width at IF input (50µs for SAR-4).

The on-tune rejection term is calculated from:

$$OTR = 0 \qquad \text{for } B_c / (B_r^2\, T) \le 1$$

$$OTR = 10 \log (B_r^2\, T / B_c) \qquad \text{for } B_c / (B_r^2\, T) > 1.$$

Figure 7 illustrates the *OTR* and the pulse width at the IF output.

FIGURE 7

Example of OTR and pulse width at the receiver IF output

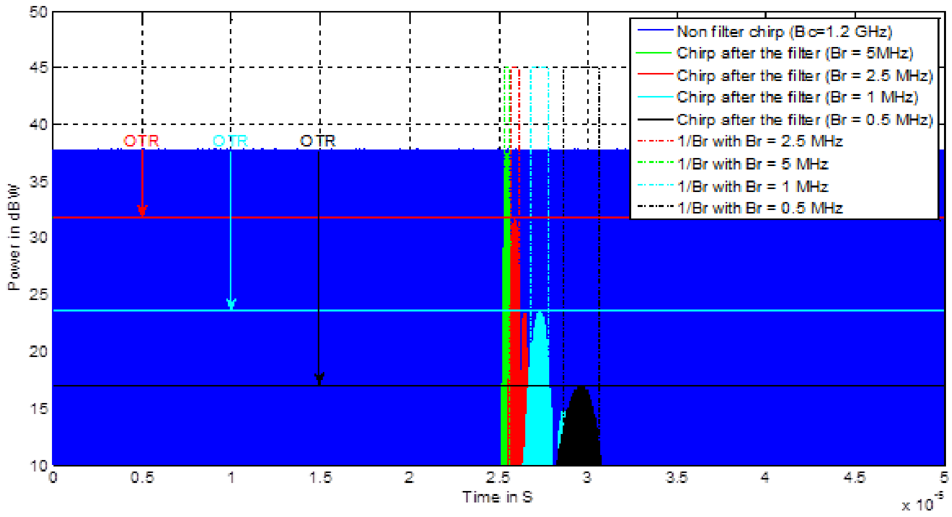

Figure 8 provides the average interference power level, I_{av}, produced by each SAR system versus the terrestrial radar receiver IF bandwidth, B_r.

FIGURE 8

SAR systems maximum *I*/*N* average

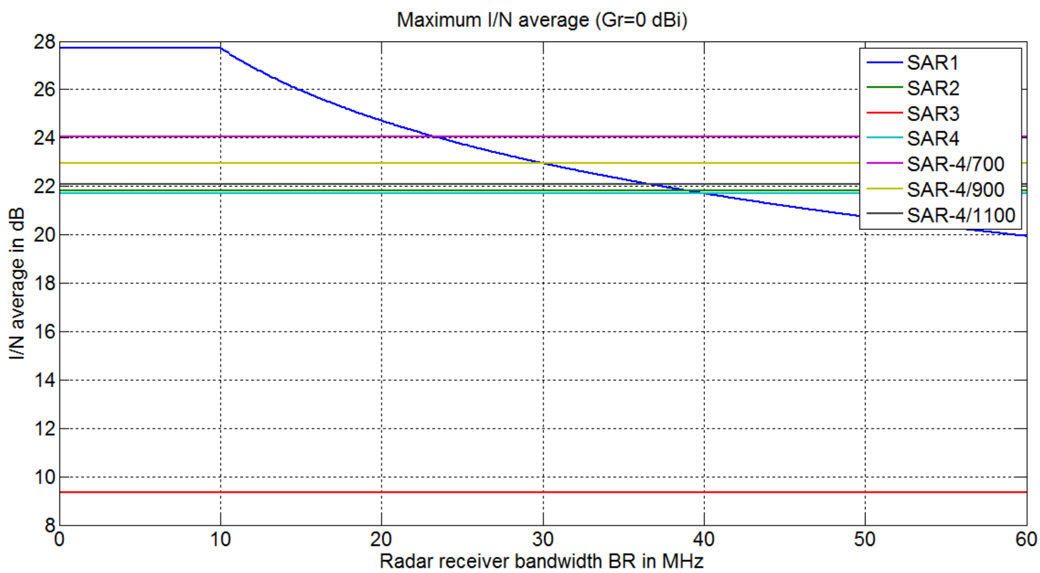

From the above results it can be concluded that the potential impact of a SAR-4 and SAR-4/700, SAR-4/900 and SAR-4/1100 systems or a SAR-2 system are similar in terms of the average interference caused.

3.4 Comparison of pulse width at IF output of radar receiver

As shown in section before, the spaceborne sensor pulse width at the IF output is calculated from:

$$\tau = \frac{B_r}{B_c} T \qquad \text{for } B_c / (B_r^2\, T) \le 1$$

$$\tau = \frac{1}{B_r} \qquad \text{for } B_c / (B_r^2\, T) > 1.$$

Figures 9 and 10 provide the pulse width at the IF output produced by each of the SAR systems versus radar receiver IF bandwidth, B_r.

FIGURE 9

SAR systems pulse width at the radar receiver IF output for up to 60 MHz IF bandwidth

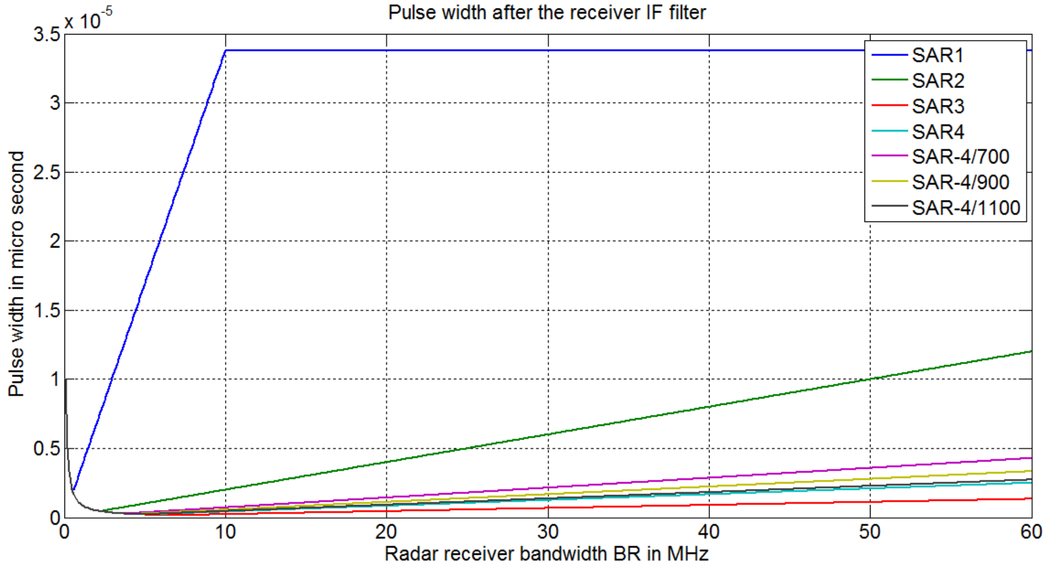

FIGURE 10

SAR systems pulse width at the radar receiver IF output for up to 10 MHz IF bandwidth

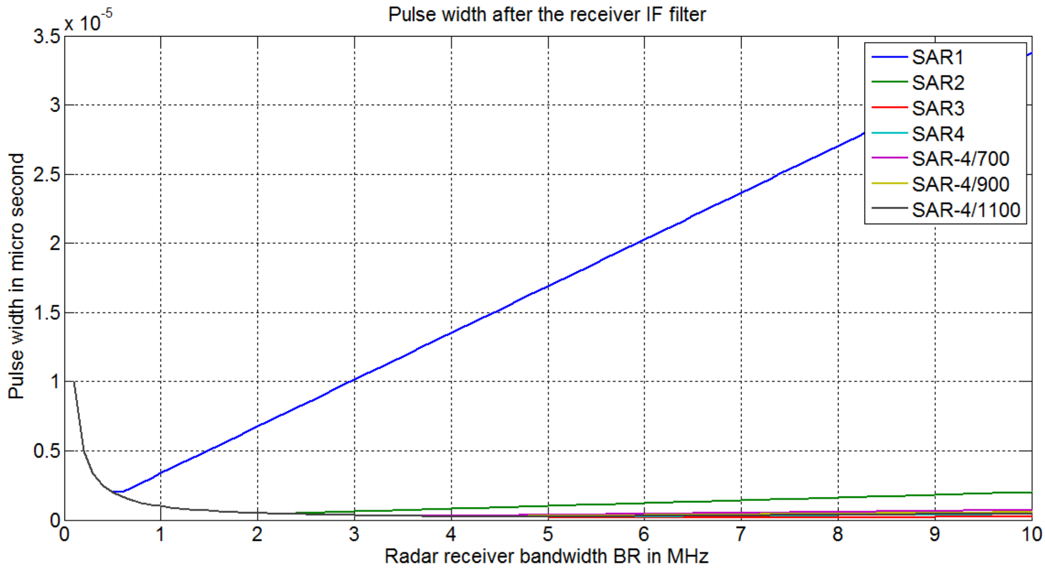

From the above result it can be concluded that the SAR-4 and SAR-4/700, SAR-4/900 and SAR-4/1100 pulse width at the radar receiver IF output is similar or shorter than the ones from SAR systems used in the Report ITU-R RS.2094.

3.5 Comparison of duty cycle at the IF output of radar receiver

Figures 11 and 12 show in direct comparison the duty cycles at the radar IF output as produced by each of the four SAR systems.

FIGURE 11

SAR systems duty cycle at the radar receiver IF output for IF bandwidth up to 60 MHz

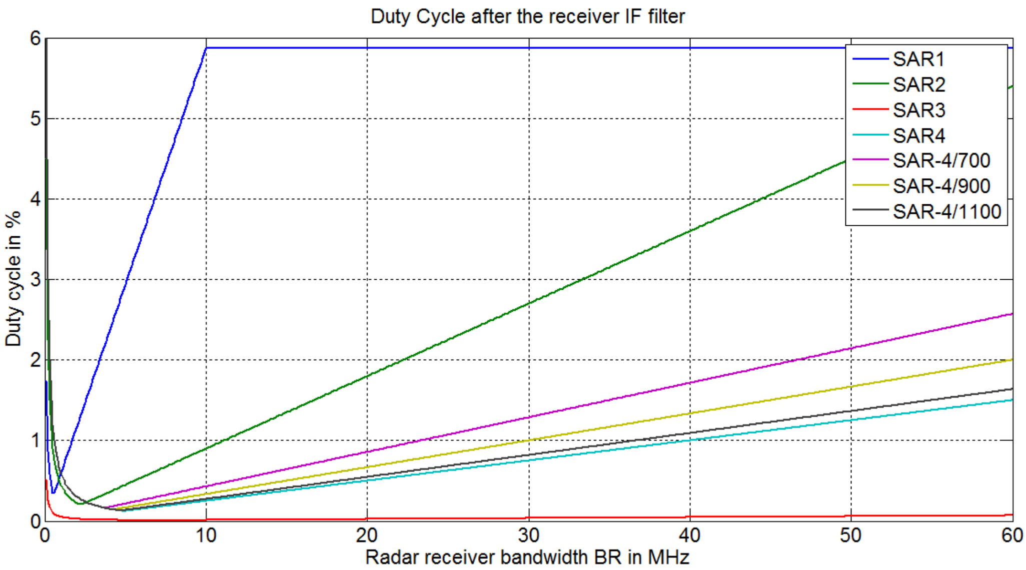

FIGURE 12

SAR systems duty cycle at the radar receiver IF output for IF bandwidth up to 10 MHz

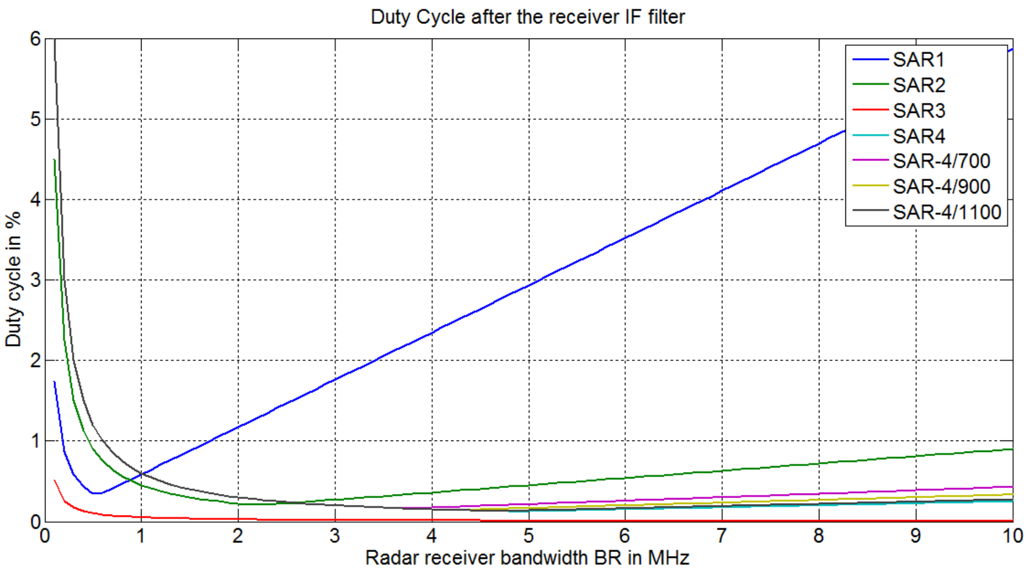

From the above result it can be concluded that the SAR-4 and SAR-4/700, SAR-4/900 and SAR-4/1100 duty cycles at the radar receiver IF output is similar or lower than the ones from SAR systems used in Report ITU-R RS.2094.

From the above result it can be concluded that the SAR-4 duty cycle at the radar receiver IF output is similar or lower than the ones from SAR systems used in the Report ITU-R RS.2094.

It can be noted that inside the current allocation (9 300-9 900 MHz) SAR-4 and SAR-4/700 (SAR-5), SAR-4/900 (SAR-6) and SAR-4/1100 (SAR-7) provides similar sharing conditions as SARs 1-3, which are already operating for several years.

3.6 Comparison of SAR-4 with the EESS waveforms tested in Report ITU-R M.2081

In this Report, four radionavigation systems were tested with waveforms representative of EESS systems. These waveforms primarily use a chirped modulation scheme. The values are scaled to the maximum 80 MHz chirp bandwidth of the test equipment. The values are shown in Table 6. The duty cycles are calculated using the scaled pulse widths. SAR-4 has been added in the table with the same scaled values for comparison.

TABLE 6

EESS waveforms

Waveform No.	**Pulse width (µs)**	**Scaled width (µs)**	**Prf (Hz)**	**Pri (ms)**	**Duty cycle (%)**	**Chirp (MHz)**	**Chirp rate (MHz/µs)**
EESS1	10	2	2 000	0.5	0.4	400/80	40
EESS2	80	16	4 500	0.22	7.2	400/80	5
EESS3	10	17.7	515	1.94	0.91	45/80	4.5
EESS4	10	1.7	5 150	0.194	0.88	460/80	46
SAR-4	**50**	**3.3**	**6 000**	**0.167**	**1.98**	**1200/80**	**24**

Table 7 gives the effective duty cycle obtained for all radio navigation radars tested in Report ITU-R M.2081. The effective duty cycle is the duty cycle of the interfering signal after the radar receiver filter (see § 3.4).

TABLE 7

Comparison of effective duty cycles for the EESS waveforms and radars tested in Report ITU-R M.2081

Waveform No.	Precision approach		ASDE		Shipborne	
	Radar G5		Radar G8		Radar S14	
	Bandwidth (MHz)	Effective duty cycle (%)	Bandwidth (MHz)	Effective duty cycle (%)	Bandwidth (MHz)	Effective duty cycle (%)
EESS1	2.5	0.08	36	0.180	25	0.125
EESS2	2.5	0.225	36	3.240	25	2.250
EESS3	2.5	0.029	36	0.412	25	0.286
EESS4	2.5	0.206	36	0.403	25	0.280
SAR-4	2.5	0.24	36	0.900	25	0.625
SAR-4/700	2.5	0.240	36	1.543	25	1.071
SAR-4/900	2.5	0.240	36	1.2	25	0.833
SAR-4/1100	2.5	0.240	36	0.982	25	0.682

The effective duty cycle of SAR-4, SAR-4/700, SAR-4/900 and SAR-4/1100 is larger than the effective duty cycle of EESS1, 3 and 4 waveforms, but still much lower than the EESS2 waveform effective duty cycle with regard to radars G8 and S14 and comparable with regard to radar G5. It may therefore be assumed that the effective duty cycle of SAR-4 will be between EESS2 and EESS1, 3 and 4.

4 Sharing studies

4.1 Sharing with the radio navigation service in the band 8 700-9 300 MHz

4.1.1 Introduction

This section provides sharing studies of EESS SAR-4 with terrestrial radars operating in the RNS in the band 8 700-9 300 MHz that were not studied in Report ITU-R RS.2094.

WRC-15 agenda item 1.12 considers an extension of the current worldwide allocation to the EESS (active) in the frequency band 9 300-9 900 MHz by up to 600 MHz within the frequency bands 8 700-9 300 MHz and/or 9 900-10 500 MHz, in accordance with Resolution **651 (WRC-12)**, subject to the sharing studies.

The 9 000-9 200 MHz frequency band is allocated to aeronautical radionavigation service (ARNS) and RLS on a primary basis for all three regions. Airport surface surveillance radars, operating in the 9 000-9 200 MHz band under the ARNS allocation, are used to provide a tool to enhance the situational awareness of air traffic controllers in an effort to reduce runway incursions and aircraft collisions. These radars provide non-cooperative aeronautical surveillance including detection and position information for all aircraft and vehicles on the airport movement area. The characteristics of these radars are in the preliminary draft revision of Recommendation ITU-R M.1796.

4.1.2 Characteristics of stations operating in the radio navigation service

The radionavigation radars operating in the band 8 700-9 300 MHz include marine radionavigation, precision approach radar (PAR), ground control approach (GCA), and airport surface detection equipment (ASDE) radars. The characteristics for all these radars are given in Recommendation ITU-R M.1796 and reproduced in Table 11.

Recommendation ITU-R M.1851 defines antenna pattern of radars using fan beams, including cosecant squared or inverse cosecant squared patterns. Recommendation ITU-R F.1245 defines pencil beams.

Recommendation ITU-R M.1796 recommends that the criterion of interfering signal power to radar receiver noise power level, I/N ratio of −6 dB, should be used as the required protection level for radiodetermination radars in the frequency band 8 500-10 680 MHz, even if multiple interferers are present.

However, Recommendation ITU-R M.1796 indicates in Annex 2 (Protection criteria for radars) para 1.2 (Pulsed interference) that:

> "The effect of pulsed interference is more difficult to quantify and is strongly dependent on receiver processor design and mode of system operation. In particular, the differential processing gains for valid-target return (which is synchronously pulsed) and interference pulses (which are usually asynchronous) often have important effects on the impact of given levels of pulsed interference. Several different forms of performance degradation can be inflicted by such interference. Assessing it will be an objective for analyses and/or testing of interactions between specific radar types. In general, numerous features of radars of the types described herein can be expected to help suppress low-duty-cycle pulsed interference, especially from a few isolated sources. Techniques for suppression of low-duty-cycle pulsed interference are contained in Recommendation ITU-R M.1372 – Efficient use of the radio spectrum by radar stations in the radiodetermination service."

In preparation for WRC-07 and the extension of the EESS (active) allocation from 300 MHz to 600 MHz, measurements were performed with some radionavigation radars and reported in Report ITU-R M.2081. The results of those measurements are also summarized in the CPM text for agenda item 1.3 (WRC-07) as follows:

> "The test and analysis results show representative radionavigation and radiolocation radars do not suffer any degradation to their performance from representative EESS (active) waveforms at an I/N of +40 dB for shipborne systems, I/N of +54 dB for airborne systems, I/N of +50 dB for ground-based systems, and an I/N of +28 dB for ground-based meteorological radars."

This statement indicates that the processing gain is an important factor which should be considered for the radars tested and would reduce the impact from SAR interference which is pulsed in nature.

Some of the radars under study in the band 9 000-9 300 MHz were measured in Report ITU-R M.2081, and since, as shown in § 2 of this Report, SAR-4 would have characteristics similar to SAR-1 to SAR-3 previously studied, it is expected that the findings of Report ITU-R M.2081 would also apply to SAR-4 and the radars measured prior to WRC-07. However, it should also be noted that Recommendation ITU-R M.1796 has been revised since and new radars were introduced that need further consideration.

TABLE 8

Characteristics of radionavigation radars in the frequency range 8 700-9 300 MHz

Characteristics	**Unit**	**System G5**	**System G6**	**System G7**	**System G8**	**System S14**	**System G21**	**System G22**
Function		Precision approach and landing radar	Airport surveillance GCA	Precision approach radar	Airport surface detection equipment	Surveillance radar (vessel and coastal)	Airport surface detection equipment	Airport surface detection equipment
Tuning range	MHz	9 000-9 200	9 025	9 000-9 200 (4 frequencies /system)	9 000-9 200 Pulse to pulse agile over 4 frequencies	9 000-9 200 or 9 225-9 300	9 000-9 200; pulse-to-pulse agile over 16 frequencies predefined hopping	9 000-9 200; pulse-to-pulse agile over 4 frequencies predefined hopping
Modulation		Frequency-agile pulse	Plain, NLFM	Plain NLFM pulse pair	Plain and LFM pulse pairs	V7N Fully coherent pulse compression radar using complex pattern of chirps at up to 6 centre frequencies with three different chirp durations	Plain and LFM pulse pairs	Two LFM pulses define a pulse pair
Peak power	kW	120	0.3105	0.5	0.07	0.05-0.1	170	50
Pulse widths	µs	0.25	1.2; 30; 96	0.65 and 25 pulse-pair	0.04 and 4.0 (compressed to 0.040)	0.150 to 40	0.040 and 4.0 (compressed to 0.040)	10.0 and 0.15 at 7 500 (both compressed to 0.040);
Pulse repetition rate	pps	6 000	12 800; 3 200-6 300; 2 120	3 470; 3 500; 5 200; 5 300	4 096 each, 8192 total	1000 – 5000	16 384 each	System maximum average 15 000
Max. duty cycle		0.0015	0.203	0.11	0.017	0.2	0.07	0.15

TABLE 8 (*continued*)

Characteristics	Unit	System G5	System G6	System G7	System G8	System S14	System G21	System G22
Pulse rise times	μs	0.02		0.15	Short pulse: 0.016 Long pulse: 0.082	~0.02	Short pulse: 0.016 Long pulse: 0.038	Short pulse: 0.020 Long pulse: 0.020
Pulse fall times	μs	0.04		0.15	Short pulse: 0.018 Long pulse: 0.06	~0.02	Short pulse: 0.023 Long pulse: 0.056	Short pulse: 0.020 Long pulse: 0.020
Antenna pattern type		Pencil/fan	Fan (csc^2)	Vertical fan and horizontal fan	Inverse csc^2	Fan beam	Inverse csc^2	Inverse csc^2
Antenna type		Planar array	Active array plus reflector	Two phased arrays	Passive array	Slotted waveguide	Passive array	Slotted waveguide
Antenna polarisation	Circular		Vertical	Right-hand circular	Right-hand circular	horizontal	Right hand circular	Right-hand circular
Main beam gain	dBi	40	37.5 (Tx) 37.0 (Rx)	Vertical fan: 36 Horizontal fan: 36	35	≥ 34	37.6	37.6
Elev. beamwidth	°	0.7	3.5 + csc^2 to 20	Vertical fan: 9.0 Horizontal fan: 0.63	19	≤ 16º @ −3dB / ≤ 55º @ −20dB	9.91	9.91
Azim. beamwidth	°	1.1	1.05	Vertical fan: 1.04 Horizontal fan: 15	0.35	≤ 0.6º @ −3dB	0.37	0.37
Horiz. scan rate	°/s	5-30	12	Vertical fan: 60, half time (60 scans/min)	360	10-48 rpm	360	360

TABLE 8 (*continued*)

Characteristics	Unit	System G5	System G6	System G7	System G8	System S14	System G21	System G22
Horiz. scan type	°	Sector: +23/+15	360	30° sector	Continuous	Continuous or sectors	Continuous	Continuous
Vert. scan rate	°/s	5-30		Horizontal fan: 20, half time (60 scans/min)	Not applicable	Not applicable	Not applicable	Not applicable
Vert. scan type		Sector: +7/-1		10° sector	Not applicable	Not applicable	Not applicable	Not applicable
Side lobe levels	dBi		7.5 average on Tx 2.9 average on Rx	Vertical fan: 17 Horizontal fan: 18.5	Az plane: ≤ +10 El plane: ≤ +20	1.5°-5° < −28 dB 5°-10° < −30 dB > 10° < −35 dB	9.15	9.15
Antenna height	m	0	0	0	30 to 100 m above ground level	Installation dependent	10 to 100 m above ground	10 to 100 m above ground
Receiver IF 3dB bandwidth	MHz	2.5	Not specified But 0.8 estimated	40	36	180 (analogue) resolution BW is 12.5 MHz or 25 MHz	50	180
Receiver noise figure	dB	3.25[1]	5 to 6.5	7.5	5.56	2.5	5.25	5.0
Min. discernible signal	dBm	–98	Not specified	–90 (S/N = 13.5 dB)	−96.2	−130 equivalent after pulse compression	–102	–115
Dynamic range	dB		65 from noise to 1 dB compression	Not specified	Not specified		Not specified	Not specified
Min. number of processed pulses			7	6	4-pulse non coherent integration		Not specified	Not specified

TABLE 8 (*end*)

Characteristics	Unit	System G5	System G6	System G7	System G8	System S14	System G21	System G22
Total chirp width	MHz		0.8 estimated	2	Short pulse: none; Long pulse: 50	80 ns to 100 µs – short, medium, long (to be clarified)	Short pulse : none Long pulse : 50	Short pulse : 35 Long pulse : 35
RF emission bandwidth 3 dB	MHz	3.6	0.8 estimated	1.1 (plain pulse), 1.8 (non-linear frequency modulation (NLFM))	43.2	Depending on profiles setup. Normally the full band is used so the −20dB BW stays within the band 9 225-9 500 GHz and the –3 dB BW is the combined BW of all center frequencies used. Default individual chirp –3dB BW is 35MHz.	50	35
RF emission bandwidth 20 dB	MHz	25	Unknown	5.8 (plain pulse), 3.15 (NLFM)	70.3		59	42

4.1.3 Sharing studies on the impact from SAR-4 emissions to RNS receivers

4.1.3.1 Study 1

Figure 13 plots the SAR-4 satellite-ground tracks for 14 orbital periods, each period of 94 minutes and 49 seconds. A SAR can pass over a contiguous territory multiple times per day. For example, there are six ground tracks going through contiguous United States of America each day (three from northeast to southwest and three from southeast to northwest).

FIGURE 13

SAR-4 ground tracks for 14 orbital periods (each 1 hr 34 min 49 sec)

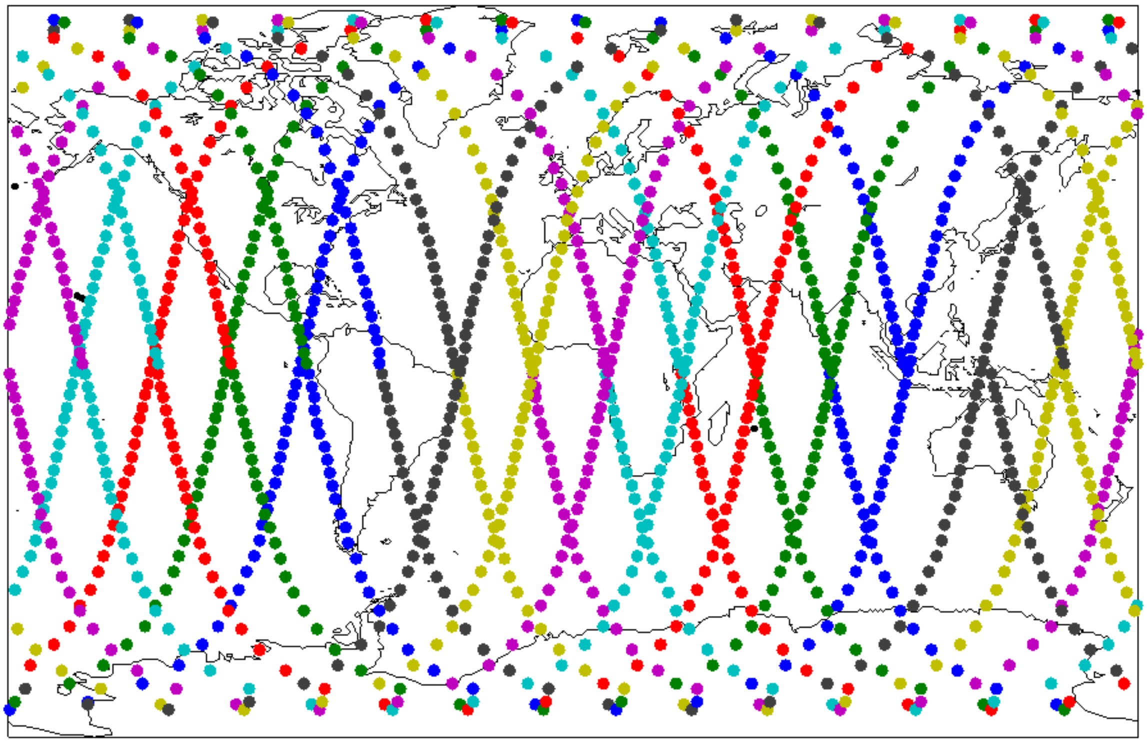

Figure 14 plots the 3-D SAR-4 antenna gain (dBi) as a function of off-axis azimuth angle and off-axis elevation angle. This antenna pattern will be used in the simulation to generate the regions of the received SAR-4 interference power in the radar receivers over the radar maximum interference power required to protect the radars.

FIGURE 14

SAR-4 antenna gain vs. off-axis elevation and azimuth angles

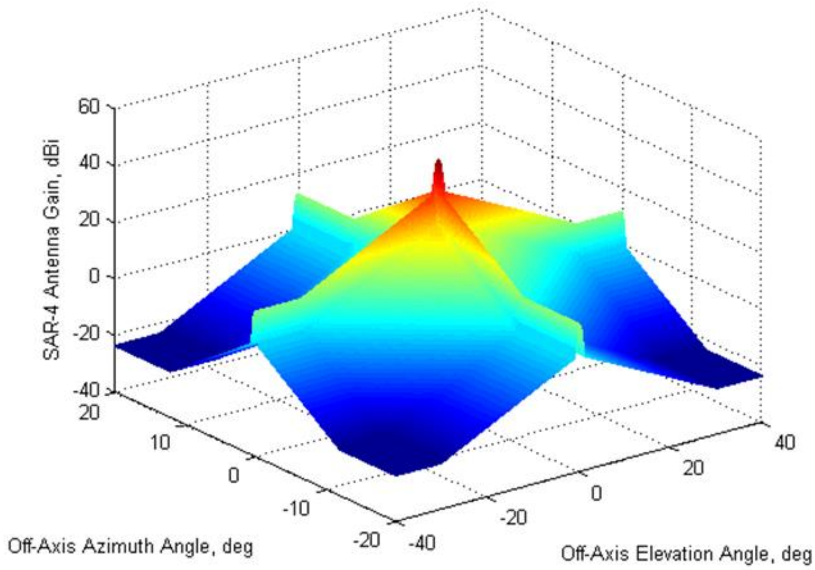

Figure 15 plots the SAR-4, SAR-4/700, SAR-4/900, and SAR-1100 off-axis angle versus the ground systems elevation angle. Since the upper limit of radar G8's elevation beam is about 19°, the upper edge of the SAR-4 elevation beam can only be 56° or less in order to avoid main-beam to main-beam interaction.

For SAR-4, SAR-4/700, SAR-4/900, and SAR-1100 the half elevation beamwidth is less than 1° to 2° and the maximum look-angle is 49.3°, therefore, main-beam to main-beam antenna coupling is probably not possible, but SAR main-beam to radar G8's far sidelobe coupling is likely. Due to the antenna design similarities between radar G8 and radars G21/G22, it is expected that main-beam to main-beam coupling will be unlikely, SAR main-beam to radars G21/G22 sidelobes is likely, but the antenna coupling for the longest duration will be sidelobe to sidelobe.

Due to the antenna design similarities between radar G8 and radars G21/G22, it is expected that main-beam to main-beam coupling will be unlikely, SAR main-beam to radars G21/G22 sidelobes is likely, but the antenna coupling for the longest duration will be sidelobe to sidelobe.

FIGURE 15

SAR-4 off-elevation main beam vs. Radar G8 elevation main beam

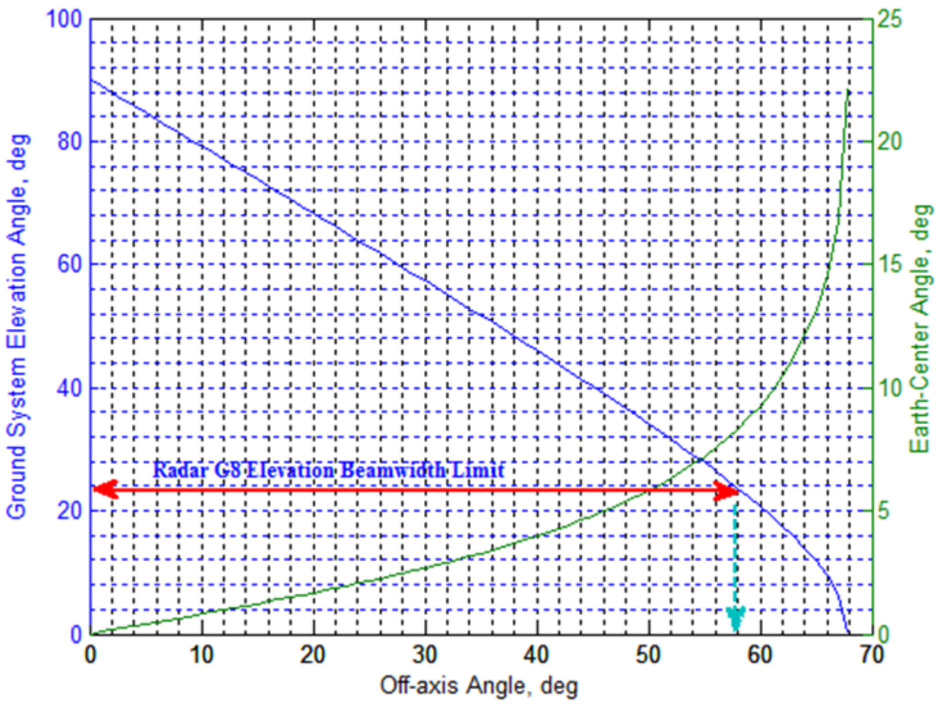

Recommendation ITU-R RS.1280 lays out the foundation of the calculation of interference to terrestrial radars – the average interference signal power level, *I* (dBW), received by a terrestrial radar from spaceborne active sensors. This Recommendation suggests that the received signal to noise of the surveillance radars may not be degraded by more than 0.5 dB longer than a single scan time, taken to be 10 seconds, although the scan time for airport surface surveillance systems is typically 1 second. This equates to an *I*/*N* power ratio of –9 dB at the receiver IF stage.

However, for this case, based on Recommendation ITU-R M.1796, an *I*/*N* ratio of −6 dB, should be used as the required protection level for radiodetermination radars in the frequency band 8 500-10 680 MHz, even if multiple interferers are present. This is defined for continuous noise type of interference. When considering pulsed interference, either a different *I*/*N* ratio or an additional processing gain needs to be considered. Recommendation ITU-R RS.1280 suggests to use such processing gain. This Recommendation also suggests that the average interfering signal power level is considered to be of interest in the case of surveillance radars (e.g. airport surface surveillance radar).

From Recommendation ITU-R RS.1280, the average interfering signal power level, *I* (dBW), received by terrestrial radar from spaceborne active sensors is calculated by:

$$I = 10 \log P_t + 10 \log (\tau\ PRF) + G_t + G_r - (32.44 + 20 \log (f\ R)) + OTR - PG \qquad (1)$$

where:

- P_t: peak spaceborne sensor transmit power (W)
- τ: spaceborne sensor pulse width (s)
- PRF: spaceborne sensor pulse repetition frequency (Hz)
- G_t: spaceborne sensor antenna gain towards terrestrial radar (dBi)
- G_r: terrestrial radar antenna gain towards spaceborne sensor (dBi)

f: frequency (MHz)

R: slant range between sensor and radar (km)

OTR: radar receiver on-tune rejection (dB)

PG: processing gain (dB), rejection of unwanted signals due to radar receiver signal processing (assumed to be zero if not known).

The on-tune rejection term is calculated by:

$$OTR = 10 \log (B_r/B_t) \quad \text{for } B_r \leq B_t$$

$$= 0 \quad \text{for } B_r > B_t$$

where:

B_r: receiver bandwidth

B_t: chirp bandwidth of the transmitted interfering signal.

Figures 16, 17, 18, and 19 show contour-regions of the ratio of received SAR-4/700, SAR-4/900 and SAR-4/1100 interference powers in the G8 radar receiver over the G8 radar maximum interference protection criteria, or I_R/I_{IPC} in dB, on the surface of the earth and the satellite line-of-sight (LoS) coverage region (dotted blue line of 0.1 degree elevation angle). Satellite position points (diamond shape) projected on the surface of the Earth are 1 minute apart.

As shown in Fig. 16, the SAR-4 interference power in a G8 radar receiver exceeds the maximum interference protection criteria (i.e. contour regions where $I_R/I_{IPC} > 0$ dB) only for a few short SAR-4 transmitting times during a few minutes single pass of the ground track and can interfere with multiple radars (if aligned along the SAR-4 ground track) simultaneously. When considering the SAR-4 main-beam to the remote sidelobe of the radar G8, the SAR-4 interference power exceeds the maximum interference protection criteria by 59.5 dB with interference apportionment between services (SA) and by 53.5 dB with no SA when accounting for an aeronautical safety margin of 6 dB.

Similarly, as shown in Fig. 17, when considering the SAR-4/700 main-beam to the remote sidelobe of the radar G8, the SAR-4/700 interference power exceeds the maximum interference protection criteria by 61.8 dB with SA and by 55.8 dB without SA, when accounting for an aeronautical safety margin of 6 dB.

Figures 18 and 19 also show similar results to Figs 16 and 17, when considering the SAR-4/900 and SAR-4/1100 main-beam to the remote sidelobe of the radar G8, the SAR interference power exceeds the maximum interference protection criteria by 60.7 dB with SA and by 54.7 dB without SA, when accounting for an aeronautical safety margin of 6 dB.

RLS, ARNS, MRNS, and proposed EESS (active) are sharing the 9 000-9 200 MHz frequency band. Hence, a per-service apportionment −6 dB was assumed with equal apportionment among the four services.

FIGURE 16

SAR-4/1200 vs. Radar G8: I_R/I_{IPC} (dB) Regions

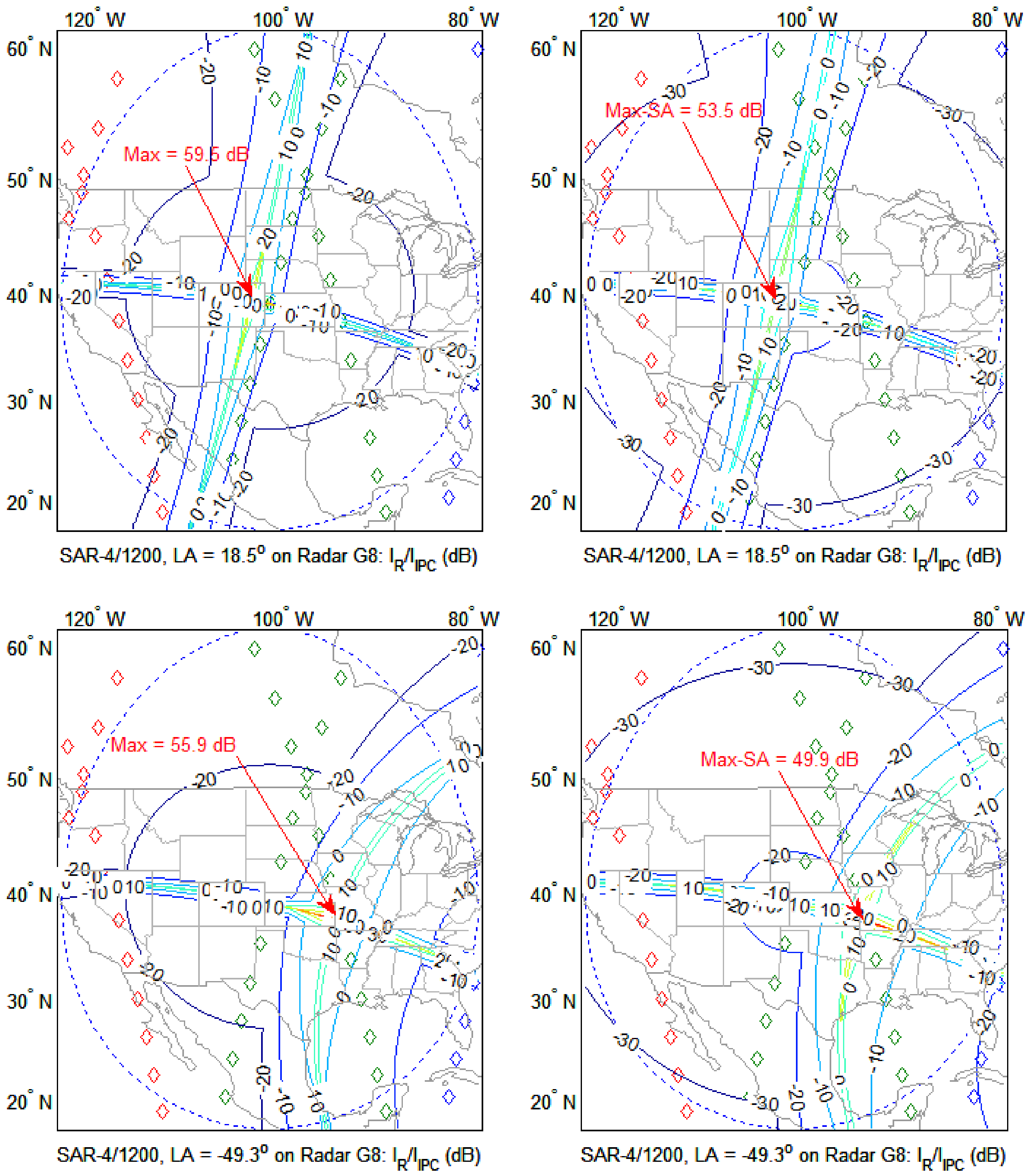

FIGURE 17

SAR-4/700 vs. Radar G8: I_R/I_{IPC} (dB) Regions

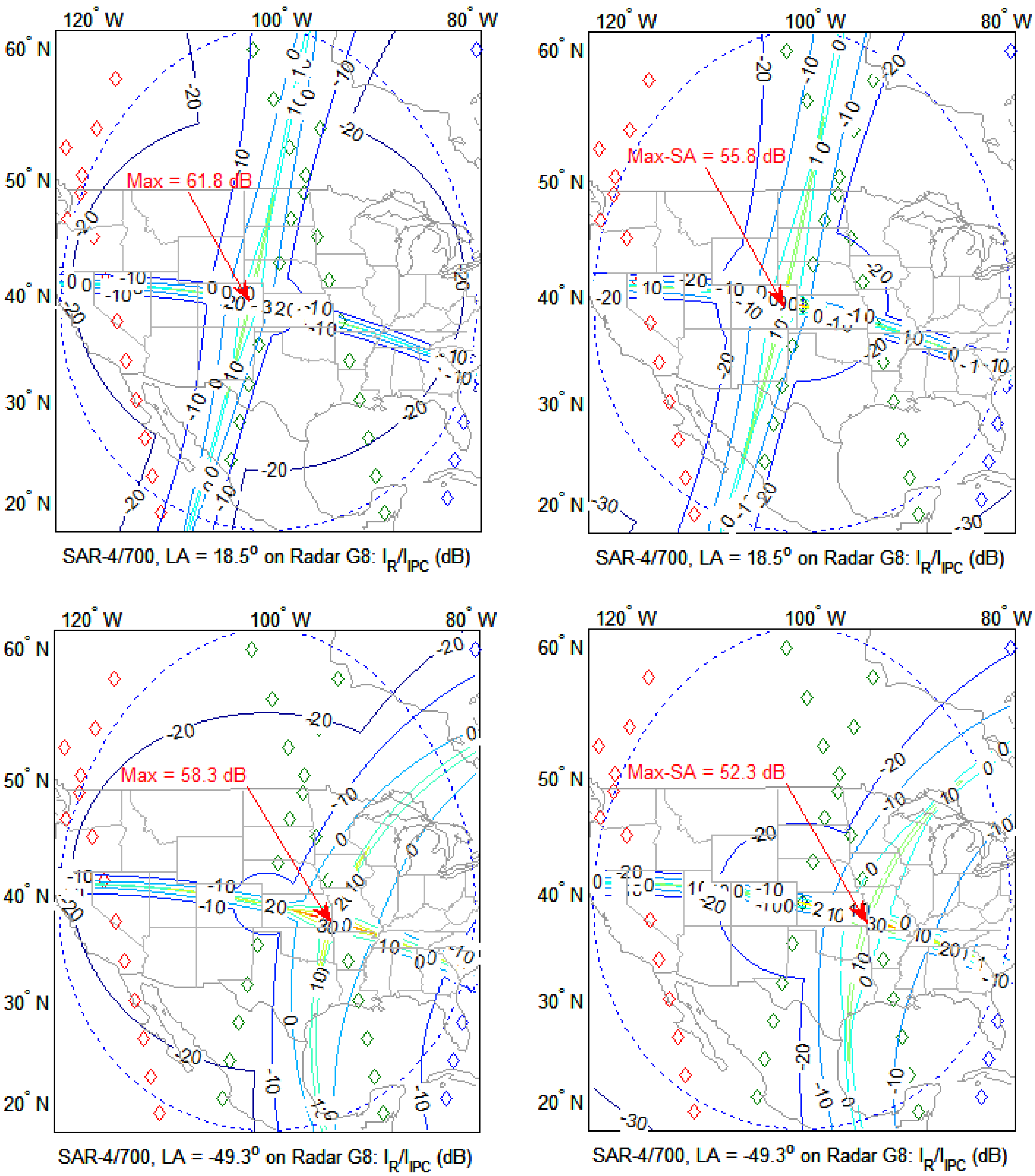

FIGURE 18

SAR-4/900 vs. Radar G8: I_R/I_{IPC} (dB) Regions

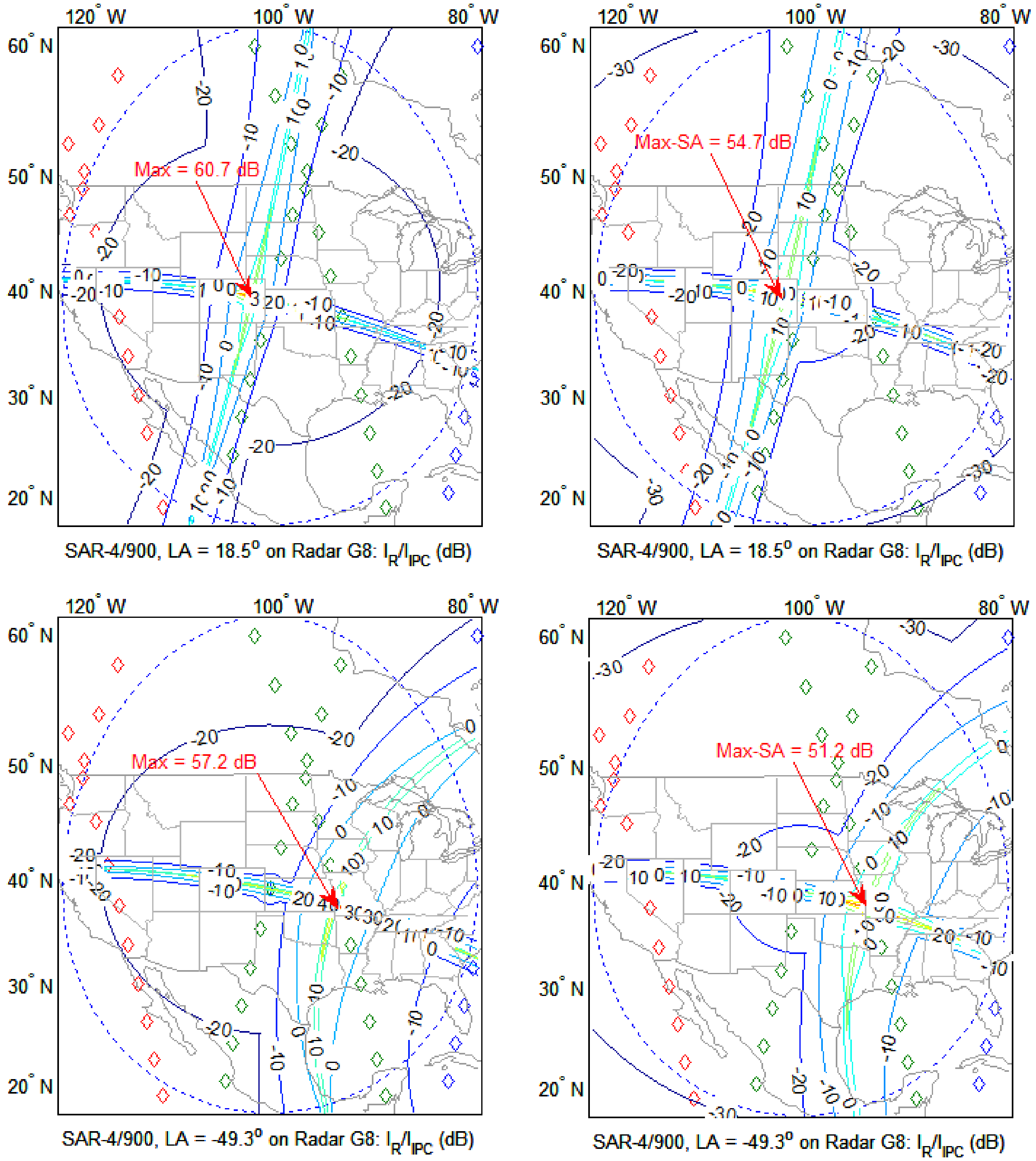

FIGURE 19

SAR-4/1100 vs. Radar G8: I_R/I_{IPC} (dB) Regions

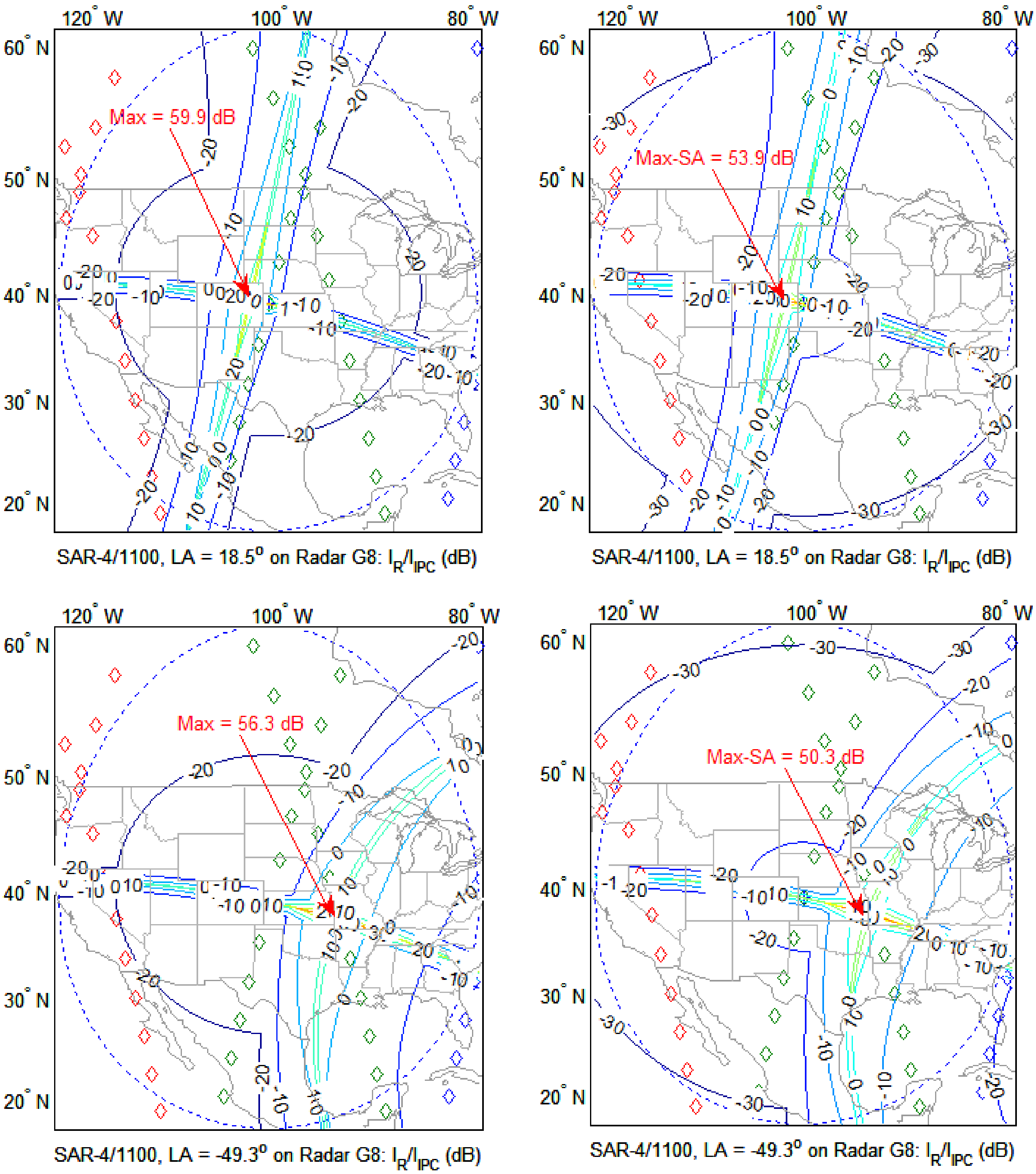

Figure 20 shows contour regions of the ratio of received SAR-4 interference power in the radar receiver over the radar G21 maximum interference protection criteria, I_R/I_{IPC} in dB, on the surface of the earth and the satellite LoS coverage region (dotted blue line of 0.1 degree elevation angle). Satellite position points (diamond shape) projected on the surface of the earth are 1 minute apart. As shown in Fig. 20, the received SAR-4 interference power in G21 radar receiver exceeds the maximum interference protection power threshold (i.e. contour regions where I_R/I_{IPC} > 0 dB) only for a SAR-4 short transmitting time during few minutes (if aligned to SAR-4 ground track) in a single pass of ground track

When considering the SAR-4 main-beam to the remote sidelobe of the radar G21, the SAR-4 interference power receiver exceeds the maximum interference protection criteria by 49 dB with SA and by 43 dB without SA, when accounting for the aeronautical safety margin of 6 dB.

Similarly, as shown in Fig. 21, when considering the SAR-4/700 main-beam to the remote sidelobe of the radar G21, the SAR-4/700 interference power exceeds the maximum interference protection criteria by 51.3 dB with SA and by 45.3 dB without SA, when accounting for the aeronautical safety margin of 6 dB.

FIGURE 20

SAR-4/1200 vs. Radar G21: I_R/I_{IPC} (dB) Regions

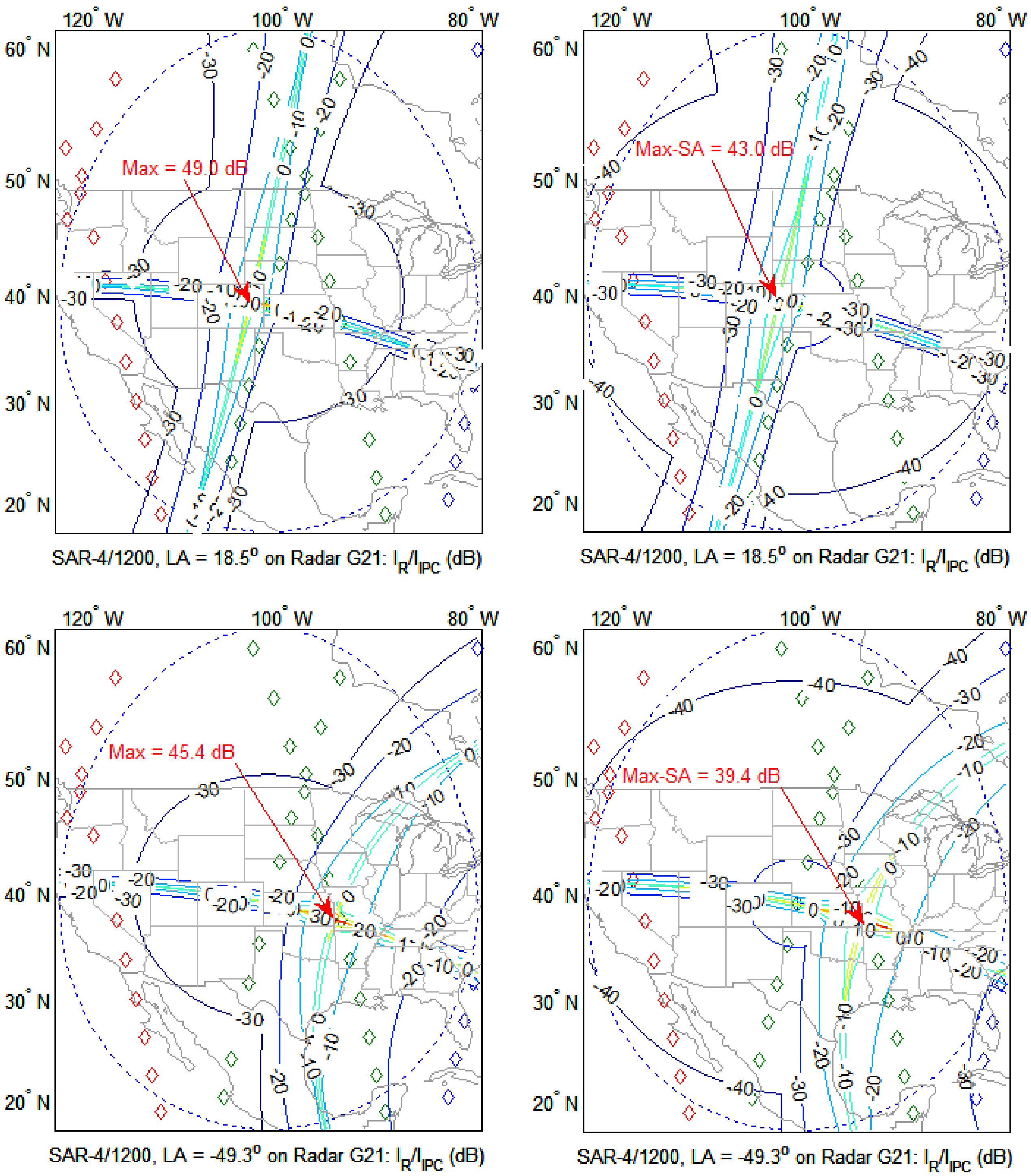

FIGURE 21

SAR-4/700 vs. Radar G21: I_R/I_{IPC} (dB) Regions

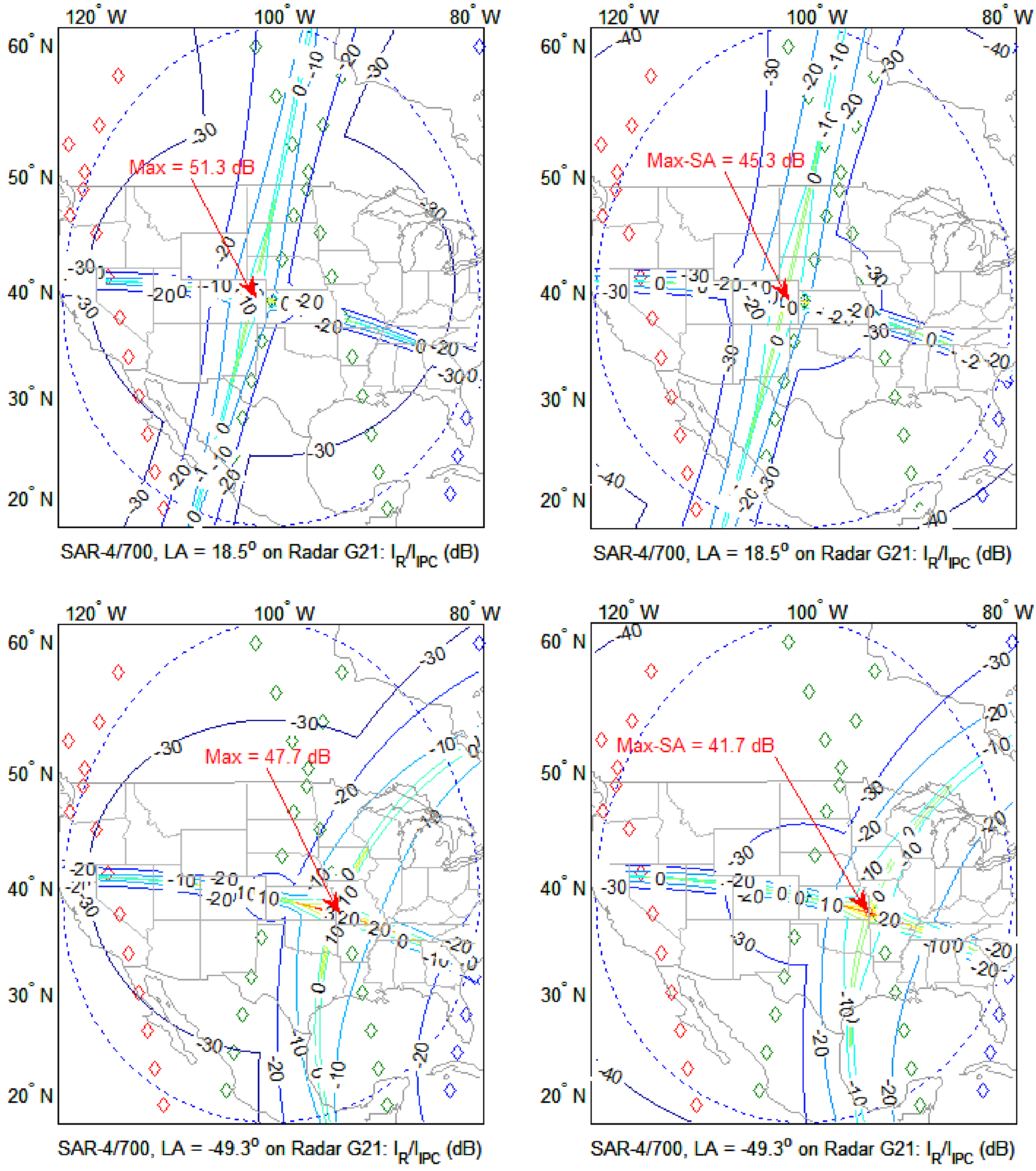

Figure 22 shows contour regions of the ratio of received SAR-4 interference power in the radar receiver over the radar G22 maximum interference protection criteria, I_R/I_{IPC} in dB, on the surface of the earth and the satellite LoS coverage region (dotted blue line of 0.1° elevation angle). Satellite position points (diamond shape) projected on the surface of the Earth are one-minute apart. As shown in Fig. 22, the received SAR-4 interference power in G22 radar receiver exceeds the maximum interference protection power threshold (i.e., region inside the ‘dark red contour’ where I_R/I_{IPC} > 0 dB) only for SAR-4 short transmitting times during few minutes (if aligned to SAR-4 ground track) in a single pass of ground track. When considering the SAR-4 main-beam to the remote sidelobe of the radar G22, the SAR-4 interference power exceeds the maximum interference protection criteria by 49.2 dB with SA and by 43.2 dB without SA, when accounting for the aeronautical safety margin of 6 dB.

Similarly, as shown in Fig. 23, when considering the SAR-4/700 main-beam to the remote sidelobe of the radar G21, the SAR-4/700 interference power exceeds the maximum interference protection criteria by 51.5 dB with SA and by 45.5 dB without SA, when accounting for the aeronautical safety margin of 6 dB.

FIGURE 22

SAR-4/1200 vs. Radar G22: I_R/I_{IPC} (dB) Regions

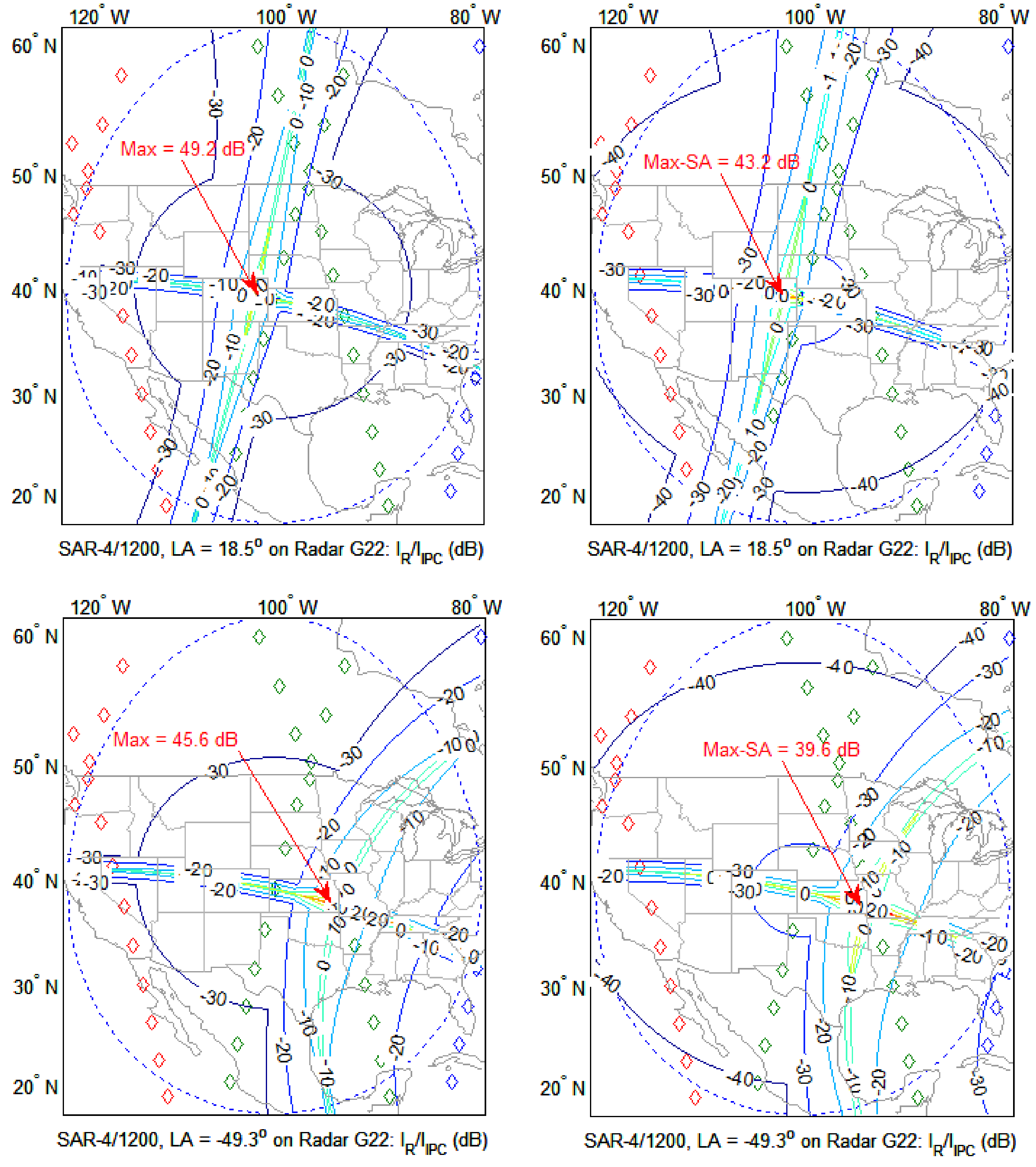

FIGURE 23

SAR-4/700 vs. Radar G22: I_R/I_{IPC} (dB) Regions

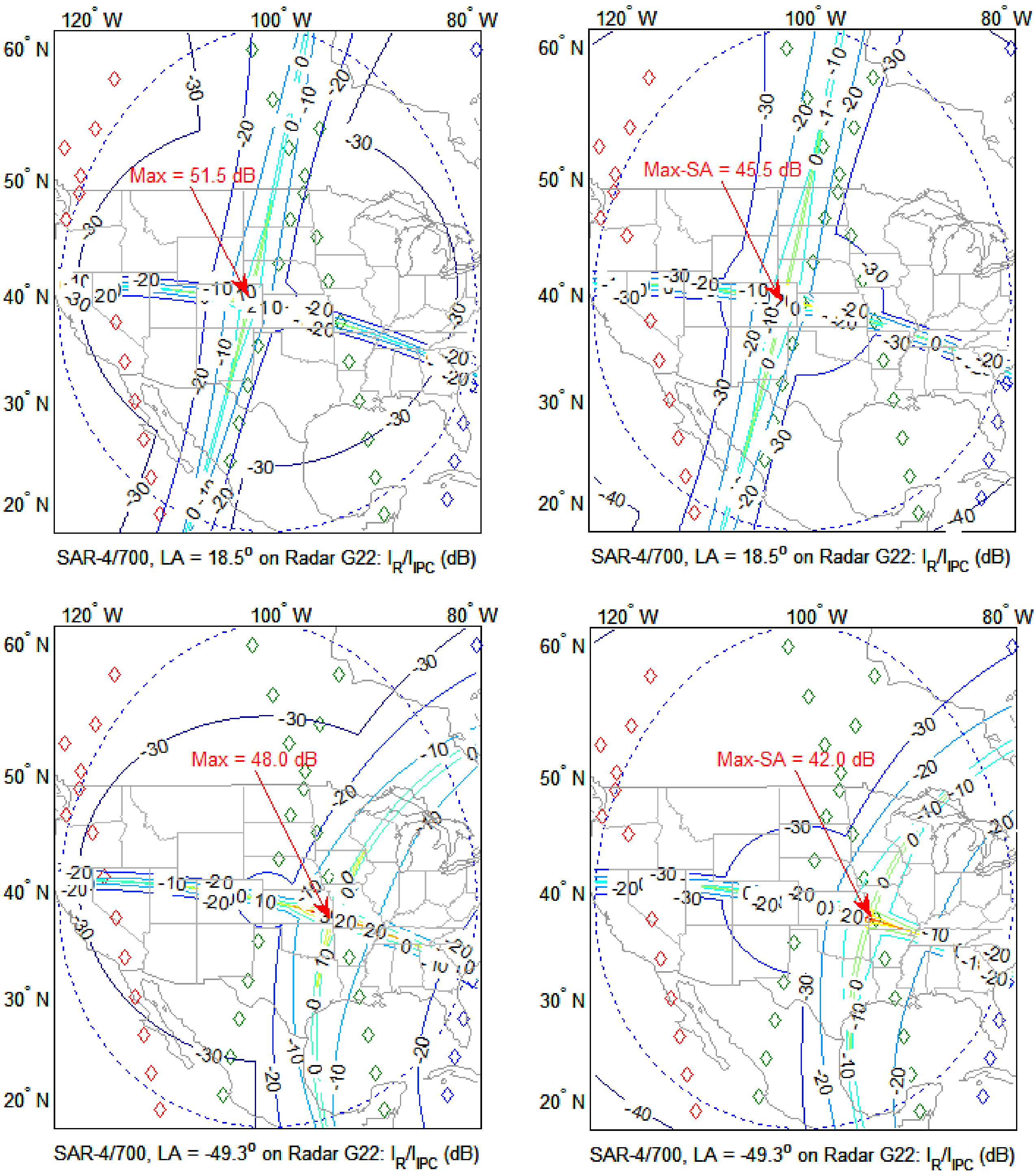

The above analysis is done for a single EESS (active), SAR-4, SAR-4/700, SAR-4/900 and SAR-4/1100, in view of the radars and did not consider the case where multiple EESS (active) satellites simultaneously illuminate the same area. Since a single EESS (active) SAR-4, SAR-4/700, SAR-4/900 and SAR-4/1100 system exceeds the required protection level for ARNS radars G8, G21 and G22, the sharing between EESS (active) and the ARNS in the 9 000-9 200 MHz is not feasible.

Simultaneous interference from overlapped side lobes of multiple SARs can result in higher interference.

Due to the safety aspects of ARNS, the addition of a minimum 6 dB aeronautical safety margin in theoretical studies is recommended by ICAO Document 9718.

Summary

The sharing results are summarized in Table 9 both with and without interference apportionment between services and with 6 dB aeronautical safety margin:

TABLE 9

Summary of results

EESS (active)	**ARNS radars**	**Effective duty cycle (%)**	**I_R/I_{IPC} with interference apportionment between services (peak dB)**	**I_R/I_{IPC} without interference apportionment between services (peak dB)**
SAR-4/1200 MHz	G8	0.9	59.5	53.5
	G21	1.25	49.0	43.0
	G22	4.5	49.2	43.2
SAR-4/700 MHz	G8	1.54	61.8	55.8
	G21	2.14	51.3	45.3
	G22	7.71	51.5	45.5
SAR-4/900 MHz	G8	1.2	60.7	54.7
SAR-4/1100 MHz	G8	0.98	59.9	53.9

The aggregate average I/N of –6 dB should be used as the required protection level for radiodetermination radars from all interference sources, including the proposed SAR. However, the effect of pulsed interference on incumbent systems is difficult to quantify and the interference level is strongly dependent on receiver-processor design and mode of system operation. In general, some radar features can help suppress low effective duty-cycle pulsed interference (of the order of 1%[2] in the radar receiver). Techniques for suppression of low-duty-cycle pulsed interference are described in Recommendation ITU-R M.1372.

[2] As shown in Report ITU-R M.2081 values of up to 2.5% have also been observed for maritime radars.

4.1.3.2 Sharing studies on the impact from SAR-4 emissions to RNS receivers (Study 2)

4.1.3.2.1 Methodology

In order to assess the potential interference conditions produced by a SAR-4 system in spotlight mode, a simulation model was developed.

Two different scenarios are analyzed called "long-term", similar to the scenario considered in Report ITU-R RS.2094, and "worst case short-term" for particular image acquisitions.

The long-term scenario consists in the deployment of 500 areas on land worldwide, which will be the object of an acquisition in the high resolution spotlight mode. They are indicated in black in Fig. 24. The radar location is in blue, collocated with one of the 500 target areas.

The track period of the SAR-4 sub satellite point repeats every 11 days. The full satellite orbit (interference) scenario has been calculated for this period at time intervals of 0.1 second. The satellite illuminates the area around the radar station when the angular conditions are met as shown in Fig. 1. The entire illumination period of the station occurs during around five seconds under varying incident angles.

FIGURE 24

Deployment of image target areas and radar for the worldwide scenario

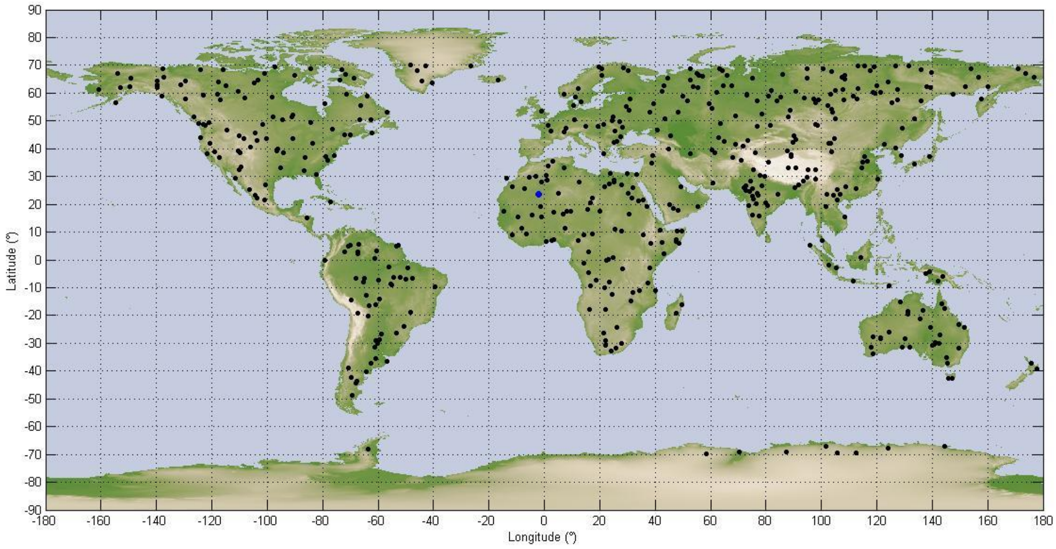

In the short-term scenario, the simulation duration is limited to 3 hours and a time step of 0.001 seconds, with 5 acquisitions, which are separated by the minimum separation distance of 45 km specified for the system. The radar is collocated with the third image area as shown in Fig. 25.

The much lower time step allows examining in more details the events where the radar antenna is pointing towards the satellite.

FIGURE 25

Deployment of image target areas and radar for worst case

4.1.3.2.2 Simulation results

4.1.3.2.2.1 Long-term scenario

The following figures provide for each type of radar the peak and average I/N cumulative distribution function (cdf) obtained from the simulations. These simulations do not take into account any processing gain of the victim radar against pulsed interference, which, as mentioned in Recommendation ITU-R RS.1280, would mitigate or eliminate any effect of pulsed interference including for high I/N values.

4.1.3.2.2.1.1 GCA radar (long-term scenario)

FIGURE 26

Peak *I*/*N* cdf for the GCA radar G6

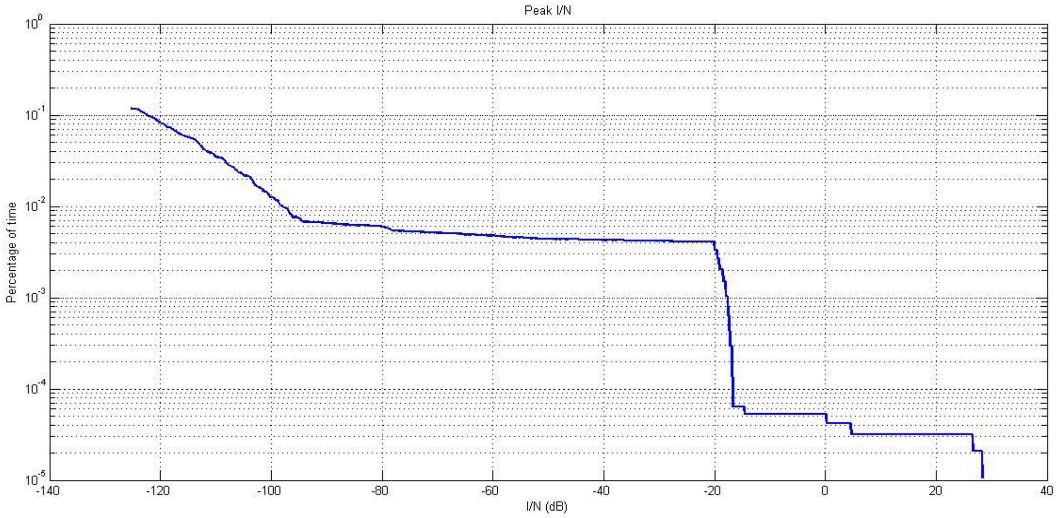

FIGURE 27

Average *I*/*N* cdf for the GCA radar G6

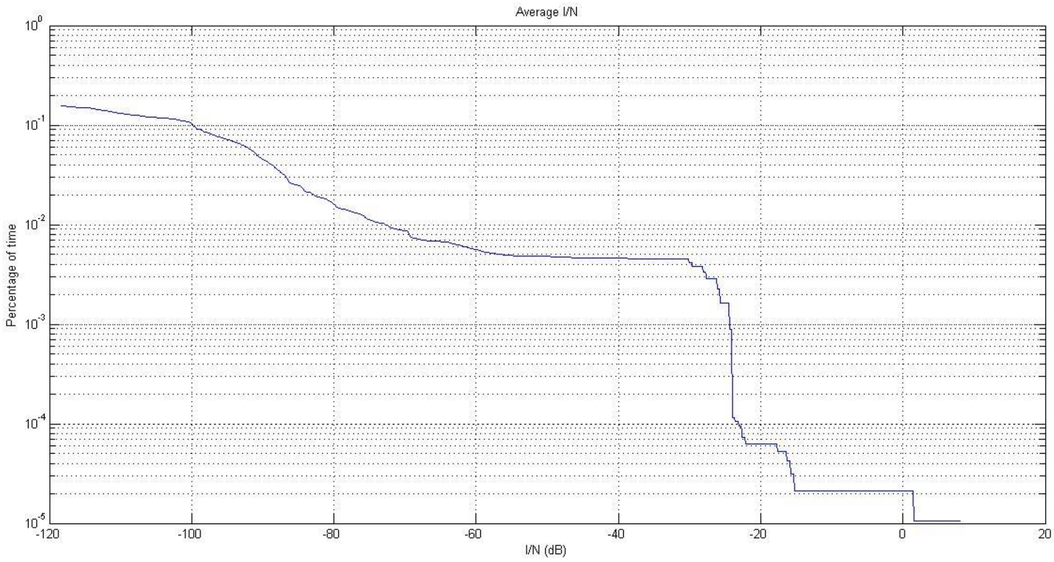

Report ITU-R M.2081 does not give any indication for this kind of radars.

It can be seen that the average *I*/*N* generated in the radar receiver does not exceed +8 dB. However, as shown in Fig. 27, it should be noted that over the 11 days orbital period of the EESS SAR satellite, such a high interference event is only noticed once. The duration of this interference event is limited to a few 100 ms, corresponding to the radar antenna pointing to the azimuth where the EESS satellite is located, while the SAR is performing an acquisition.

It should be noted that a 14 dB radar processing gain would alleviate any harmful interference from SAR-4 in the GCA radar.

FIGURE 28

Average *I*/*N* vs time for the GCA radar G6

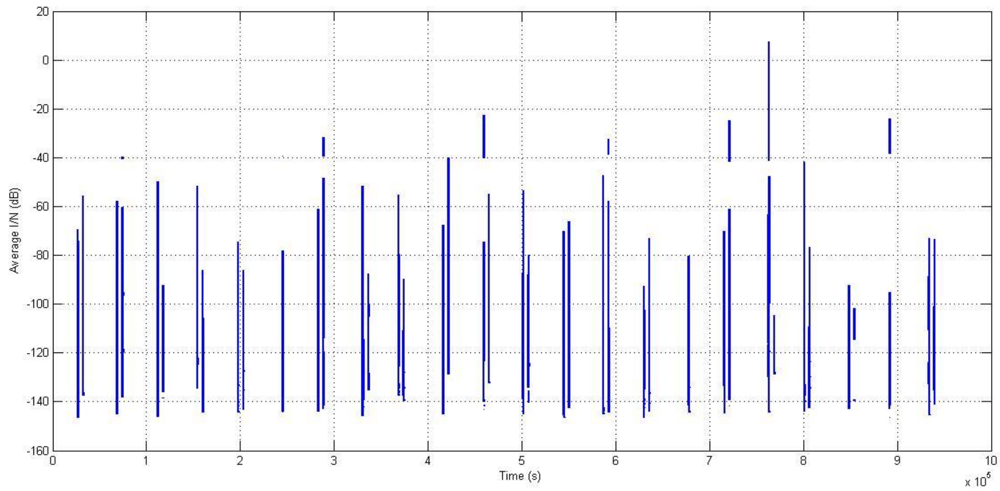

4.1.3.2.2.1.2 Precision approach radar (PAR) (long-term scenario)

Figures 29 and 30 have been derived for east-west oriented runways.

FIGURE 29

Peak *I*/*N* cdf for the PAR radars G5 and G7

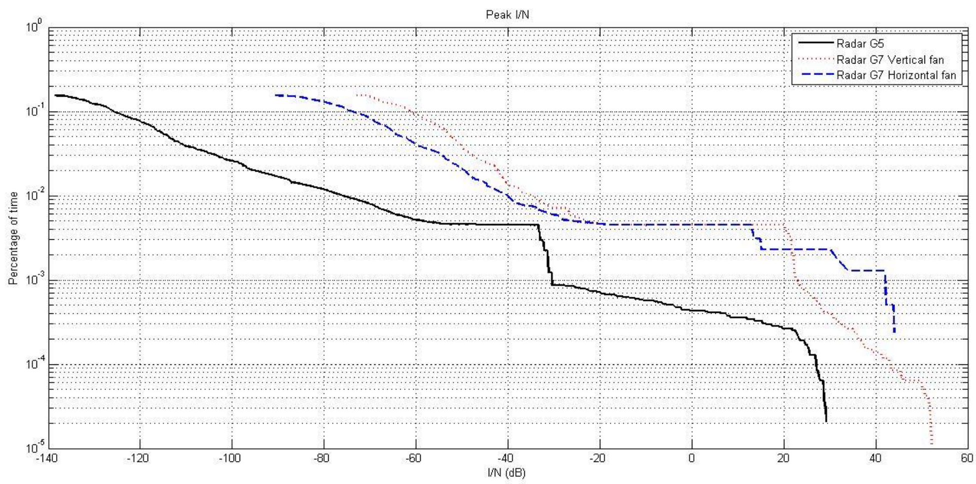

FIGURE 30

Average *I*/*N* cdf for the PAR radars G5 and G7

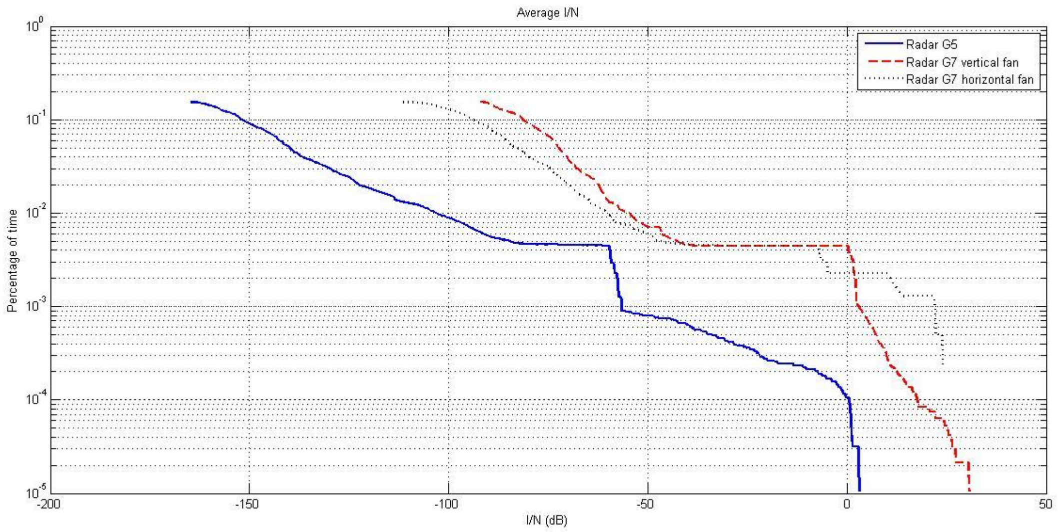

Report ITU-R M.2081 indicates that for PAR radars there is no effect detected for peak *I*/*N* lower than +20 dB for EESS1 waveform and +25 dB for EESS4 waveform. There would therefore be very infrequent faint speckling on radar G5, limited to a period lower than 3 seconds per 11 days. With regard to radar G7, week speckling could appear on the horizontal and vertical fans. This would be limited in time, less than 10 (2 times 5) seconds over the 11 days, and only for a runway oriented in the worst case azimuths.

The average *I*/*N* may reach +30 dB for the radar G7 vertical fan, but limited to very small interference durations. As shown in Fig. 31, there would be up to five potential high interference events during the 11 days satellite orbital period if actual transmissions would occur. Each of these high interference event durations may correspond to the SAR illumination duration of 5 to 7 seconds.

It should be noted that a radar processing gain exceeding 36 dB would alleviate any potential impact of SAR-4 emissions into PAR radars.

FIGURE 31

Average *I*/*N* vs time for the PAR radar G7 (vertical fan)

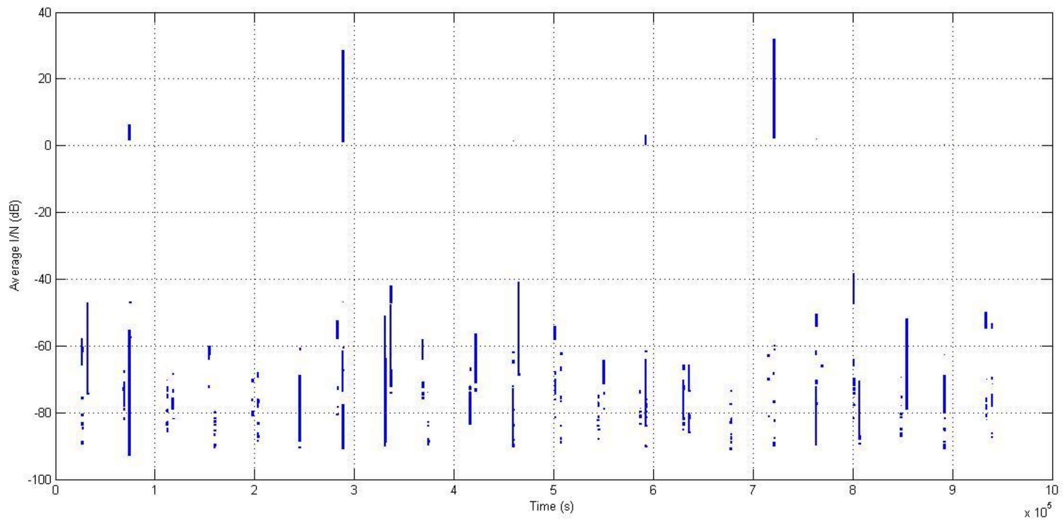

FIGURE 32

Zoom of the second high interference event for the PAR radar G7 (vertical fan)

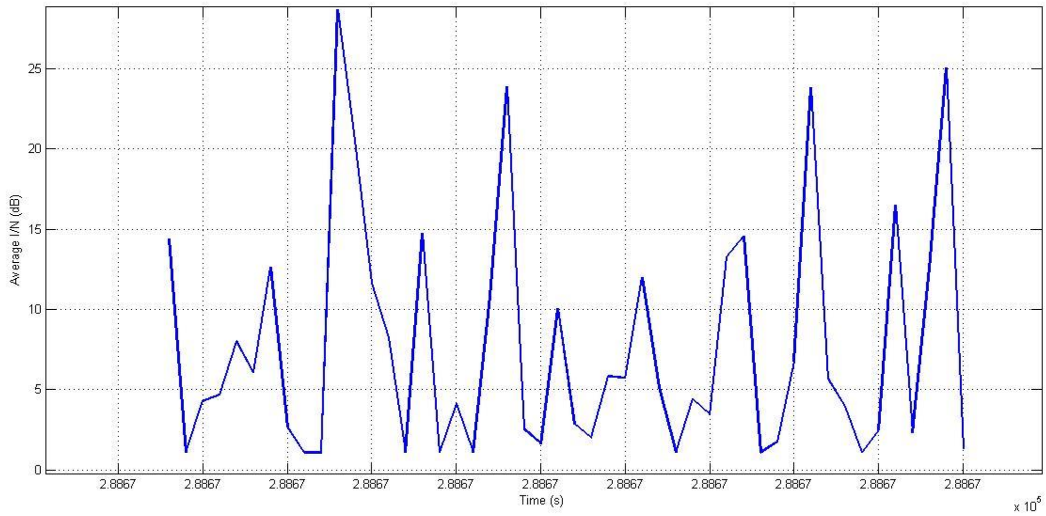

4.1.3.2.2.1.3 Airport surface delection equipment (ASDE) radar (long-term scenario)

FIGURE 33

Peak *I*/*N* cdf for the ASDE radars G8, G21 and G22

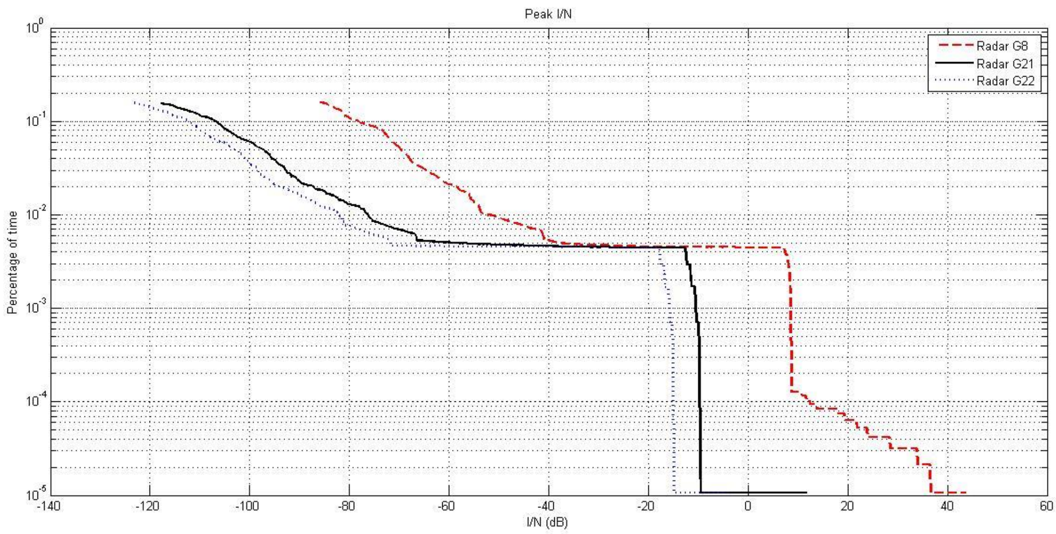

FIGURE 34

Average *I*/*N* cdf for the ASDE radars G8, G21 and G22

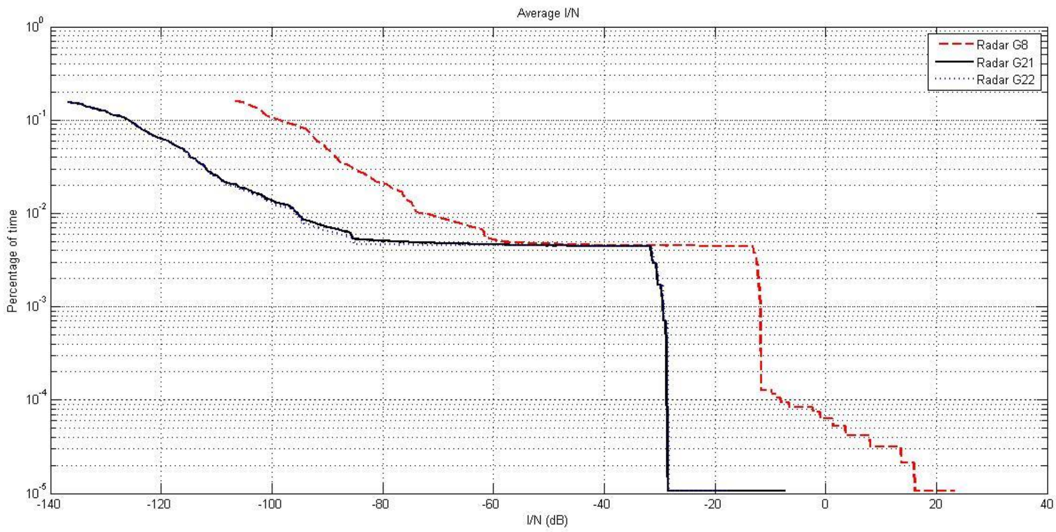

In general, some radar features can help suppress low effective duty-cycle pulsed interference (of the order of 1% in the radar receiver). Report ITU-R M.2081 indicates that for EESS2, that have similar characteristics as a SAR-4, there are few strobes at a peak *I*/*N* of 50 dB for radar G8. However, the measurements in this Report did not take into account the impact on the probability of detection of radar G8.

The average *I*/*N* does not exceed 22 dB for a G8-type radar. This study considers the varying side lobe levels on the terrestrial radars while previous studies consider fixed side lobe levels and interference apportionment and aeronautical safety margin. Therefore, the results differ from other studies. Depending on the operational transmission schedule, such high interference events may only appear up to four times during any 11 days EESS orbital period as shown in Fig. 21. As shown in Fig. 35, even then, they would only occur if the radar antenna is pointing in azimuth direction towards the satellite location at the moment when a SAR picture is actually acquired. Based on this *I*/*N* value obtained, an average radar processing gain of 32 dB would help to reduce interference effects into the G8 radar receiver. Simultaneous interferences from overlap sidelobes of multiple SARs can result in higher interference.

FIGURE 35

Average *I*/*N* vs time for the ASDE radar G8

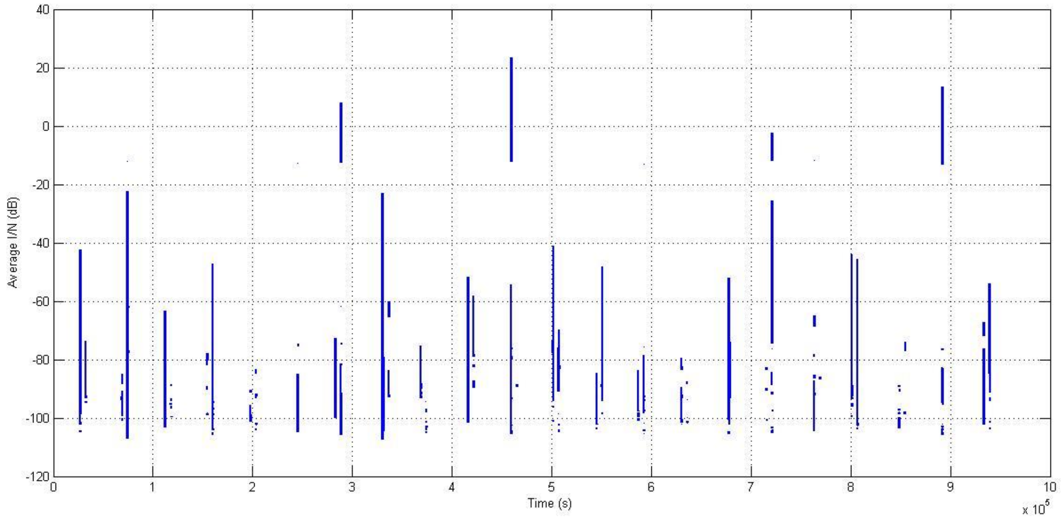

FIGURE 36

Zoom of the second interference event for the ASDE radar G8

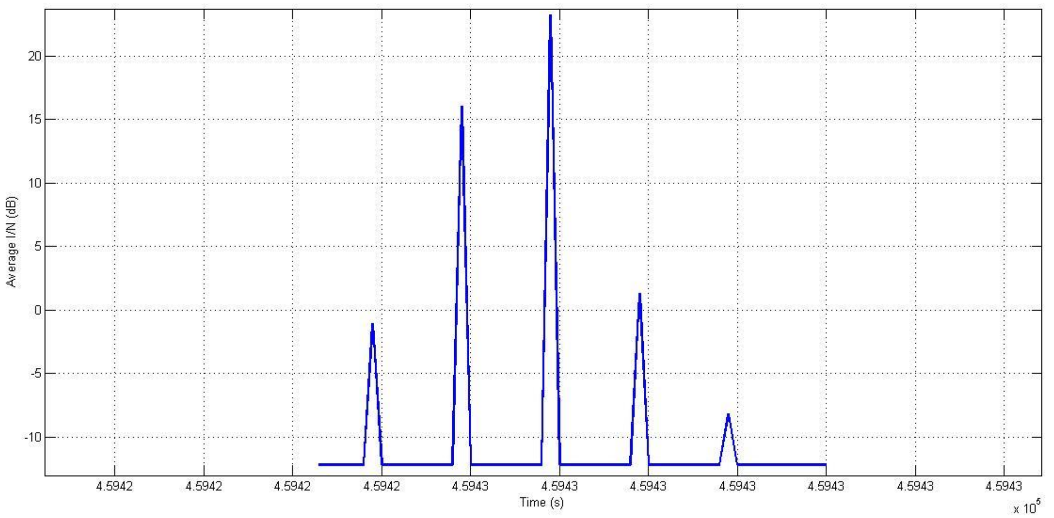

4.1.3.2.2.1.4 Maritime radars (long-term scenario)

FIGURE 37

Peak *I*/*N* cdf for the maritime radar S14

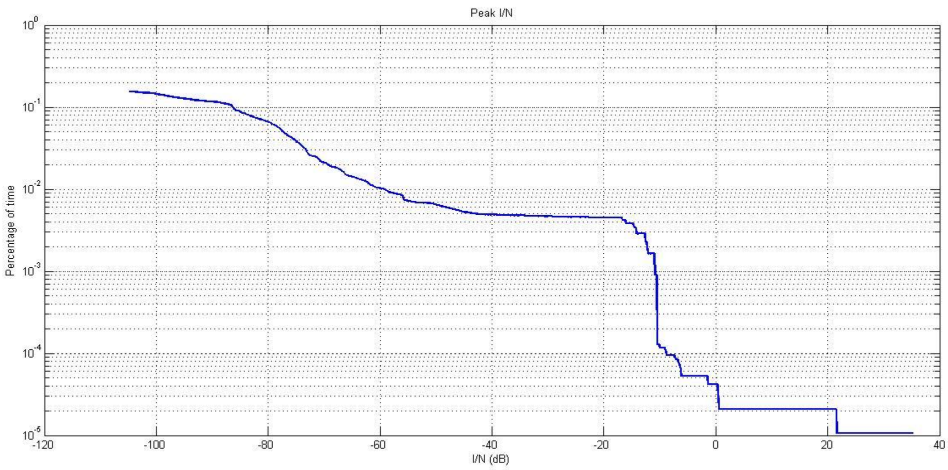

FIGURE 38

Average *I*/*N* cdf for the maritime radar S14

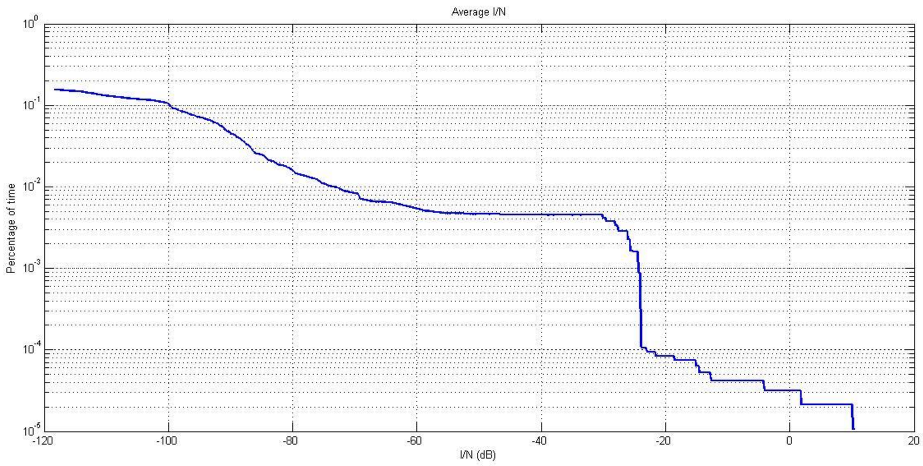

Report ITU-R M.2081 indicates that for all EESS and chirp waveforms there is no effect up to peak *I*/*N* of 40 dB. This is also confirmed by measurements results given in Recommendation ITU-R M.1796 at 9 410 MHz.

The average *I*/*N* never exceeds +10 dB. A processing gain of 16 dB for the maritime radar would therefore suppress any interference effect into this radar type.

4.1.3.2.2.2 Short-term scenario

For each of the identified radars the azimuth and elevation pointing angles are chosen randomly from one time step to the next within limits given in Table 3. The results are given in terms of peak and average *I*/*N* vs. time in Fig. 39 to Fig. 46. These simulations do not take into account any processing gain of the victim radar against pulsed interference, which, as mentioned in Recommendation ITU-R RS.1280, would help to reduce the interference effect of pulsed interference including for high *I*/*N* values.

4.1.3.2.2.2.1 GCA radar (short-term scenario)

FIGURE 39

Peak *I*/*N* values for the GCA radar G6

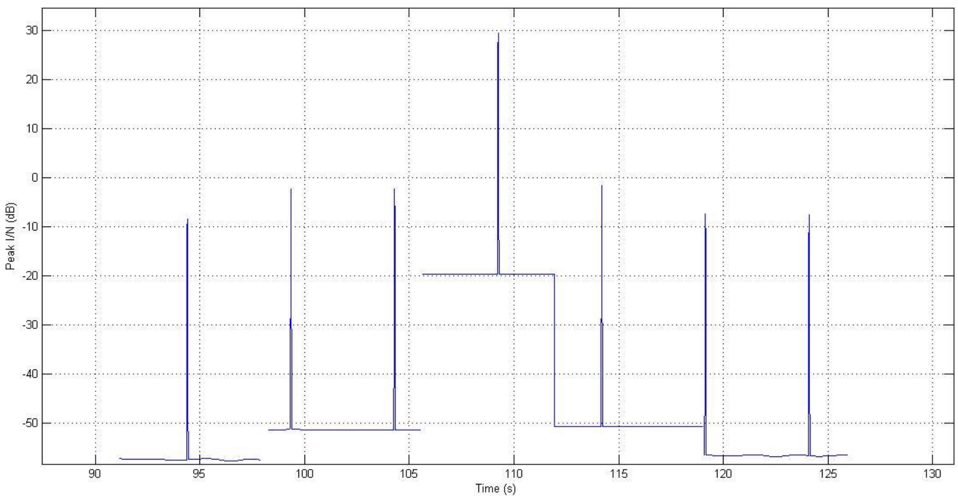

FIGURE 40

Average *I*/*N* values for the GCA radar G6

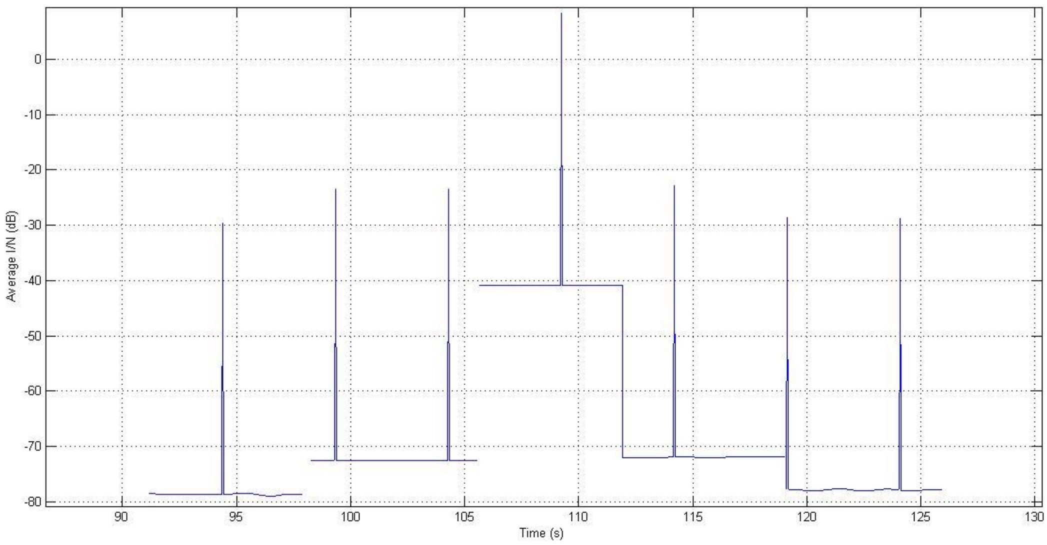

The five acquisitions are clearly visible on Figs 27 and 28. The passage of the radar antenna is also clearly visible. An *I*/*N* of −6 dB is only exceeded if and when the SAR-4 is performing an acquisition over a radar location.

4.1.3.2.2.2.2 PAR radar (short-term scenario)

FIGURE 41

Peak *I*/*N* values for the vertical fan of the PAR radar G7 (horizontal fan)

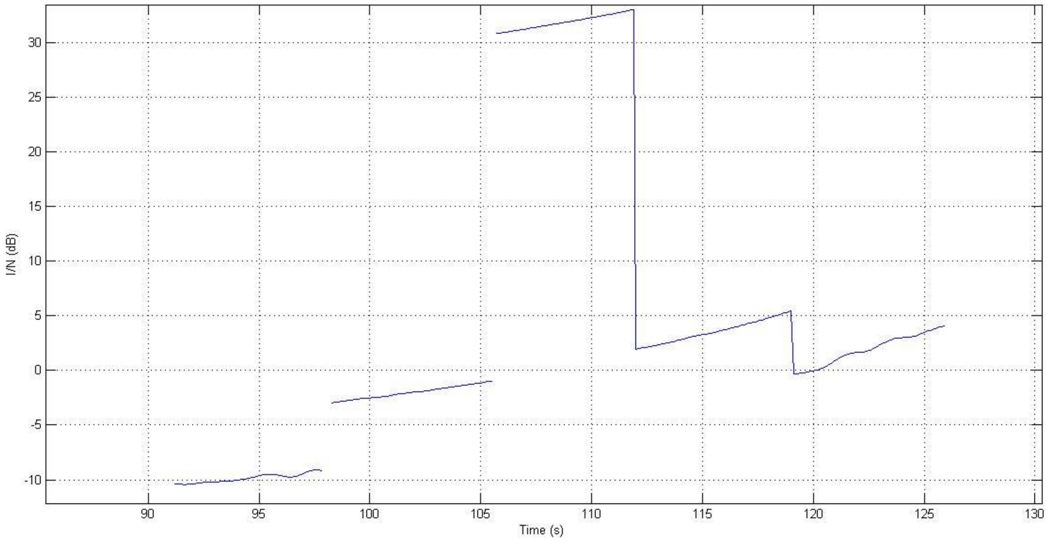

FIGURE 42

Average *I*/*N* values for the vertical fan of the PAR radar G7 (horizontal fan)

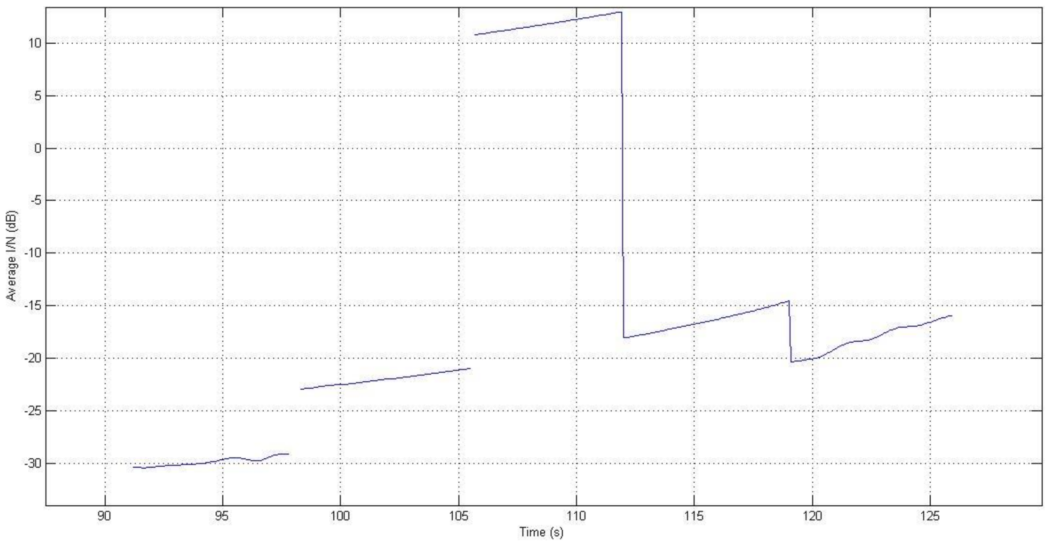

In Figs 41 and 42, the runway has been assumed as to be oriented in the azimuth 260° which corresponds to a worst case regarding potential EESS interference. It should be noted that main-beam to main-beam coupling would be impossible, since the maximum elevation angle for such radars is around 10°, whereas the SAR system is only able to perform acquisitions between 35° and 70° elevation. The satellite would therefore always be in the far sidelobe during a SAR acquisition of the radar area. Here again the *I*/*N* criterion of –6 dB is only exceeded if and when the SAR-4 is performing an acquisition including the radar site.

4.1.3.2.2.2.3 ASDE radar (short-term scenario)

FIGURE 43

Peak *I*/*N* cdf for the ASDE radar G22

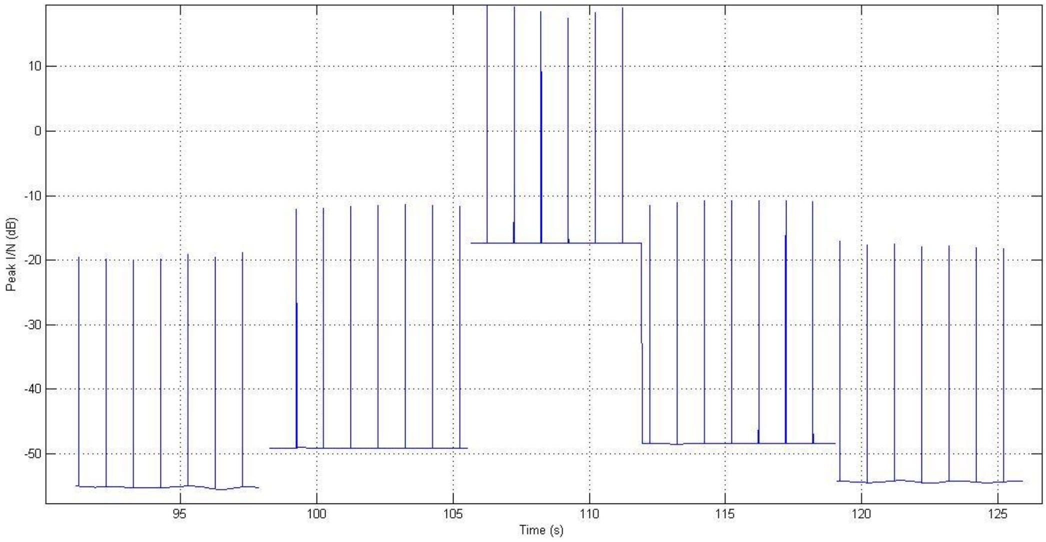

FIGURE 44

Average *I*/*N* cdf for the ASDE radar G22

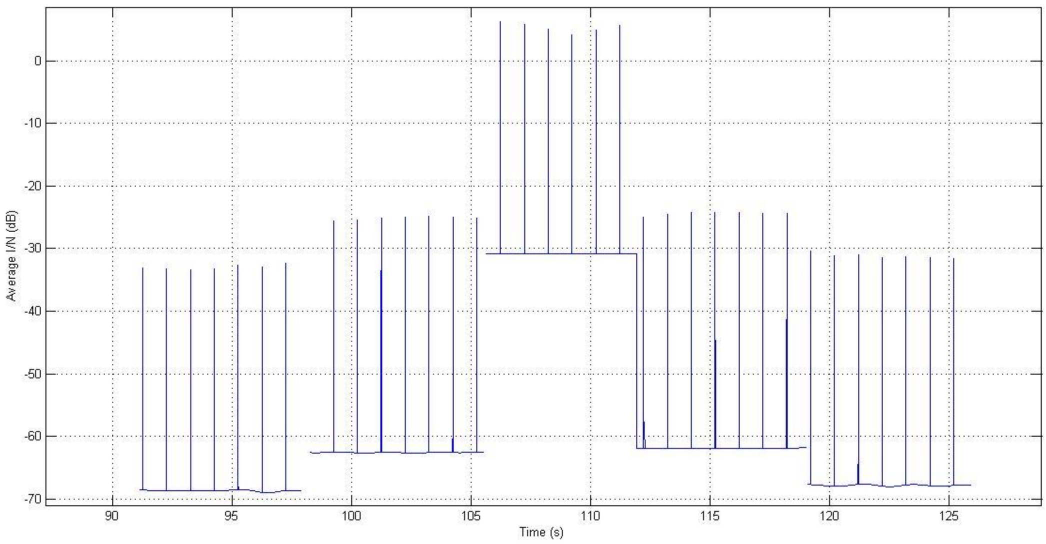

From the Figures above, the *I*/*N* value of −6 dB is exceeded in times when the SAR is illuminating the radar site within its main beam. Here once again, main-beam to main-beam coupling would basically be impossible because of geometrical conditions. The peaks observed come from the side lobes of the radar in elevation.

This study considers the varying side lobe levels on the terrestrial radars while previous studies consider fixed side lobe levels and interference apportionment and aeronautical safety margin. Therefore, the results differ from other studies. Due to the large effective duty cycles of all SAR-4 modes seen by radar G22 (up to 7.71 %), there may be no radar processing gain for radar G22.

4.1.3.2.2.2.4 Maritime radar (short-term scenario)

FIGURE 45

Peak *I*/*N* values for the maritime radar S14

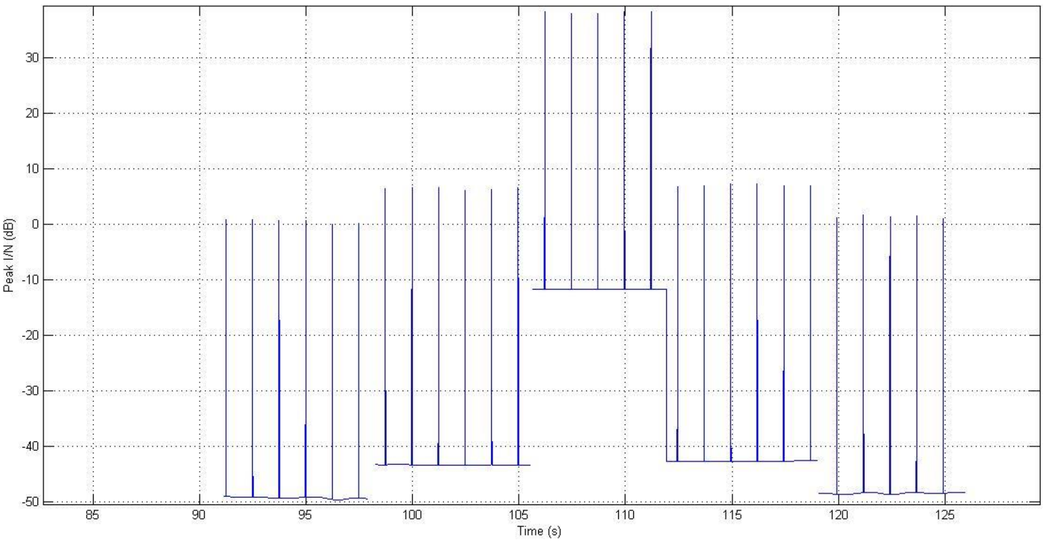

FIGURE 46

Average *I*/*N* values for the maritime radar S14

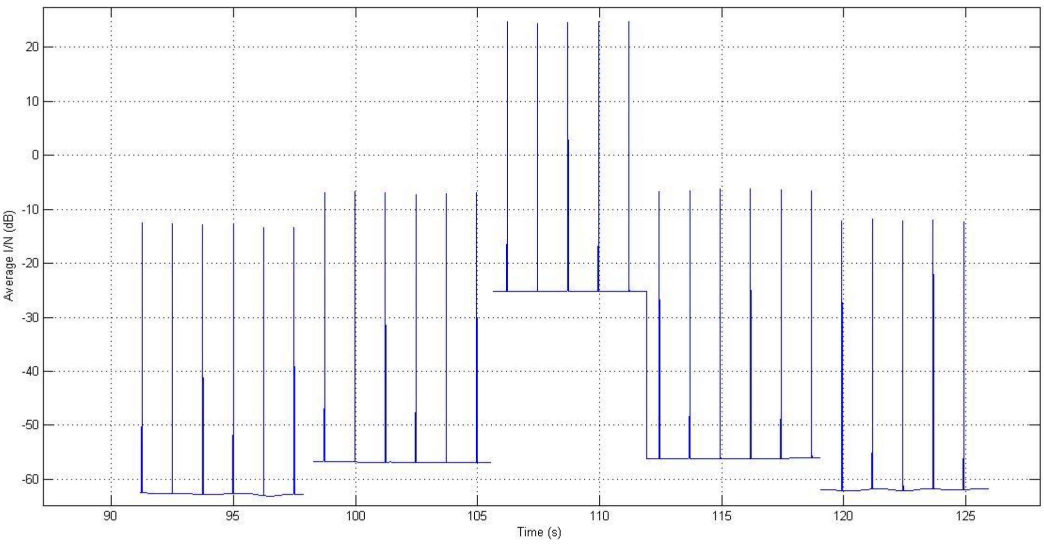

For simulation simplicity the radar S14 which is normally shipborne has been located on land.

Also in this case the average *I*/*N* would only exceed –6 dB when the SAR-4 is illuminating the radar with its main beam and the main beam of the radar antenna is oriented towards SAR-4.

4.1.3.3 Sharing studies on the impact from SAR-4 emissions to RNS receivers (Study 3)

This section deals with the SAR-4 system impact to operation of shipborne, ground-based, and airborne radars for the scenario given in Fig. 47.

This scenario assumes that SAR-4 is moving on a circle orbit at the altitude of around 510 km. The motion path of SAR-4 is shown by blue curve in Fig. 47. The orbit projection to the Earth's surface is shown by black curve. Here the potential area of evaluation limited by the distance of 190 km and 740 km from the SAR-4 orbit projection to the Earth's surface is also shown.

During the flight SAR-4 makes measurements in the corresponding points A, B, C, D and E in the orbit areas –3, –2, –1, 0. +1, +2, +3 (highlighted with green color in Fig. 47). With this the time period of going through each area and time period of each evaluation is 5 s. At the orbit sections between these areas the measurements are not made and time period of going through these orbit sections (the time period between the measurements) is 1 s. The SAR-4 speed along the orbit is 7.63 km/s.

The speed of sub-satellite point movement is 7.06 km/s.

FIGURE 47

Scenario of SAR-4 system impact to ground-based radar

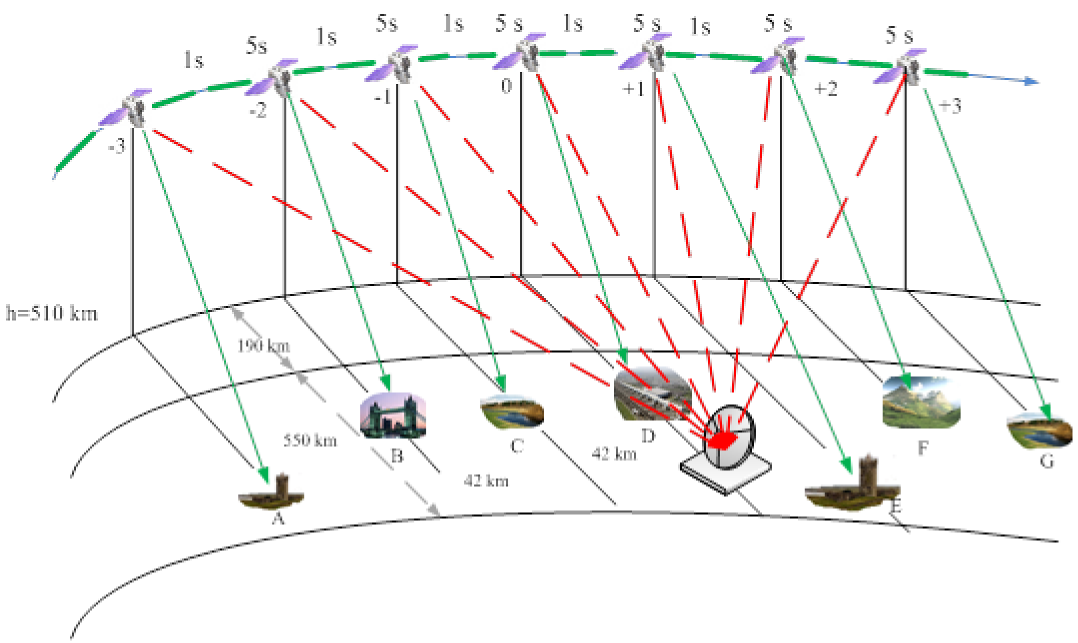

In the vicinity of point D the radiodetermination radar which experiences interference from SAR-4 emissions is located. The interference impact lines are shown in Fig. 50 by red dotted lines. In each of seven considered cases the main beam of radar antenna pattern is directed on azimuth to the SAR-4 sub-satellite point. As the case may be interference caused by SAR-4 can fall into the radar receiver input on the main lobe or side/back lobe of the antenna pattern.

The technical characteristics of SAR-4 given in § 2 of this Report were used in the studies. The technical characteristics of G6, G7, G8 ground-based radars and S3 maritime radar were taken from Recommendation ITU-R M.1796 (see Table 8).

There are no specific protection criteria for the presented radar types in Recommendation ITU-R M.1796-1. Therefore the general protection criteria I/N = –6 dB given in Recommendation ITU-R M.1461 is proposed for evaluation of the interference impact. However, the effect of pulsed interference on incumbent systems is difficult to quantify and the interference level is strongly dependent on receiver-processor design and mode of system operation. In general, some radar features can help suppress low effective duty-cycle pulsed interference (of the order of 1%[3] in the radar receiver). Techniques for suppression of low-duty-cycle pulsed interference are described in Recommendation ITU-R M.1372. Since the protection criteria specified in Recommendation ITU-R M.1461 does not take into account the pulse interference from SAR-4 therefore the effective e.i.r.p. value ($e.i.r.p._{eff}$) defined by the following equation is proposed to use :

$$e.i.r.p._{eff} = e.i.r.p.(C) + 10\lg(Q/100)$$

where:

e.i.r.p. (*C*): SAR-4 transmitter e.i.r.p. towards the radio determination radar antenna, dBW

Q: duty cycle (%).

Then the interference-to-noise ratio taking into account the pulse interference from SAR-4 is defined by the following equation:

$$I/N = EIRP_{eff} + G_{recrls} + 20\lg(\lambda/4\pi R) - 10\lg(kT_N \Delta F) - PG$$

where:

$G_{rec\ rls}$: Antenna gain of the radiolocation receiver, which suffers interference from SAR-4 (dB)

λ: Operational wavelength (m)

R: Distance between SAR-4 transmitter and RLS receiver (m)

k : Boltzmann constant (dBW/K Hz)

T_N : RLS receiver noise temperature (degree)

ΔF : Receiver frequency band (Hz)

PG: processing gain (dB), rejection of unwanted signals due to radar receiver signal processing.

The considered radar types have narrow antenna pattern in the vertical plane and do not scan antenna pattern in the vertical plane or do it in the very narrow angle sector.

To evaluate the interference effect to operation of these radars the calculations were carried out for the minimum (α_{min}) and maximum (α_{max}) arrival angles of interference which corresponds to the remote and closest boundary of measurement area.

The calculations of the minimum and maximum arrival angles of interference were carried out for all seven orbit areas given in Fig. 50. The evaluation results of arrival angles are presented in Table 10 below.

TABLE 10

Minimum and maximum arrival angles for different orbit areas

Orbit area	**–3**	**–2**	**–1**	**0**	**+1**	**+2**	**+3**
α_{min} (degrees)	34.1	34.4	34.5	35	34.5	34.4	34.1
α_{max} (degrees)	68.5	67.8	69	70	69	67.8	65.5

[3] As shown in Report ITU-R M.2081 values of up to 2.5% have also been observed for maritime radars.

The analysis of the interference arrival angles showed that interference impact can be only at the side and back lobes of antenna pattern for the considered radar types.

To evaluate the interference effect to operation of these radars the calculations were carried out for the minimum (α_{min}) and maximum (α_{max}) interference arrival angles which correspond to the remote and closest boundary of measurement area.

Estimates of maximum effective *I*/*N* at the receiver front end of the concerned radars for maximum interference arrival angle are shown in Table 11.

TABLE 11

Estimates of maximum effective *I*/*N* for maximum interference arrival angle in relation to radiodetermination radars operating in the frequency band 8 700-9 300 MHz

Radar	G6	G7	G8	S3
Operation frequency range, GHz	9.025	9.0-9.2	9.0-9.2	8.5-10.0
$I/N_{eff\ max}$ (0)	25.8	25.6	30.3	26.8
$I/N_{eff\ max}$ (−1 & +1)	–4.3	–4.5	0.2	–3.3
$I/N_{eff\ max}$ (−2 & +2)	–10.0	–10.2	–5.5	–9.0
$I/N_{eff\ max}$ (−3 & +3)	–14.4	–14.6	–9.9	–13.4
$I/N_{eff\ max}$ (−58 & +58)	–3.2	–7.5	–2.8	–6.3

Estimates of *I*/*N* at the receiver front end of the radars concerned for minimum interference arrival angle are shown in Table 12.

TABLE 12

Estimates of maximum effective *I*/*N* for minimum interference arrival angle in relation to radiodetermination radars operating in the frequency band 8 700-9 300 MHz

Radar	G6	G7	G8	S3
Operation frequency range, GHz	9.025	9.0-9.2	9.0-9.2	8.5-10.0
$I/N_{eff\ min}$ (0)	21.5	21.3	26.0	22.5
$I/N_{eff\ min}$ (−1 & +1)	–1.4	–1.6	3.1	–0.4
$I/N_{eff\ min}$ (−2 & +2)	–10.8	–11.0	–6.3	–9.8
$I/N_{eff\ min}$ (−3 & +3)	–13.4	–13.6	–8.9	–12.4
$I/N_{eff\ min}$ (−58 & +58)	–2.5	–6.8	–2.1	–5.6

Analysis of the obtained results shows that for any interference arrival angle the maximum *I*/*N* level would be produced when conducting SAR-4 measurements in point D (orbit area **0**) when distance between the interference source and the victim radiodetermination radar would be minimal. Variation of I/N level for the orbit area concerned is as follows:

25.6-30.3 dB for maximum interference arrival angle;

21.3-26.0 dB for minimum interference arrival angle.

The above level of *I*/*N* significantly exceeds in case of main beam to main beam coupling the *I*/*N* threshold value (*I*/*N* = –6dB) specified in Recommendation ITU-R M.1461. The excess level would be between 27.3 dB and 36.3 dB depending on the interference arrival angle.

When SAR-4 moves along orbit areas −1 & +1 the *I*/*N* threshold value would be exceeded in case of main beam to main beam coupling for all radars under consideration and for both minimum and maximum angles. Maximum excess of *I*/*N* threshold value would be of 9.1 dB. It is achieved for G8 radar with minimum interference arrival angle.

When SAR-4 moves along orbit areas −2 & +2 the *I*/*N* threshold value could be exceeded in case of main beam to main beam coupling only for G8 radar. The excess level would be 0.5 dB.

When SAR-4 moves along orbit areas −3 & +3 the *I*/*N* values for all types of the radars would be significantly lower of *I*/*N* = –6 dB.

Analysis of the obtained results show that the most part of the radiodetermination radars concerned would receive interference level from SAR-4 exceeding the *I*/*N* threshold in the measurement or adjacent areas and in case of main beam to main beam coupling Duration of unacceptable interference impact for G6, G7 and S3 radars would be 15 s and it would not exceed 25 s for G8 radar assuming main beam coupling during these periods.

Concurrently, interference effect produced by SAR-4 emissions when it was in the radar visibility sector (areas −58 & +58 of SAR-4 orbit) was analyzed. The estimations assumed that SAR-4 emission would fall into radar receiving antenna pattern main lobe irrespective of the radar scan sector. The estimations show that protection level specified in Recommendation ITU-R M.1461 would be exceeded for most radars under consideration. The excess would increase with SAR-4 approaching the location of the victim radar. The excess level would be a function of radar antenna beam width and of its scan sector.

The results of the conducted studies also show possibility of occurrence of more than 30 dB excess of *I*/*N* = −6 dB at the radar receiver front end which may result in substantial degradation of radar performance and in some cases in partial or complete loss of operability during a short period of time (seconds).

In case the radar processing gain PG is taken to 0 dB then:

1) SAR-4 creates an *I*/*N* higher than −6dB into the radar receiver mainly when it is located in the exposure area of SAR-4 in spotlight mode and is seen by the radar main beam.

2) when the radar receiver is located outside the SAR-4 exposure area there is no interference.

A radar processing gain from 32 to 36 dB is sufficient to remove the interference in the exposure area assuming no interference apportionment between service.

4.1.4 Sharing studies on the impact of RNS emissions on SAR-4 receiver

4.1.4.1 Scenario

We consider a deployment of 200 ASDE radars of type G21 which is the most powerful radar listed in Table 6, deployed worldwide in the band 9 000-9 200 GHz. They are represented in Fig. 48 as black. The blue dots represent the area where an image in high resolution mode may be taken by the SAR system. It has been assumed that 500 image areas were randomly positioned and not necessarily co-located with the radars.

FIGURE 48

Deployment of radars and image areas

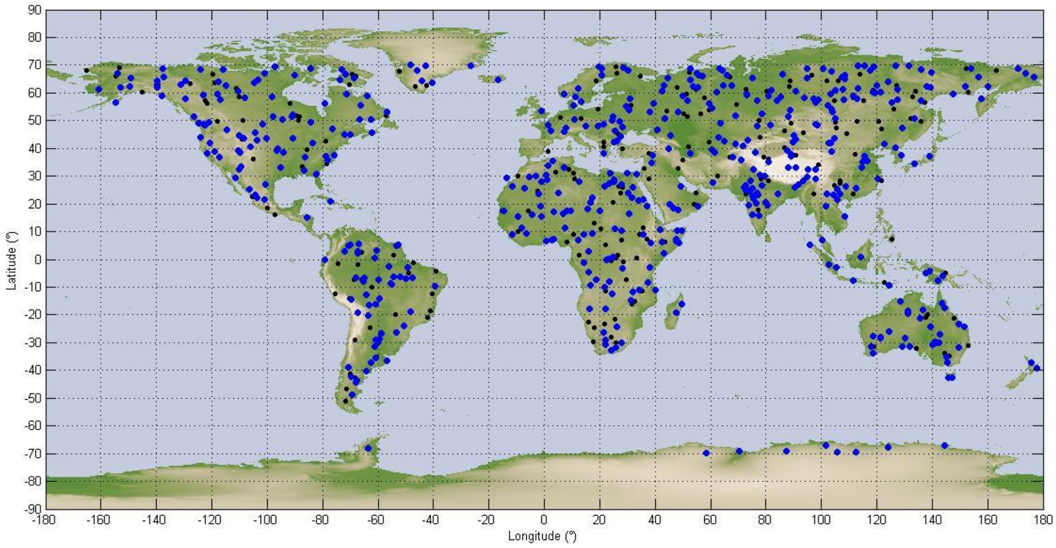

The simulation is run for 11 days with a time step of 1 second. Each time the satellite is within visibility of one area of interest (blue dot) within the relevant azimuth and incidence angles, this area is illuminated, for a duration which varies between 3 and 7 seconds. The SAR-4 receiver will also be activated only during this portion of time. It is assumed that the rest of the time it is inactive. The aggregate interference from all radars in visibility during the acquisition is calculated and converted in *I*/*N*. The noise value is calculated in the 200 MHz of the band 9 000-9 200 MHz.

4.1.4.2 SAR Processing gain

The SAR protection criterion against CW interference is an *I*/*N* of −6 dB, not to be exceeded more than 1% of the time for systematic interference, which is the case here. It is understood here that the reference time for this 1% allowance is the time when the SAR system is in operation (3% of the total time). When compared to the total simulation duration, the effective percentage of time of interference allowance should be in fact 1% * 3% which is 0.03% of the time. When dealing with pulsed interference however, the processing gain of the SAR system should be taken into account, as explained in Recommendation ITU-R RS.1166.

The allowable interference levels as specified above may differ upon consideration of the interference mitigation effect of SAR processing discrimination and modulation characteristics of the radiolocation/radionavigation systems operating in the band.

The allowable *I*/*N* at the entrance of the SAR processing is as follows:

$$I/N_e = I/N_s \cdot \frac{G_{N_{AZ}}}{G_{I_{AZ}}} \cdot \frac{G_{N_{RNG}}}{G_{I_{RNG}}}$$

where:

I/N_e: ratio of the interference-to-noise at the processor input

I/N_s: ratio of the interference-to-noise at the processor output

$G_{N_{AZ}}$: processing gain of noise in azimuth

$G_{I_{AZ}}$: processing gain of the interfering signal in azimuth

$G_{N_{RNG}}$: processing gain of noise in range

G_{IRNG}: processing gain of the interfering signal in range.

$$G_{N_{AZ}} = T_I PRF$$

where:

G_{NAZ}: azimuth processing gain

T_I: SAR azimuth integration time

PRF: pulse repetition frequency.

The integration time T_I in spotlight mode is between three and seven seconds. A value of five seconds has been considered in TABLE 13.

TABLE 13

Range and azimuth processing gains for noise and interference for SAR-4 at 9.6 GHz

Parameter	Value
PRF (Hz)	6000
T_I (s)	5
I/N_s (dB)	−6
G_{NAZ} (dB)	44.8
G_{IAZ} (dB)	0 to 9.5
G_{NRNG} (dB)	0
G_{IRNG} (dB)	2.3
I/N_e (dB)	+26 to +36

A peak *I*/*N* value of +26 or +36 dB would therefore be acceptable against pulsed interference.

4.1.4.3 Results

The results obtained for a deployment of 200 G21 ASDE radars are given in terms of cdf of the *I*/*N* in Fig. 49.

FIGURE 49

***I/N* cdf for 200 radars ASDE G21 in the band 9-9.2 GHz**

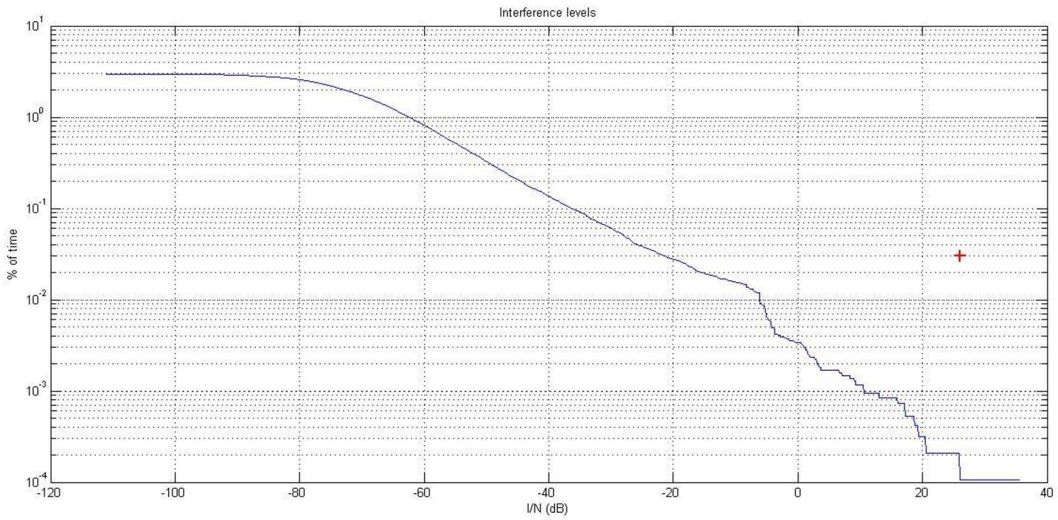

The maximum *I*/*N* is +38 dB and is obtained for 0.0001% of the total time. The *I*/*N* obtained for 1% of the time when the sensor is active is −20 dB, 46 dB below the interference protection criterion when taking into account the SAR processing gain as explained in § 4.1.4.2. A much larger number of radars is expected to be deployed worldwide, however, due to the margin obtained, this is not expected to be a problem, unless this number exceeds 7 000 000.

In this simulation the interference power of all 200 radars has been aggregated, while in reality those radars are pulsed, and the different pulses do not arrive at the same time in the SAR receiver and do not aggregate in power. This would depend of course on the duty cycle of the interfering radars.

4.1.4.4 Summary and preliminary conclusions (RNS in 8 700-9 300 MHz)

When taking into account the test results contained in Report ITU-R M.2081 where radionavigation radars have been tested against various EESS waveforms similar to SAR-4, it is possible to conclude that the SAR emissions would not be a problem for radionavigation radars operating in the band 8 700-9 300 MHz. In addition, the acquisition time of SAR-4 in high resolution mode is very limited.

On the other hand the static analysis of the maximum interference from SAR-4 to the radiodetermination radars shows that the *I*/*N* value at the receiver input can achieve 31 dB. Therefore the additional studies of interference impact consequences to the radiodetermination radars operating in the frequency band 8 700-9 300 MHz are required.

When considering the SAR processing gain as explained in Recommendation ITU-R RS.1166, it is possible to show that these radionavigation radars should not be a problem for SAR-4.

4.2 Sharing with the radiolocation service in the band 8 700-9 300 MHz

4.2.1 Introduction

This section deals with sharing with radars operating in the radio location service in the band 8 700-9 300 MHz.

4.2.2 Characteristics of stations operating in the radio location service

Two systems have been for further studies in the band 8 700-9 300 MHz. they are given in Table 14. It should be noted that these radars are also operating in the band above 9 300 MHz already allocated to EESS (active) and used by multiple SAR systems. In addition, several key parameters are missing, such as the IF bandwidth, which is required to compute the noise level and *I*/*N* values. An IF bandwidth of 10 MHz has been assumed consistent with the lower pulse width of 0.15 µs, assuming no modulation for this pulse width.

The sweeping patterns in azimuth and elevation are not clear for radar G20. It has been assumed that the radar antenna was rotating mechanically in azimuth and that an electronically scan of +/−60° was performed in addition. It was assumed that the antenna was pointing to 40° elevation and a scan in elevation of +/−40° was performed around this value, so that the azimuths covered range from 0 to 80°.

TABLE 14

Radiolocation system parameters in the band 8 700-9 300 MHz

Characteristics	Units	System A12	System G20
Function		Multipurpose surveillance, scanning, tracking	Multipurpose surveillance, scanning, tracking
Tuning range	MHz	8 500-9 900	9 200-9 900
Modulation		Adaptive Pulse, FM	Adaptive Pulse, FM
Peak power	kW	0.03-10	0.03-10
Pulse widths	µs	0.15-300 adaptive	0.15-30 adaptive
Pulse repetition rate	pps	1 000-50 0000 adaptive	1 000-20 000 adaptive
Max. duty cycle		0.8 (pulse) 1 (FM)	0.60 (pulse) 1 (FM)
Pulse rise times	µs	Not specified	Not specified
Pulse fall times	µs	Not specified	Not specified
Antenna pattern type	Antenna pattern type	Digital beam forming	Digital beam forming
Antenna type		Active array	Active planar array
Antenna polarisation		Linear / Circular	Linear/circular
Main beam gain	dBi	35-42	36-42
Elev. beamwidth	°	1.6 @42 dBi	4 @ 36 dBi 2 @ 42 dBi
Azim. beamwidth	°	1.6 @42 dBi	2.5 @ 36 dBi 1.3 @ 42 dBi
Horiz. scan rate	°/s	Not applicable	Not applicable
Horiz. scan type	°	± 60° Electronic scan ± 120° with additional mechanical repositioner	± 60° electronic scan N*360° mechanical
Vert. scan rate	°/s	Not applicable	Not applicable
Vert. scan type		± 60° Electronic scan ± 120° with additional mechanical repositioner	± 40° electronic
Side lobe levels	dBi	Depends on beamforming	Depend on beamforming
Antenna height	m	Aircraft altitude	~ 10 m

TABLE 14 (*end*)

Characteristics	**Units**	**System A12**	**System G20**
Receiver IF 3dB bandwidth	MHz	Not specified	Not specified
Receiver noise figure	dB	6	6
Min. discernible signal	dBm	–130	–122

4.2.3 Sharing studies on the impact of SAR-4 emissions on RLS receivers

4.2.3.1 Study 1

4.2.3.1.1 Methodology

In order to assess the potential interference conditions produced by a SAR-4 system in spotlight mode, the same simulation model was used, with the same scenarios.

4.2.3.1.2 Simulation results

4.2.3.1.2.1 Long-term scenario

Figures 50 and 51 show the cdf of the peak *I*/*N* values obtained for both radars A12 and G20, and interference caused by a SAR-2 system transmitting within the current EESS allocation, and a SAR-4, that may use the extended allocation. For both radars the azimuth and elevation angles are chosen randomly from one time step to the other within the limits defined in Table 8.

FIGURE 50

Peak *I*/*N* values for SAR-2 and SAR-4 and radars A12 and G20

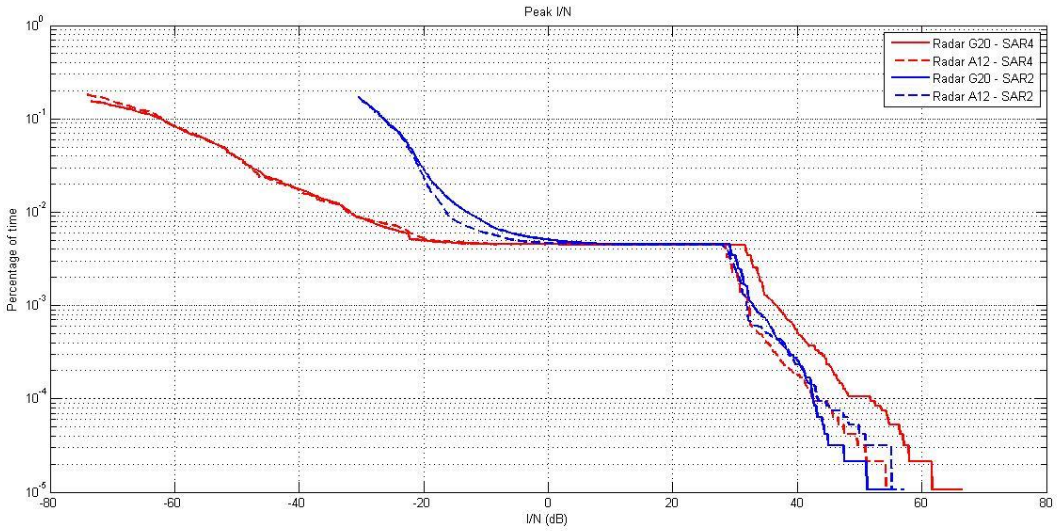

FIGURE 51

Average *I*/*N* values for SAR-2 and SAR-4 and radars A12 and G20

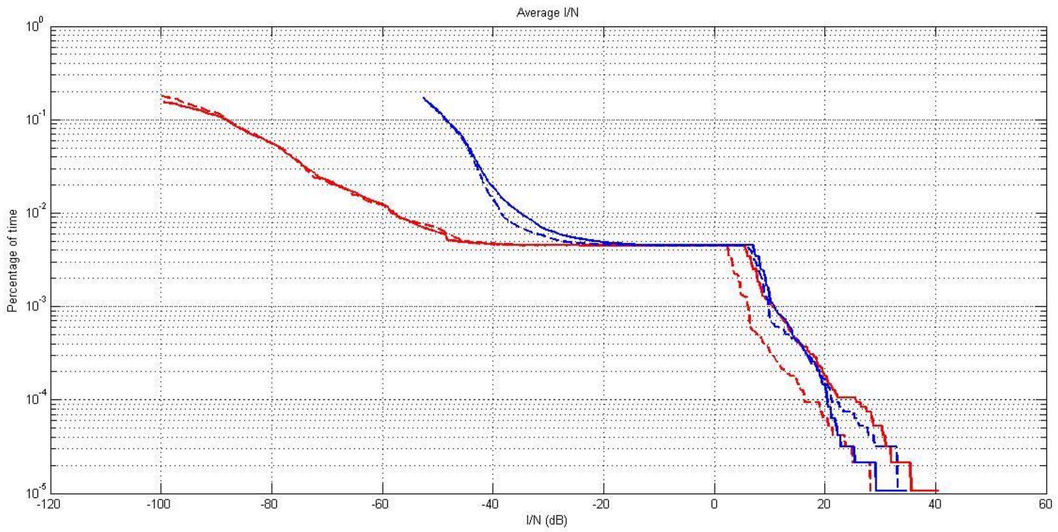

It can be seen that in case of main beam to main beam coupling the peak *I*/*N* can reach values as high as 60 dB. However these extremely high values are obtained for very low percentages of time in the order of 0.00001%, which is less than 100 ms per 11 days.

For radar A12, this supposes a fixed aircraft, whereas in reality from one acquisition to another the aircraft would have disappeared from the target area. In addition, during one month, the pointing angle of the radar would also change, thus decreasing the *I*/*N* values. The impact of SAR-4 may be compared to the impact of SAR-2, which is operational and using the existing allocation. SAR-4 would create a slightly higher interference, up to 64 dB. Therefore, if no interference has been noticed until today on either radars A12 or G20, it is expected that none will be observed after the extension of the allocation to EESS (active).

4.2.3.2 Sharing studies on the impact of SAR-4 emissions on RLS receivers (Study 2)

4.2.3.2.1 Introduction

This section addresses the sharing performance simulation analyses between the EESS SAR and RLS radars in the band 8 700-9 300 MHz based on the spectrum characteristic modeling method. The sharing effects are analyzed between the EESS SAR and RLS radars including G20 and A12 in the band 8 700-9 300 MHz by simulating the different parameters of the EESS SAR and radars.

4.2.3.2.2 Interference simulation analyses from spaceborne SAR with adjustable parameters to pulse radars

This section provides the interference simulation results from spaceborne SAR with adjustable parameters as pulse width, repeat period and bandwidth to pulse radars while keeping the same parameters of pulse radars and the peak power of spaceborne SAR. The simulation results display the signal waveforms by signal processing of pulse radars.

(1) Interference effect under the condition of keeping the same parameters of spaceborne SAR pulse width and bandwidth, with the repeat period adjustable.

The result of interference effect analysis from SAR interference signals under the condition of same pulse width and bandwidth and adjustable repeat period is shown in Table 15 and Fig. 52 (a)-(c).

TABLE 15

Interference effect analysis from SAR interference signals under the condition of same pulse width and bandwidth and adjustable repeat period

Number	Pulse width (μs)	Repeat period (μs)	Bandwidth (MHz)
1	50	100	1200
2	50	200	1200
3	50	400	1200
Simulation result	When the pulse width and bandwidth of SAR interference signals are keeping the same, the amplitude of interference pulse train basically remains with the increasing repeat period, while the appearing times reduce during a set time.		
Basic conclusion	The interference amplitude keeps the same when repeat period of SAR pulse increased, while the decreasing appearing times of interference pulse will reduce the average interference power.		

FIGURE 52

Interference effect analysis from SAR interference signals under the condition of same pulse width and bandwidth and adjustable repeat period

(a) Simulation result when repeat period is 100 μs

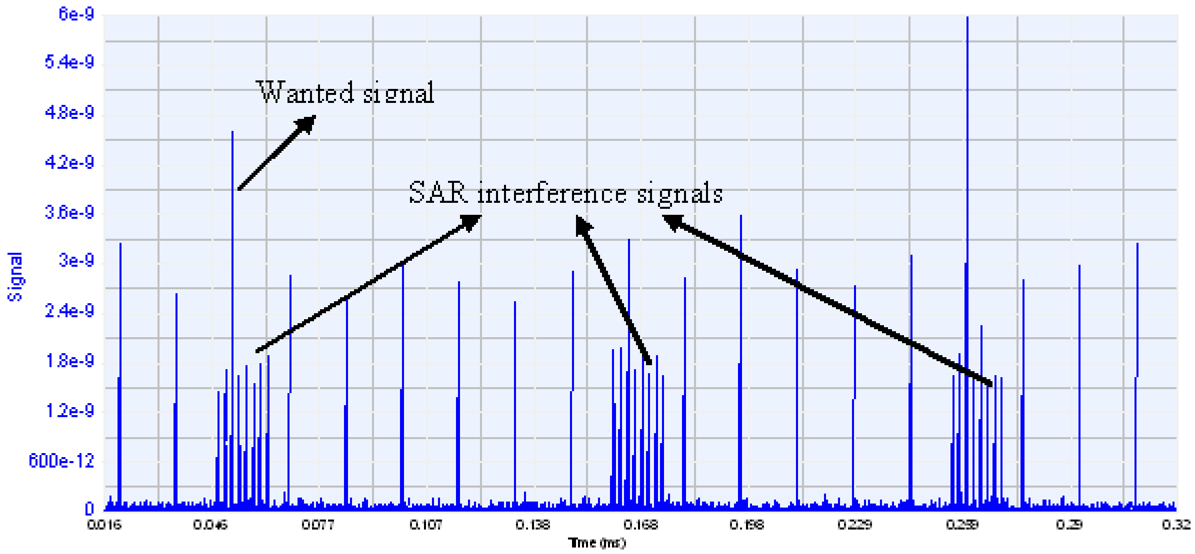

(b) Simulation result when repeat period is 200 µs

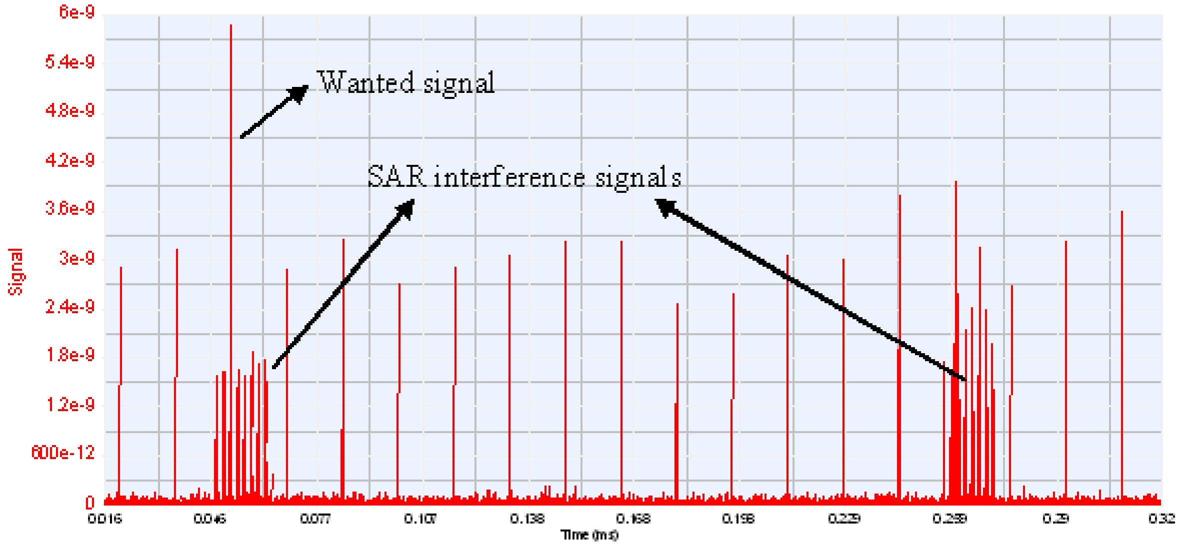

(c) Simulation result when repeat period is 400 µs

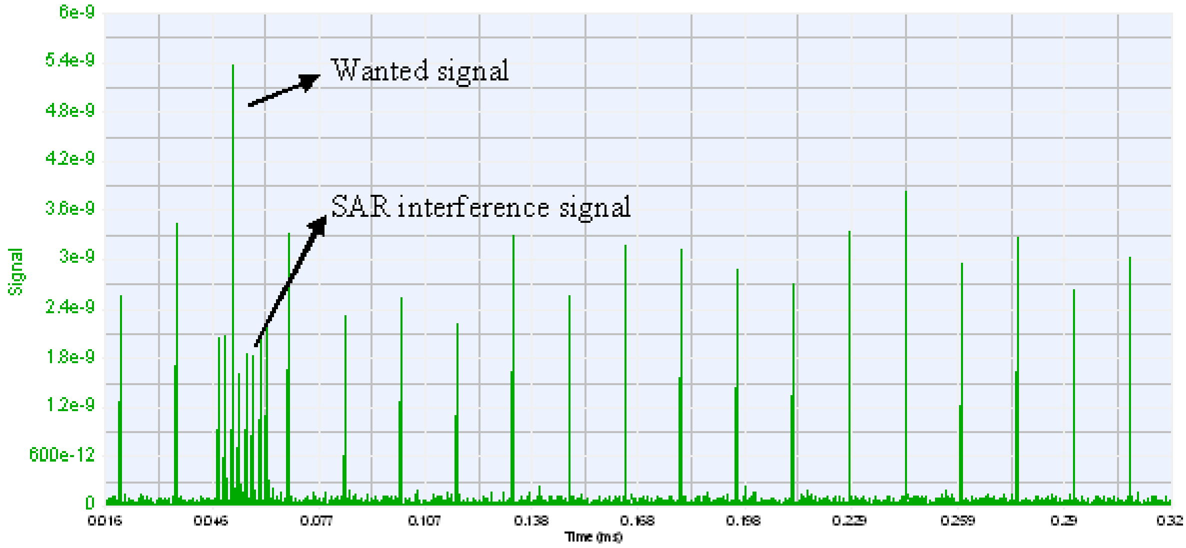

(2) Interference effect under the condition of keeping the same parameters of spaceborne SAR repeat period and bandwidth, with the pulse width adjustable.

The result of interference effect analysis from SAR interference signals under the condition of same repeat period and bandwidth and adjustable pulse width is shown in Table 16 and Fig. 53 (a)-(c).

TABLE 16

Interference effect analysis from SAR interference signals under the condition of same repeat period and bandwidth and adjustable pulse width

Number	Pulse width (µs)	Repeat period (µs)	Bandwidth (MHz)
1	10	100	1200
2	20	100	1200
3	40	100	1200
Simulation result	When repeat period and bandwidth of SAR interference signals remain the same, the amplitude of interference pulse train gradually increases with the increasing pulse width.		
Basic conclusion	When repeat period and bandwidth of SAR interference signals remain the same, the interference amplitude to pulse radar increases with the increasing pulse width, which will raise the average interference power.		

FIGURE 53

Interference effect analysis from SAR interference signals under the condition of same repeat period and bandwidth and adjustable pulse width

(a) Simulation result when pulse width is 10 µs

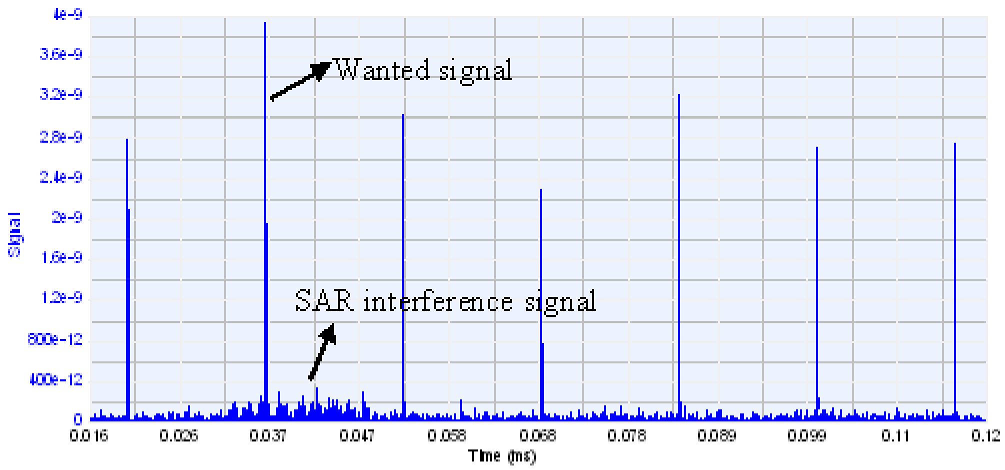

(b) Simulation result when pulse width is 20 µs

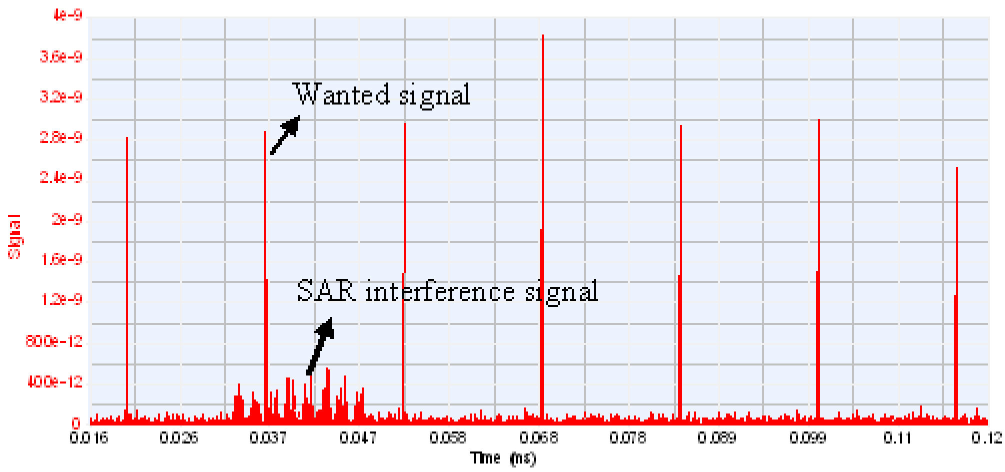

(c) Simulation result when pulse width is 40 µs

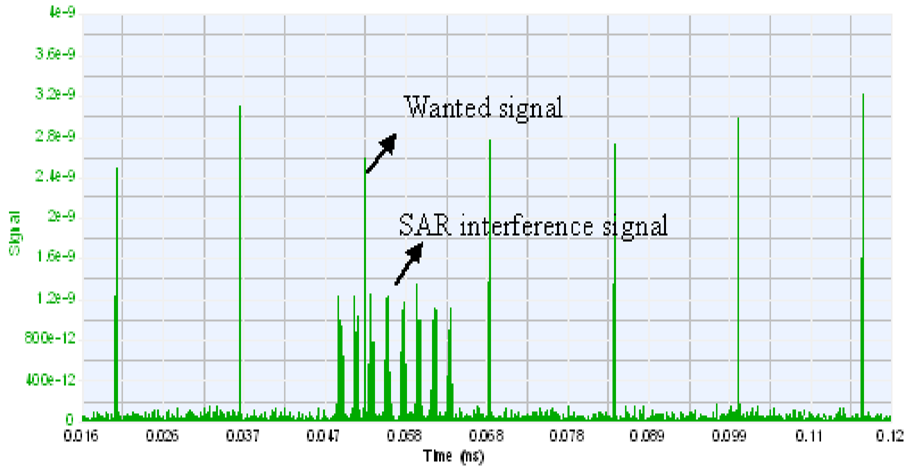

(3) Interference effect under the condition of keeping the same parameters of spaceborne SAR pulse width and repeat period, with the bandwidth adjustable.

The result of interference effect analysis from SAR interference signals under the condition of same pulse width and repeat period and adjustable bandwidth is shown in Table 17 and Fig. 54 (a)-(c).

TABLE 17

Interference effect analysis from SAR interference signals under the condition of same pulse width and repeat period and adjustable bandwidth

Number	Pulse width (µs)	Repeat period (µs)	Bandwidth (MHz)
1	50	200	600
2	50	200	900
3	50	200	1200
Simulation result	When pulse width and repeat period of SAR interference signals remain the same, the suppression of interference signal towards wanted signal becomes weaker with the increasing bandwidth, and the interference reduces.		
Basic conclusion	When pulse width and repeat period of SAR interference signals remain the same, the suppression to wanted signals and interference become weaker with the increase of bandwidth.		

FIGURE 54

Interference effect analysis from SAR interference signals under the condition of same repeat period and bandwidth and adjustable pulse width

(a) Simulation result when bandwidth is 600 MHz

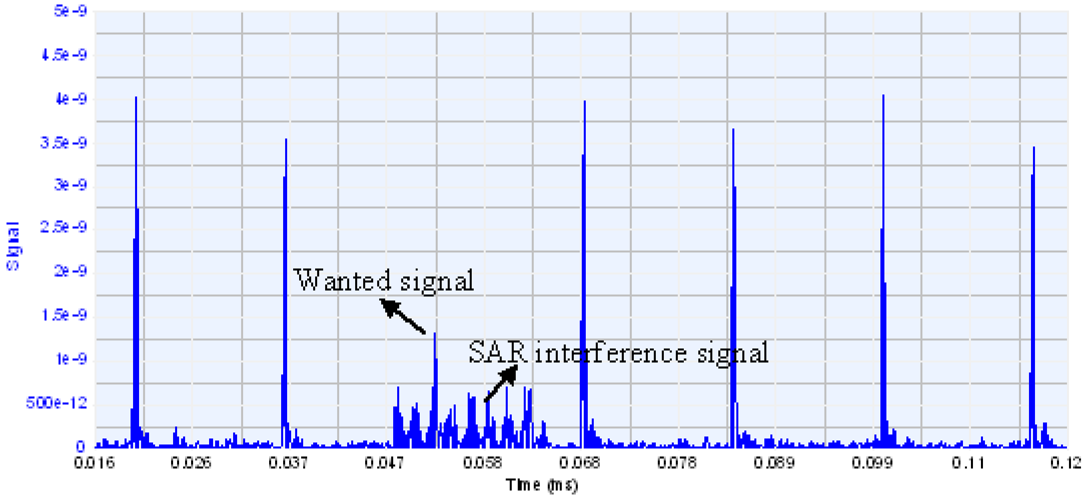

(b) Simulation result when bandwidth is 900 MHz

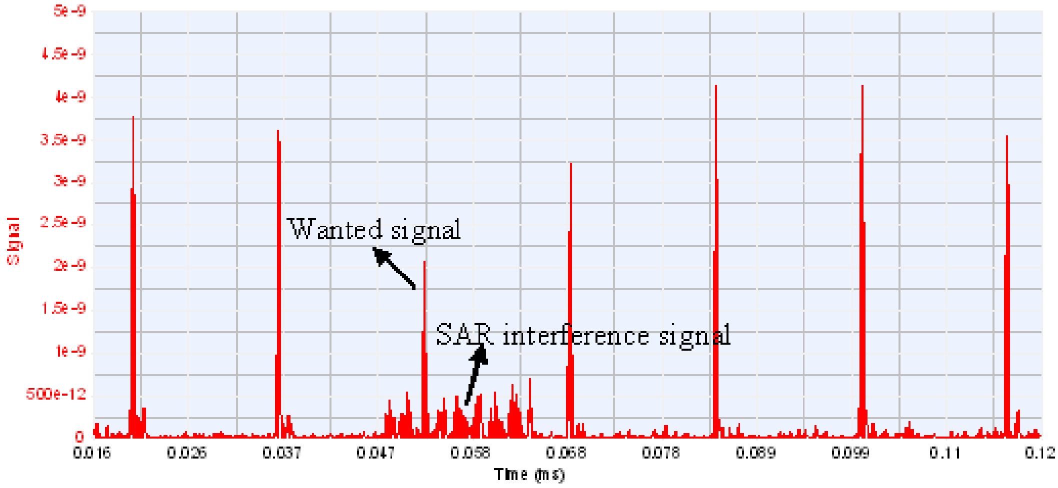

(c) Simulation result when bandwidth is 1 200 MHz

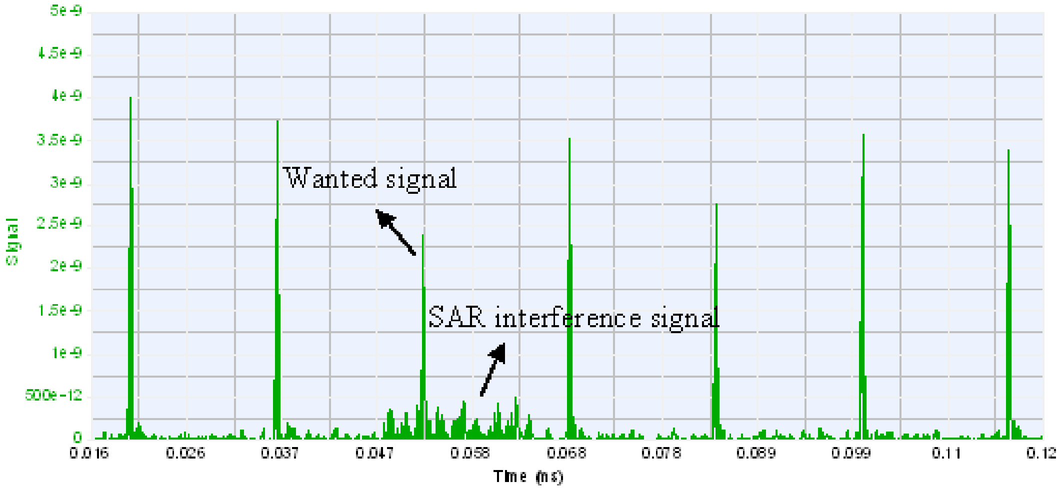

4.2.3.2.3 Interference simulation analyses from spaceborne SAR-4 to pulse radars with adjustable parameters

This section provides the interference simulation results from spaceborne SAR-4 to pulse radars with adjustable parameters pulse width, pulse repetition frequency, bandwidth, and pulse compression ratio. The simulation results display the signal waveforms by signal processing of pulse radars.

(1) Interference effect under the condition of keeping the same parameters of pulse width and bandwidth of pulse radar, with the pulse repetition frequency adjustable.

The result of interference effect analysis from SAR-4 interference signals under the condition of same pulse width and bandwidth and adjustable repeat period of pulse radar is shown in Table 18 and Fig. 55 (a)-(c).

TABLE 18

Interference effect analysis from SAR under the condition of same pulse width and bandwidth and adjustable repeat period of pulse radar

Number	Pulse width (µs)	Repeat period (µs)	Bandwidth (MHz)	Pulse compression ratio
1	1.6	20	37.5	60
2	1.6	40	37.5	60
3	1.6	80	37.5	60
Simulation result	When pulse width and bandwidth of pulse radar with adjustable repeat period remain the same, the amplitude of interference signal from spaceborne SAR-4 signal is basically identical; while the interference of false target appears, the duration of which will become longer with the increasing repeat period of pulse radar.			
Basic conclusion	The length of pulse radar repeat period does little effect to the interference signals, while the duration of interference pulse is in proportion to repeat period of pulse radar.			

FIGURE 55

Interference effect analysis from SAR under the condition of same pulse width and bandwidth and adjustable repeat period of pulse radar

(a) Simulation result when repeat period is 20µs

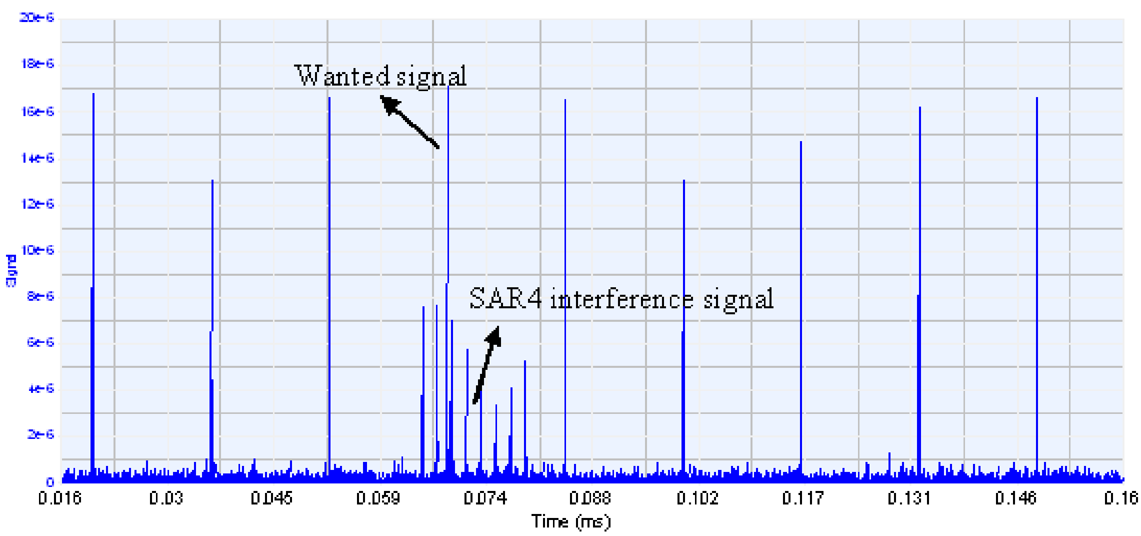

(b) Simulation result when repeat period is 40 µs

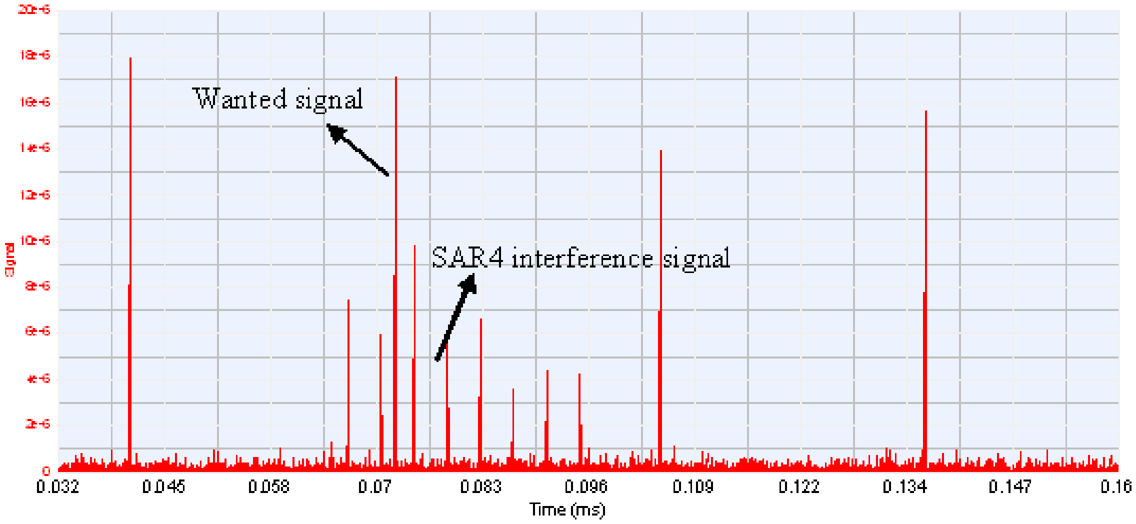

(c) Simulation result when repeat period is 80 µs

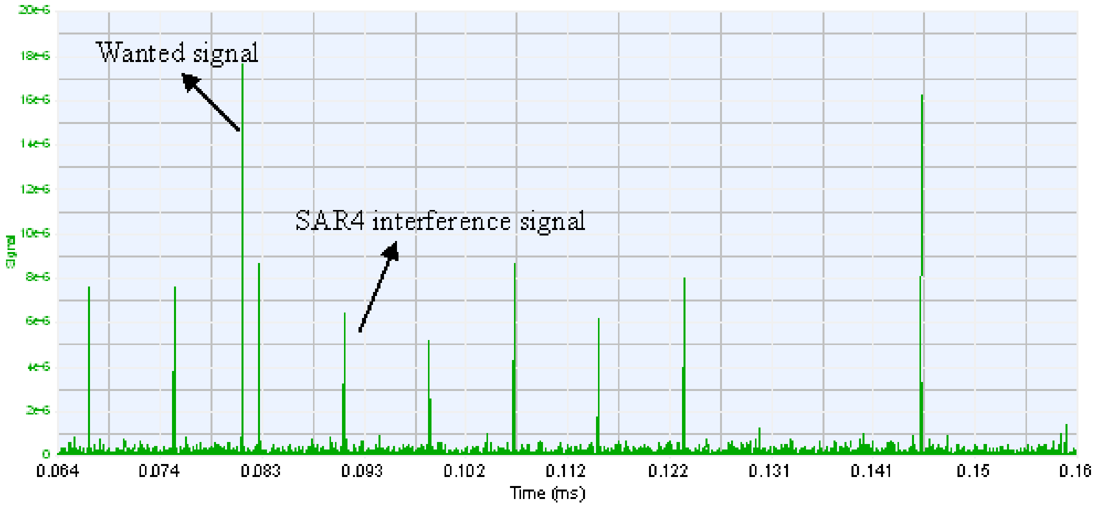

(2) Interference effect under the condition of keeping the same parameters of repeat period and bandwidth of pulse radar, with the pulse width adjustable.

The result of interference effect analysis from SAR-4 interference signals under the condition of same repeat period and bandwidth and adjustable pulse width of pulse radar is shown in Table 19 and Fig. 56 (a)-(c).

TABLE 19

Interference effect analysis from SAR under the condition of same repeat period and bandwidth and adjustable pulse width of pulse radar

Number	Pulse width (µs)	Repeat period (µs)	Bandwidth (MHz)	Pulse compression ratio
1	1.6	8	37.5	60
2	3.2	8	37.5	120
3	6.4	8	37.5	240
Simulation result	The SAR interference signal reduces markedly with the increase of pulse width of pulse radar, for one reason of which is the increase of pulse compression ratio, for another is the greater compression resulted from the increase of pulse width.			
Basic conclusion	When repeat period and bandwidth of pulse radar remain the same, the wider the pulse width is, the weaker the interference becomes.			

FIGURE 56

Interference effect analysis from SAR under the condition of same pulse width and bandwidth and adjustable repeat period of pulse radar

(a) Simulation result when pulse width is 1.6 µs

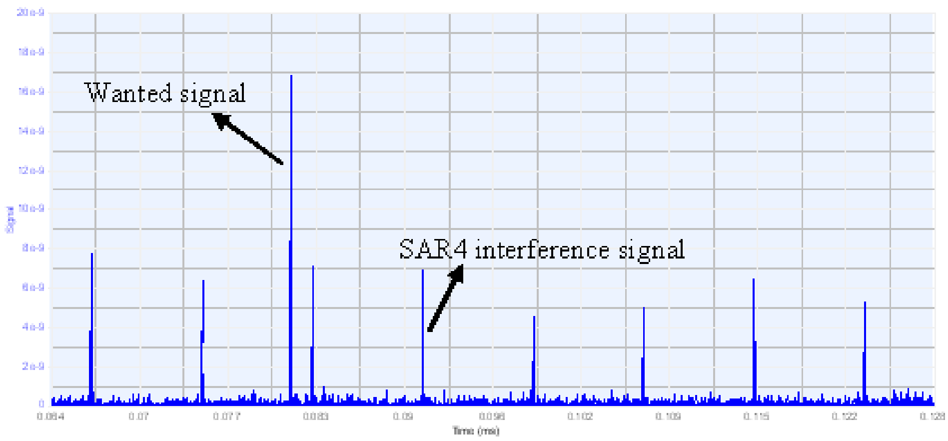

(b) Simulation result when pulse width is 3.2 µs

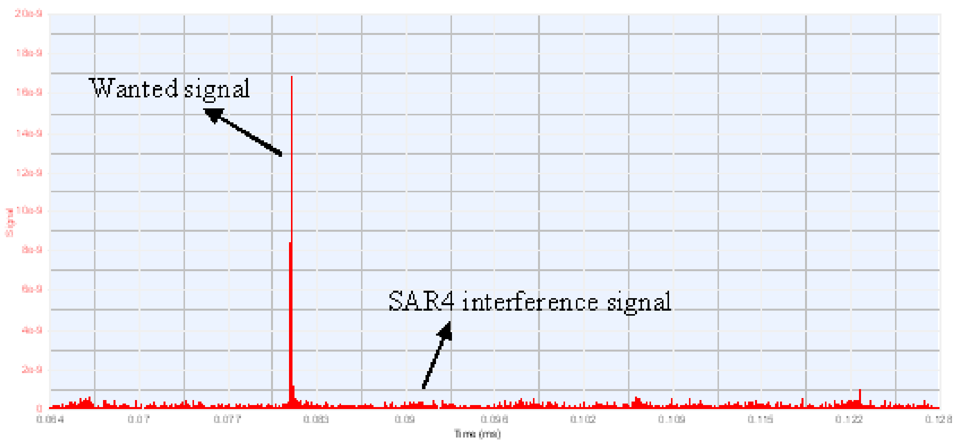

(c) Simulation result when pulse width is 6.4 µs

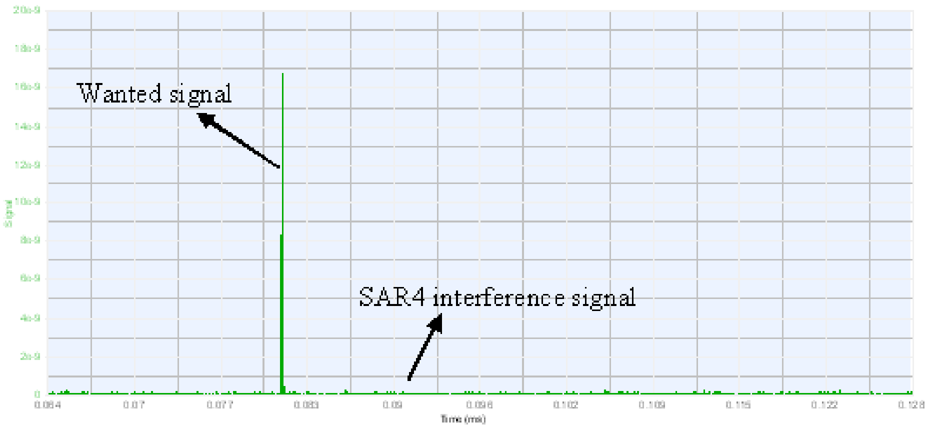

(3) Interference effect under the condition of keeping the same parameters of pulse compression ratio and repeat period of pulse radar, with the pulse width and bandwidth adjustable.

The result of interference effect analysis from SAR-4 interference signals under the condition of same pulse compression ratio and repeat period, and adjustable pulse width and bandwidth of pulse radar is shown in Table 20 and Fig. 57 (a)-(d).

TABLE 20

Interference effect analyses from SAR under the condition of same pulse compression ratio and repeat period, and adjustable pulse width and bandwidth of pulse radar

Number	Pulse width (µs)	Repeat period (µs)	Bandwidth (MHz)	Pulse compression ratio
1	2	16	30	60
2	4	16	15	60
3	8	16	7.5	60
4	12	16	5	60
Simulation result	When pulse compression ratio remains the same, though the amplitude of wanted signals stays identical, interference becomes weaker with the increase of pulse width and the decrease of bandwidth.			
Basic conclusion	When pulse compression ratio and repeat period remain the same, interference rejection capability is rapidly enhanced with the increase of pulse width and the decrease of bandwidth.			

FIGURE 57

Interference effect analyses from SAR under the condition of same pulse compression ratio and repeat period, and adjustable pulse width and bandwidth of pulse radar

(a) Simulation result when pulse width is 2 µs and bandwidth is 30 MHz

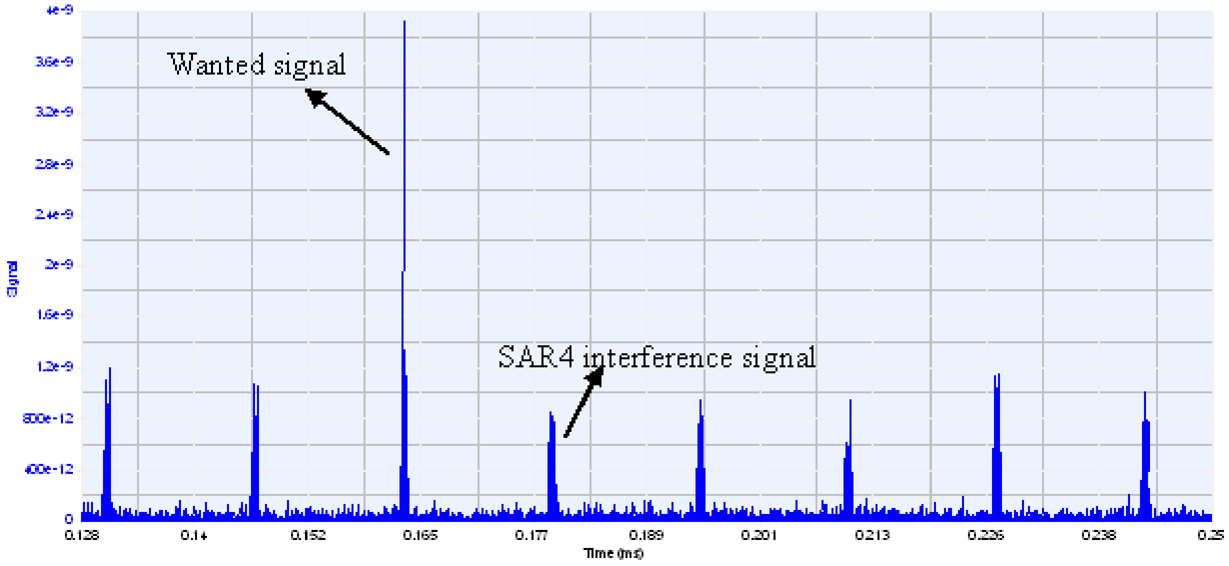

(b) Simulation result when pulse width is 4 µs and bandwidth is 15 MHz

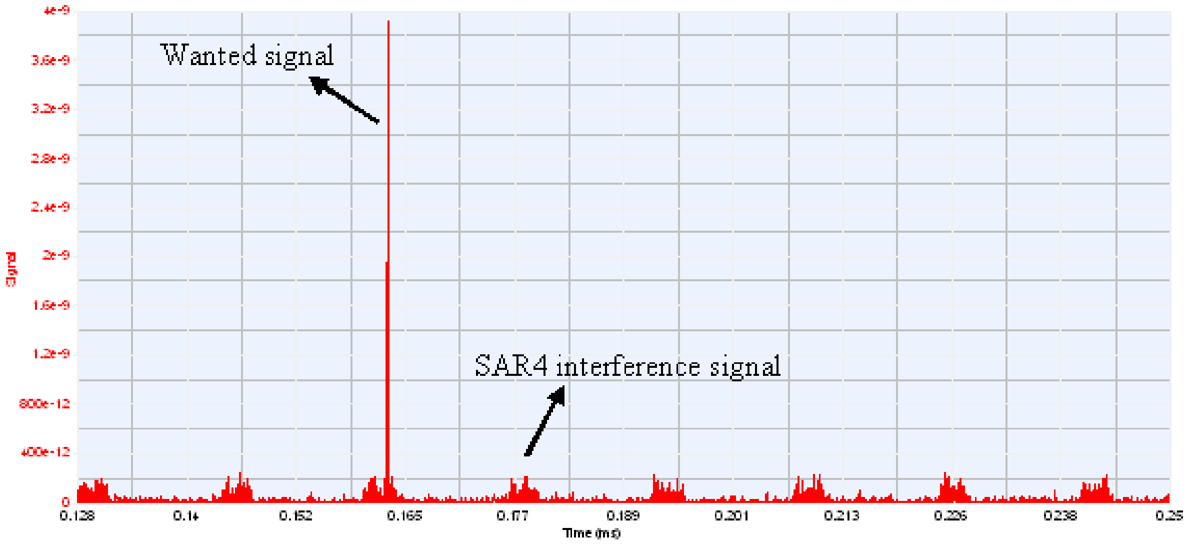

(c) Simulation result when pulse width is 8 µs and bandwidth is 7.5 MHz

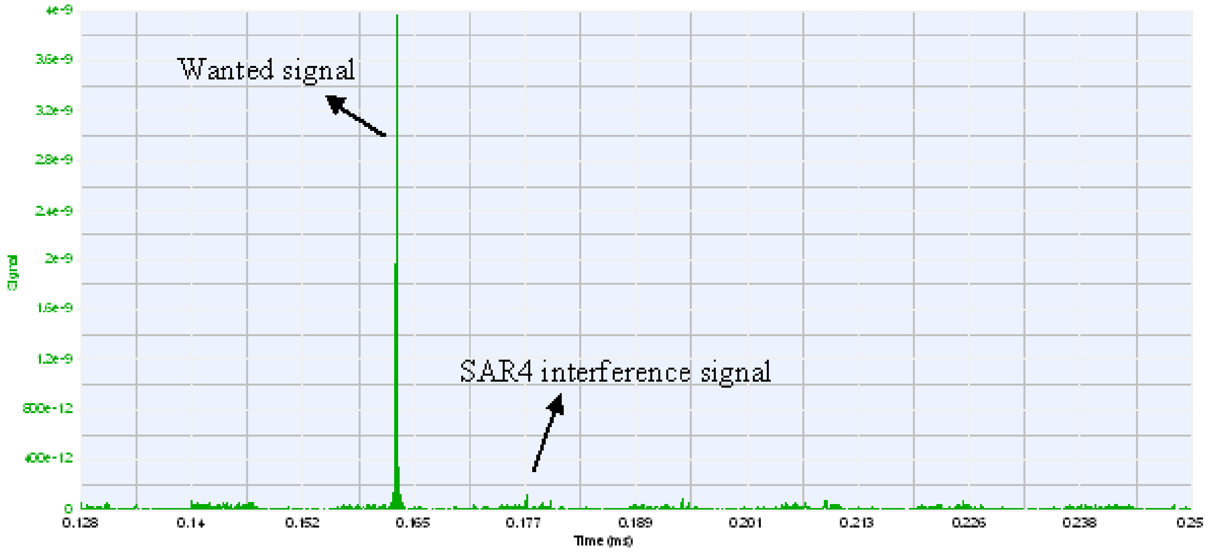

(d) Simulation result when pulse width is 12 µs and bandwidth is 5 MHz

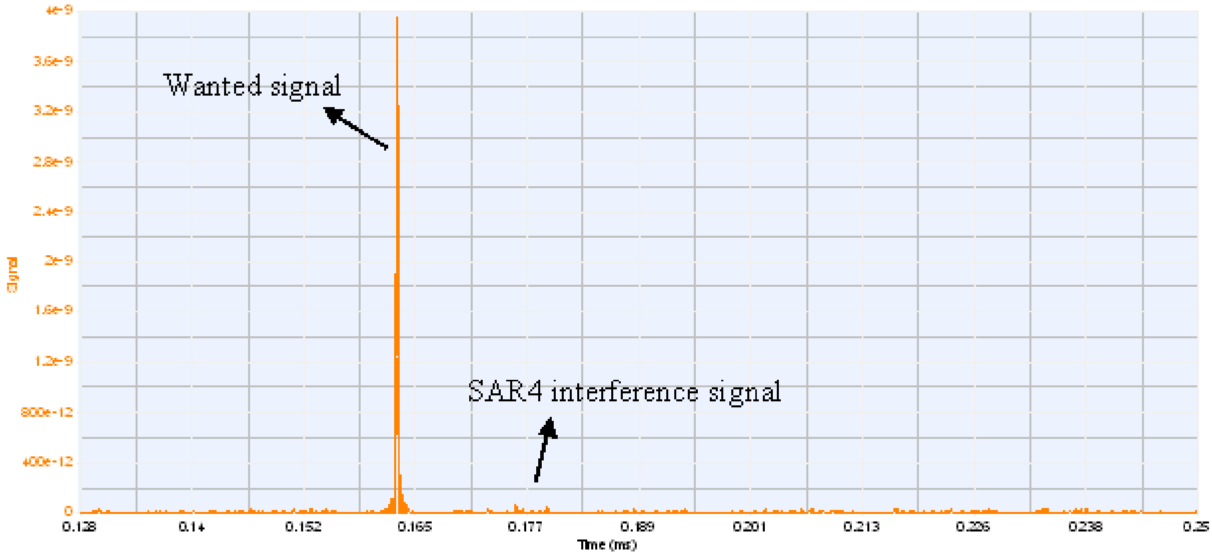

4.2.3.2.4 Protection criteria for pulse radars sharing with spaceborne SAR-4

Surveillance and tracking radars usually take 0.8 as detection probability to determine whether the radars are performing in a normal way.

Based on the simulation parameter setting, the interference criteria or the power ratios of I/N of pulse radars are shown in Fig. 62 and Table 24.

Figure 58 shows curves of radar detection probabilities with I_{av}/N for pulse width of 15 µs and 24 µs; it is the interference criterion listed in Table 20 when detection probability is equal to 0.8. $P_{j\text{-}av}$ and $P_{j\text{-}peak}$ in Table 23 stand for the average power and peak power of SAR interference signals in the front-end of pulse radar receiver, and the difference of which is 5.2 dB (the duty cycle is 30%); N is the internal noise power of radar; I_{peak} is the peak power of interference after the intermediate-frequency filter, the difference of the two parameters is –1.8 dB (viz. OTR value of intermediate-frequency filter in 4 MHz); I_{av} is the average power of equivalent interference of I_{peak}, the difference of the two parameters is –28.2 dB (duty cycle change of pulse width through filter).

FIGURE 58

Simulation results of interference criteria to pulse radars

(a) Simulation result of radar A12

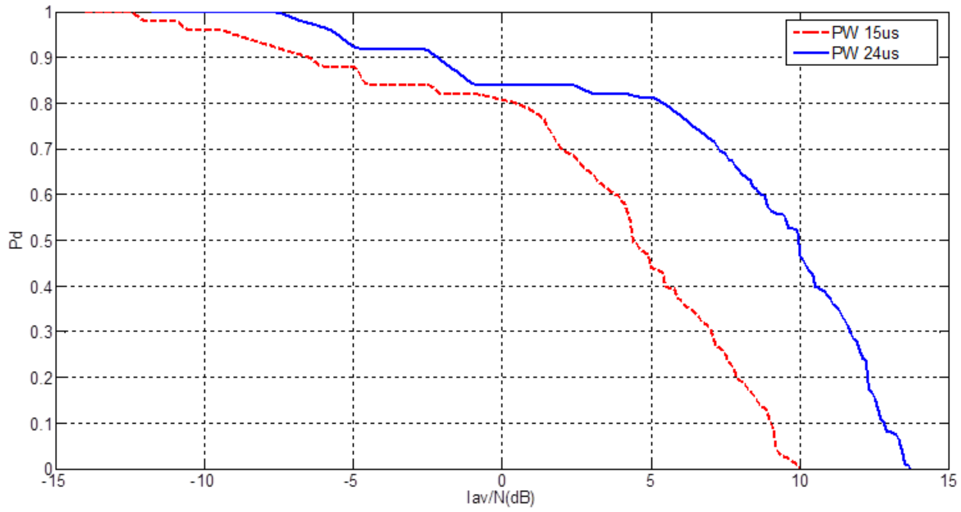

(b) Simulation result of radar G20

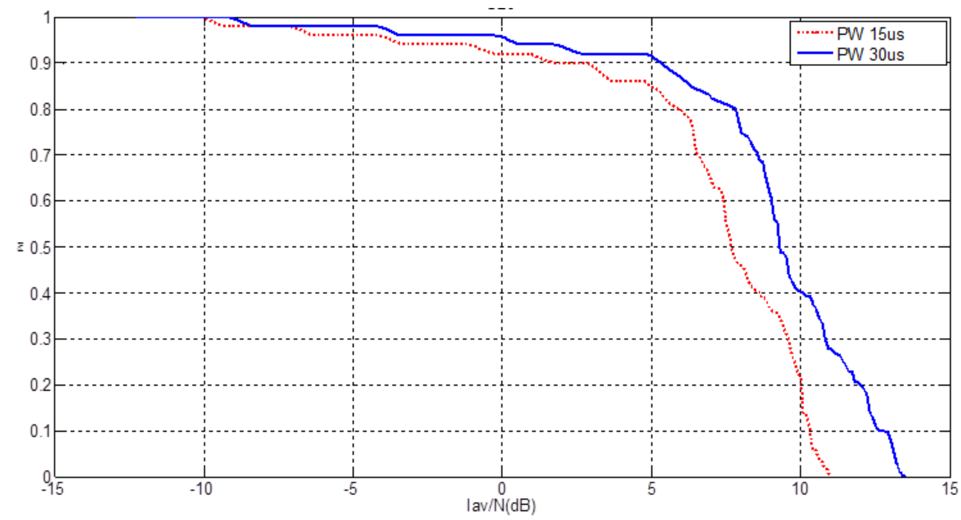

TABLE 21

Simulation calculation results of interference criteria for pulse radars

Type of radar	Pulse width (µs)	Repeat period (µs)	Bandwidth (MHz)	$P_{j\text{-}av}$ (dBm)	$P_{j\text{-}peak}$ (dBm)	N (dBm)	$P_{j\text{-}peak/N}$	$I_{peak/N}$	$I_{av/N}$
A12	15	20	4	–76.7	–71.5	–102	30.5	28.7	0.5
	24	30	4	–72	–66.8		35.2	33.4	5.2
G20	15	50	4	–71.3	–66.1	–102	35.9	34.1	5.9
	30	50	4	–69	–64		37.8	36.0	7.8

4.2.3.2.5 Summary of results of study 2

The analysis of interference simulations from EESS SAR-4 to pulse radars indicates that:

– the interference level keeps basically constant when the repeat period of SAR pulse increasing, while the decreasing appearance times of interference pulse will reduce the average interference power;

– the interference level rises with the increasing pulse width of SAR interference signals, which also raises the average interference power;

– the wanted radar signals decreases when the bandwidth of SAR signal increases, and the interference effect becomes weaker;

– the pulse repetition frequency of radar does not affect the amplitude of received interference signals from SAR, and the duration of interference is in proportion to the pulse repetition frequency of the radar;

– the amplitude of pulse radar received from SAR interference signals decreases with the increase of pulse width of pulse radar, and the interference rejection capability is also enhanced.

Simulations of interference for pulse radars indicate that:

– when the pulse width of radar A12 is 15 μs and 24 μs, the allowable maximum ratio of average interference to noise power is 0.5 dB and 5.2 dB, respectively, and the allowable maximum ratio of peak interference to noise power is 28.7 dB and 33.4 dB, respectively;

– when the pulse width of radar G20 is 15 μs and 30 μs, the allowable maximum ratio of average interference to noise power is 5.9 dB and 7.8 dB respectively, and the allowable maximum ratio of peak interference power to noise power is 34.1 dB and 36 dB, respectively.

It can be seen that pulsed radars with signal processing techniques, such as pulse compression, have a strong capability of interference mitigation.

4.2.4 Sharing studies on the impact of RLS emissions on SAR-4 receiver

4.2.4.1 Scenario

In Fig. 59, the black dots represent the location of 50 G20 radars transmitting in the band 8 700-9 300 MHz. The blue dots represent the area where an image in high resolution mode may be taken by the SAR system. It has been assumed that 500 image areas were randomly positioned and not necessarily co-located with the radars.

FIGURE 59

Deployment of radars and image areas

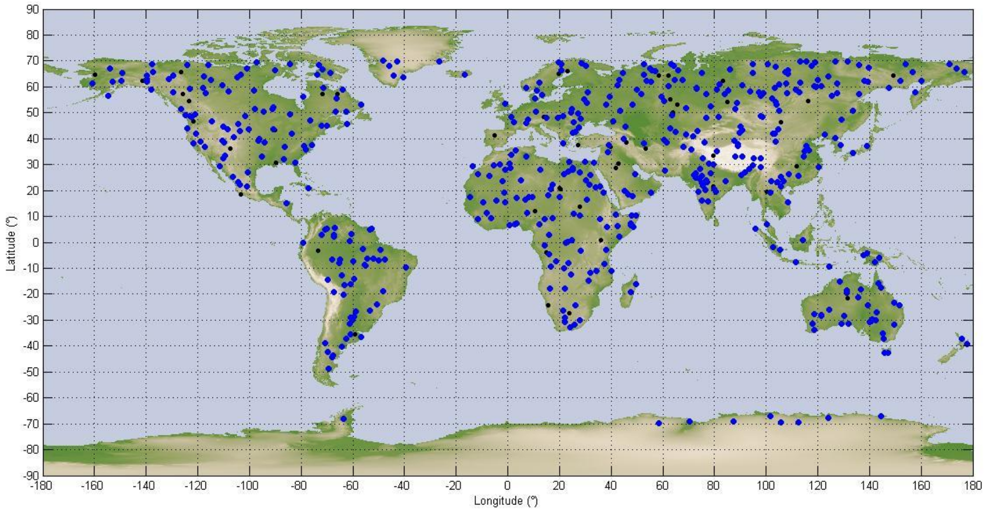

The simulation is run for 11 days with a time step of one second. Each time the satellite is within visibility of one area of interest (blue dot) within the relevant azimuth and incidence angles, this area is illuminated, for a duration which varies between three and seven seconds. The SAR receiver will also be activated only during this portion of time. It is assumed that the rest of the time it is inactive. The aggregate interference from all radars in visibility during the acquisition is calculated and converted in *I*/*N*. The noise value is calculated in 600 MHz.

As explained in § 4.1.4.2, the SAR protection criterion is an *I*/*N* of 26 to 36 dB, not to be exceeded in more than 1% of the time for random or non-systematic interference, which is the case here, but would not be the case for radar A12 which is airborne. It is understood here that the reference time for this 1% allowance is the time when the SAR system is in operation (3% of the total time). When compared to the total simulation duration, the effective percentage of time of interference allowance should be in fact 1% times 3% which is 0.03% of the time.

4.2.4.2 Results

The results obtained for a deployment of 50 G20-radars are given in terms of cdf of the *I*/*N* in Fig. 60.

FIGURE 60

***I*/*N* cdf for 50 radars in the band 8.7-9.3 GHz**

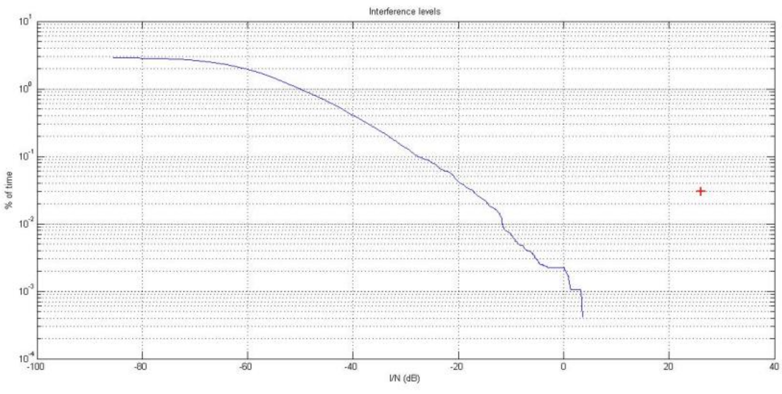

The maximum *I*/*N* is +4 dB and is obtained for 0.0001% of the total time. The *I*/*N* obtained for 1% of the time when the sensor is active is –17.2 dB, more than 40 dB below the protection criterion.

4.3 Sharing with the radiolocation service in the band 10.0-10.5 GHz

4.3.1 Introduction

This section deals with sharing with radars operating in the RLS in the band 10.0-10.5 GHz.

4.3.2 Characteristics of stations operating in the radio location service

The frequency band 9 900-10 500 MHz is used by maritime, terrestrial and aeronautical radars. Typical technical characteristics of these radars are described in Recommendation ITU-R M.1796. Analysis of technical characteristics for the radars reflected in Recommendation ITU-R M.1796 showed that the frequency band 9 900-10 500 MHz is used by terrestrial radars A1, A4, A7 (a, b, c, e, f), S2, S3, G4, and G14.

Table 22 contains technical characteristics of the above mentioned radars except those for radar A1 because required data are not available in Recommendation ITU-R M.1796. It was also assumed that the levels of far side and rear lobes in the radar antenna patterns were 27 dB below the level of the antenna main lobe.

TABLE 22

Technical characteristics of radars A4, G4, G14, and S2

Radar type	A4	G4	G14	S2
Frequency band (GHz)	10.0-10.5	10.0-10.5	10.15-10.65	10.0-10.5
Emission type	CW, FMCW	CW, FMCW	CW	CW, FMCW
Receiver noise figure *N* (dB)	3.6	3.4	3.6	3.5
Receiver 3 dB IF bandwidth (MHz)	0.48	0.52	0.5	0.5
N Receiver inherent noise level (dBW)	–143.5	–143.4	–143.4	–143.5
Max gain (dBi)	35.5	42.2	42.0	43.0
Level of near-side lobes (dBi)	15.5	22.2	22.0	23.0
Average Level of far-side lobes and rear emission (dBi)	–18.92	–12.22	–12.42	–11.42
Antenna pattern azimuthal width, (°)	2.5	1	1.2	1
Antenna pattern elevation width, (°)	2.5	1	2	1
Elevation scan sector, (°)	± 60	Sector: 90+sweep (mechanical)	Unspecified	Sector: +83/–30 (mechanical)
Azimuthal scan sector, (°)	± 60	360	unspecified	360
Average antenna pattern used	COS (Rec. ITU-R M.1851)	COS (Rec. ITU-R M.1851)	COS (Rec. ITU-R M.1851)	COS (Rec. ITU-R M.1851)

The following Figure presents the radar S2 average antenna pattern using Recommendation ITU-R M.1851, Table 5, equation (14).

FIGURE 61

Radar S2 antenna pattern

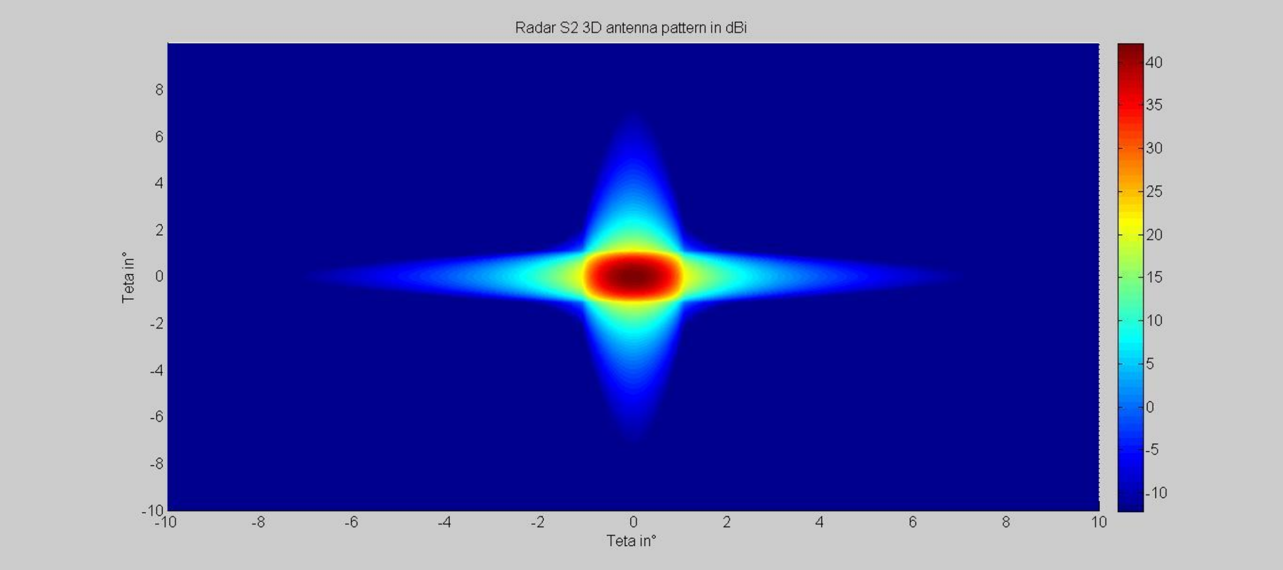

Protection criteria vs. pulsed interference for the above mentioned radars are unavailable in Recommendation ITU-R M.1796-1. Therefore the general protection criteria I/N = –6 dB given in Recommendation ITU-R M.1461 is proposed to use for evaluation of the interference impact.

However, the effect of pulsed interference on incumbent systems is difficult to quantify and the interference level I is strongly dependent on receiver-processor design and mode of system operation. In general, numerous radar features can help suppress low effective duty-cycle pulsed interference. Techniques for mitigation of low-duty-cycle pulsed interference are described in Recommendation ITU-R M.1372. Since the protection criteria specified in Recommendation ITU-R M.1461 does not take into account the pulse interference effect from EESS SAR-4, the effective e.i.r.p. value ($e.i.r.p._{eff}$) defined with account of duty cycle is proposed to use

$$e.i.r.p._{eff} = e.i.r.p.(C) + 10\lg(Q/100)$$

where:

e.i.r.p. I: SAR-4 transmitter e.i.r.p. towards the radio determination radar antenna (dBW)

Q: duty cycle (%).

All three systems identified in Recommendation ITU-R M.1796 in the band 10.0-10.5 GHz are tracking radars, either airborne, ship borne, or land based. They use either CW or FMCW waveforms, with an IF bandwidth around 500 kHz.

A purely CW waveform does not allow for a determination of the distance, whereas a FMCW waveform permits it. The basic principle of either a CW or FMCW radar relies on a bank of Doppler filters with a relatively small bandwidth which allows for a determination of the Doppler of the target which is being tracked. This bank of filters is done through an FFT that will smear the SAR signal on all frequencies.

As indicated by Fig. 62, the CW radar receiver declares detection at the output of a particular Doppler bin if that output value passes the detection threshold within the detector box. Since the narrow band filter (NBF) bank is implemented by an FFT, only finite length data sets can be processed at a time. The length of such blocks is normally referred to as the dwell time or dwell interval. The dwell interval determines the frequency resolution or the bandwidth of the individual NBFs.

Assuming a 1 kHz bandwidth for each individual Doppler filter and a 0.5 MHz bandwidth for the IF filter then $N_{FFT} = 2B/\Delta f = 1024$ points FFT (the factor 2 is needed to account for both positive and negative Doppler shifts) and a 1 ms dwell time.

This would contain six EESS SAR-4 pulses and the average *I*/*N* value should therefore be considered instead of the peak *I*/*N*.

FIGURE 62

Basic diagram of CW radar

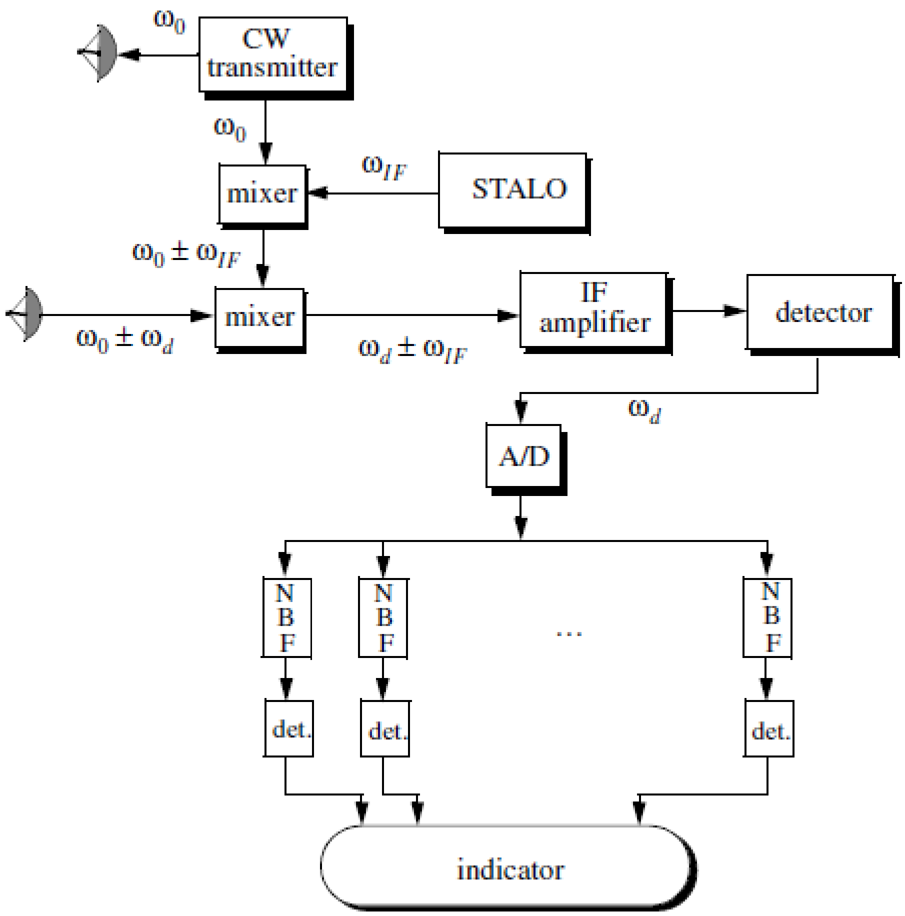

4.3.3 Sharing studies on the impact of EESS SAR-4 emissions on RLS receivers

Four sharing studies were performed.

Study 1 – Approach A: worst case analysis

This study computes the worst case effect on radar for the worst case configuration (when RLS receiver has the maximum possible gain towards the EESS SAR satellite and is located at measuring point and the victim radars are located in along track plain). That is why complex average pattern along track for EESS SAR-4 specified in Recommendation ITU-R RS.2043 (red curve in Fig. 11,) was used in *I*/*N* estimations. The effect of EESS SAR satellite movement over 11 days (typical repetition period of the EESS SAR-4 satellite orbit) is not taken into account in this study.

Study 1 – Approach B: Probability and average time that *I*/*N* of −6dB is exceeded

This study is the same as Study 1 but in addition is computing the probability that *I*/*N* of –6dB is exceeded and the average time during which the exceedance of –6dB might occur. This study takes into account radar receiver location anywhere in the possible measurement zone in the EESS SAR-4 visibility area. The EESS SAR-4 satellite repetition period over 11 days is also not taken into account in this study.

Study 2: Dynamic analysis

This study simulates the movement of the EESS SAR-4 satellite over 11 days and provides associated statistics (cumulative probability distribution function) on the average *I*/*N* level as received by the RLS receiver.

Study 3: Impact on EESS SAR-4 pulsed interference into FMCW radars

This study addresses the sharing performance simulation analyses between the EESS SAR and RLS radars in the band 9 900-10 500 MHz based on the spectrum characteristic modeling method.

4.3.3.1 Worst case static analysis (Study 1)

This section discusses effect from SAR-4 on operation of shipboard, ground-based and air-borne radars for the scenario given in Fig. 63.

FIGURE 63

Scenario of SAR-4 effect on terrestrial radar

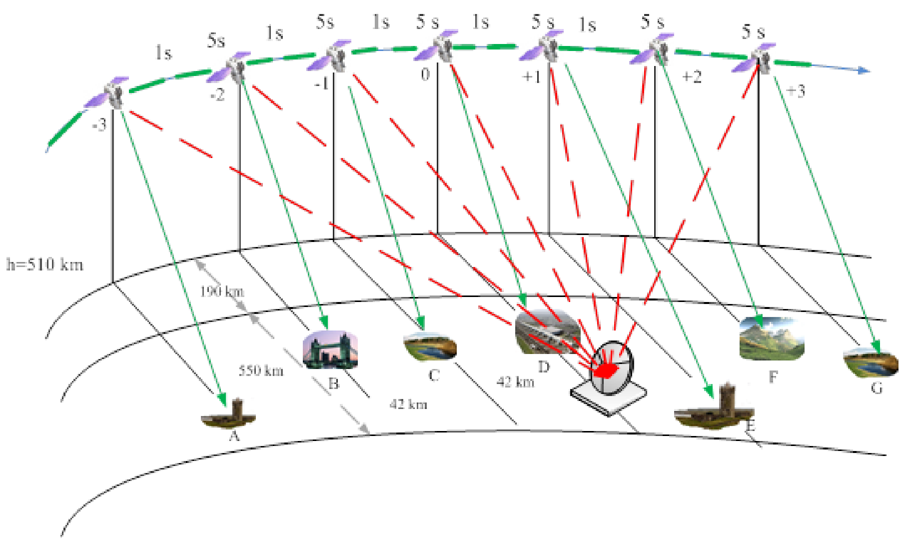

This scenario assumes that SAR-4 is moving on a circle orbit at the altitude of around 510 km. The motion path of SAR-4 is shown by a blue curve in Fig. 53. The orbit projection to the Earth’s surface is shown by a black curve. Here the potential area of measurements limited by the distance of 190 km and 740 km from the SAR-4 orbit projection to the Earth’s surface is also shown.

During the flight SAR-4 makes measurements in the corresponding points A, B, C, D, E, F and G in the orbit areas –3,–2, –1, 0, +1, +2, +3 (highlighted by green color in Fig. 66). With this the time period of going through each area (time period of each measurement) is 5 s. At the 1 s intervals between these areas the measurements are not made and time period of going through these distances and the time period between the measurements is 10 s. The EESS SAR-4 velocity along the orbit is 7.63 km/s. The velocity of the corresponding sub-satellite point is 7.06 km/s. Due to

EESS SAR-4 orbit parameters the interval between repeated measurements in any point can be 11 days.

In the vicinity of point D the radiodetermination radar which experiences interference from EESS SAR-4 emissions is located. The interference impact lines are shown by red dotted lines in Fig. 66. In each of the seven considered cases the main beam of radar antenna pattern is directed to the SAR-4 sub-satellite point. As the case may be, interference caused by EESS SAR-4 can fall into the radar receiver input on the main lobe or side/back lobe of the antenna pattern.

For the evaluation of interference impact for each of the possible locations of EESS SAR-4 the following values were calculated:

– maximum and minimum interference arrival angles (α_{max} and α_{min}) which correspond to the closest and widest boundary of the measurement area;
– maximum and minimum distance between the radar receiver and SAR-4 (L_{max} and L_{min});
– maximum and minimum propagation losses.

The indicated parameters are shown in Fig. 64. The evaluation of the indicated values while conducting measurements at point D is given in Table 23.

FIGURE 64

Mutual location of radar and SAR

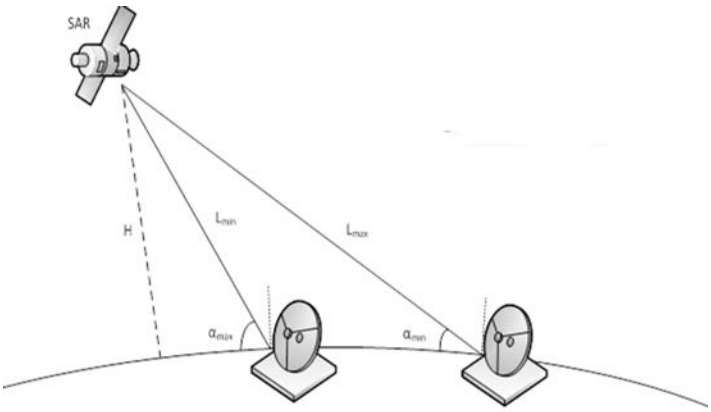

TABLE 23

Results of calculations

Maximum angle of arrival (°)	70
Minimum distance (km)	540
Minimum interference propagation loss (dB)	167
Minimum angle of arrival (°)	35
Maximum distance (km)	830
Maximum interference propagation loss (dB)	171

Estimation of the minimum and maximum interference arrival angles were carried out for other orbit areas of EESS SAR-4. The calculation results are given below in Table 24.

TABLE 24

Minimum and maximum interference arrival angles for different orbit parts

Orbit area	−3	−2	−1	0	+1	+2	+3
α_{min} (°)	34.1	34.4	34.5	35	34.5	34.4	34.1
α_{max} (°)	68.5	67.8	69	70	69	67.8	65.5

Estimation of *I*/*N* took into consideration relative location of terrestrial radar antenna and position of EESS SAR-4 as well as probable interference falling into the terrestrial radar antenna main lobe. Such probability resulted from EESS SAR-4 scan sector (minimum and maximum angle of interference arrival) as well as the terrestrial radar antenna vertical (elevation) scan sector.

Counter alignment of the antenna main lobes would be impossible for a case when the angle of interference arrival α_{min} exceeds vertical scan sector of the terrestrial radar antenna. For that case it was assumed that SAR-4 interference affected radar far-side or rear lobes.

In calculations of interference from SAR-4 to operation of the radiolocation systems the pulse emissions of SAR-4 system is proposed to take into account by using the effective e.i.r.p. value ($e.i.r.p._{eff}$):

The value of interference-to-noise ratio was estimated using the following equation:

$$I/N = e.i.r.p._{eff} + G_{rec\,rls} + 20\,lg(\lambda/4\pi R) - 10\,lg(kT_N \Delta F) - PG$$

where:

- $e.i.r.p._{eff}$: effective e.i.r.p. of SAR-4 transmitter with consideration of duty cycle (dBW)
- $G_{rec\,rls}$: gain of radar receiver antenna affected by SAR-4 interference (dBi)
- λ: operational wavelength (m)
- R: distance between SAR-4 transmitter and radar receiver (m)
- k: Boltzmann constant (dBW/K Hz)
- T_N: radar receiver noise temperature (K)
- ΔF: radar receiver bandwidth (Hz)
- PG: processing gain (dB), rejection of unwanted signals due to radar receiver signal processing.

Calculations on the basis of assumptions shown in Table 28 estimated of spatial counter alignment probability for pointing the main lobes of the EESS SAR-4 transmitter antenna and that of the victim radar receiver. The analysis results were used in estimating *I*/*N* of the radar receiver.

4.3.3.1.1 Study 1 Approach A

To evaluate the interference effect to operation of these radars the calculations were carried out for the minimum (α_{min}) and maximum (α_{max}) interference arrival angles which correspond to the remote and closest boundary of measurement area.

Estimates of maximum effective *I*/*N* at the receiver front end of the radars concerned for maximum interference arrival angle are shown in Table 25. Estimates of maximum effective *I*/*N* for minimum interference arrival angle are shown in Table 26. In both cases, the radar antenna main beam is pointing towards EESS SAR-4. The characteristics of radars A7 and S3 are located in Recommendation ITU-R M.1796.

The noise performance of the receiver is defined as:

$$P = kT_0(10^{\frac{NF(dB)}{10}} - 1) \cdot \Delta F$$

TABLE 25

Estimates of maximum effective *I/N* for maximum interference arrival angle in relation to radiodetermination radars operating in the frequency band 9 900-10 500 MHz

Radar	A4	A7(1)	G4	G14	S2	S3(1)
Operation frequency range (GHz)	10.0-10.5	9.38-10.12	10.0-10.5	10.15-10.65	10.0-10.5	8.5-10.0
I/N_{eff} (0) (dB)	60.7	27.4	68	37.4	68.6	27.1
I/N_{eff} (−1 & +1) (dB)	28.7	–4.6	36	5.4	36.6	–4.9
I/N_{eff} (−2 & +2) (dB)	24.6	–8.7	31.9	1.3	32.5	-9
I/N_{eff} (−3 & +3) (dB)	21.4	–11.8	28.7	–1.8	29.4	–12.1
I/N_{eff} (−58 & +58) (dB)	–3.2	–6.5	4.1	–25.8	4.7	–6.8

(1) It should be noted that radars A7 and S3 operate in the frequency band 9.3-9.9 GHz which is already allocated to the EESS (active)

TABLE 26

Estimates of maximum effective *I/N* for minimum interference arrival angle in relation to radiodetermination radars operating in the frequency band 9 900-10 500 MHz

Radar	A4	A7(1)	G4	G14	S2	S3(1)
Operation frequency range, GHz	10.0-10.5	9.38-10.12	10.0-10.5	10.15-10.65	10.0-10.5	8.5-10.0
I/N_{eff} (0)	56.3	23.3	63.6	33.1	64.3	22.8
I/N_{eff} (−1 & +1)	41.3	8.3	48.6	18.1	49.3	7.8
I/N_{eff} (−2 & +2)	23.3	–9.7	30.6	0.0	31.2	–10.3
I/N_{eff} (−3 & +3)	21.2	–11.8	28.5	–2	29.2	–12.3
I/N_{eff} (−58 & +58)	–2.5	–5.4	4.8	–26.5	5.4	–6.1

(2) It should be noted that radars A7 and S3 operate in the frequency band 9.3-9.9 GHz which is already allocated to the EESS (active)

Analysis of the obtained results as depicted in Tables 25 and 26 shows that all considered radiodetermination radars would be affected with interference which level significantly exceeds in the worst case of radar location and when the radar is pointing toward EESS SAR with the maximum possible gain the specified *I*/*N* threshold value of *I*/*N* = –6 dB when EESS SAR-4 conducts measurements in point D (flight in orbit area **0** when distance between SAR-4 and the radars would be minimal. Probable excess would be between 29.3 dB and 74.6 dB.

When EESS SAR-4 conducts measurements in points C and E (orbit areas –1 & +1), the *I*/*N* threshold value would be exceeded in the worst case of radar location and when the radar is pointing toward EESS SAR-4 with the maximum possible gain for all types of radars under consideration. Potential excess of the specified protection criterion could be from 1.4 dB to 54.6 dB.

When EESS SAR-4 conducts measurements in points B and F (orbit areas –2 & +2), the *I*/*N* threshold value would be significantly exceeded in the worst case of radar location and, when the radar is pointing toward EESS SAR-4 with the maximum possible gain for radars A4, G4, G14 and S2. Potential excess of the specified protection criterion could be from 6.0 dB to 38.5 dB.

When EESS SAR-4 conducts measurements in points A and G (Orbit areas –3 & +3) the *I*/*N* threshold level might be significantly exceeded in the worst case of radar location and when the radar is pointing toward EESS SAR with the maximum possible gain for radars A4, G4 and S2 but for radar G14 the excess was minor.

The interference may exceed an *I*/*N* of –6 dB at any time between the appearance and disappearance of the satellite when flying over a radar site and when the main beam of radar is pointing to EESS SAR-4.

The results of the studies also show the possibility of occurrence of *I*/*N* values exceeding –6 dB by more than 65 dB at the radar receiver front end which may result in substantial degradation of radar performance during a short period of time (seconds).

4.3.3.1.2 Study 1 – Approach B

The diagrams in Fig. 65 provide the maximum average *I*/*N* level produced by EESS SAR-4 at the radar A4 receiver input (while radar A4 is pointing towards EESS SAR-4) assuming a processing gain, P_G, of 0 dB for elevation angles of 70° and 35°, respectively.

FIGURE 65

Maximum average *I*/*N* for an elevation angle 70° and 35° for radar A4

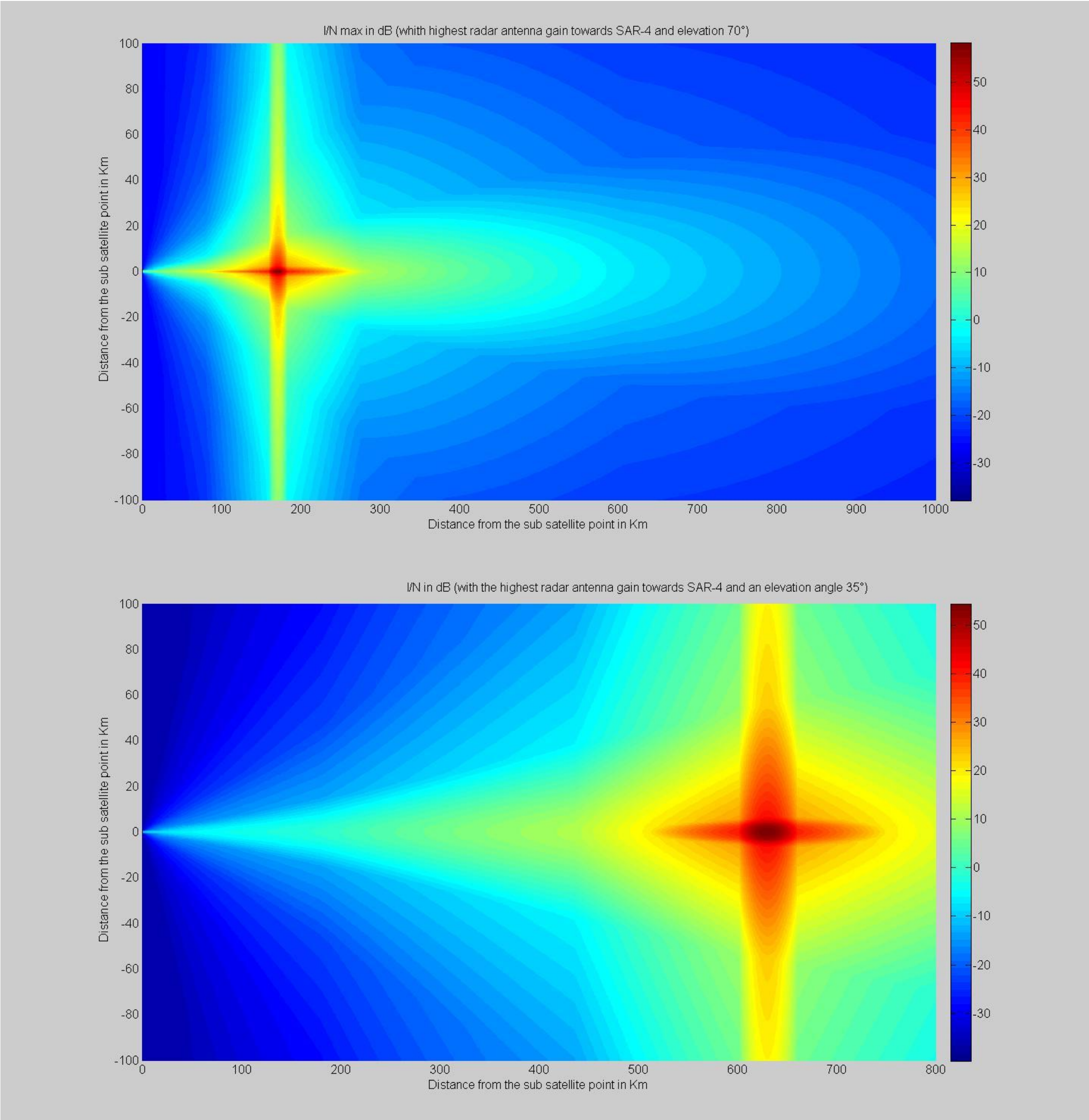

The diagrams in Fig. 66 provide the maximum average *I*/*N* level produced by EESS SAR-4 at the radar G4 receiver input (radar G4 pointing towards EESS SAR-4) assuming a processing gain, P_G, of 0 dB for an elevation angle of 70° and 35°, respectively.

FIGURE 66

Maximum average *I*/*N* for an elevation angle 70° and 35° for radar G4

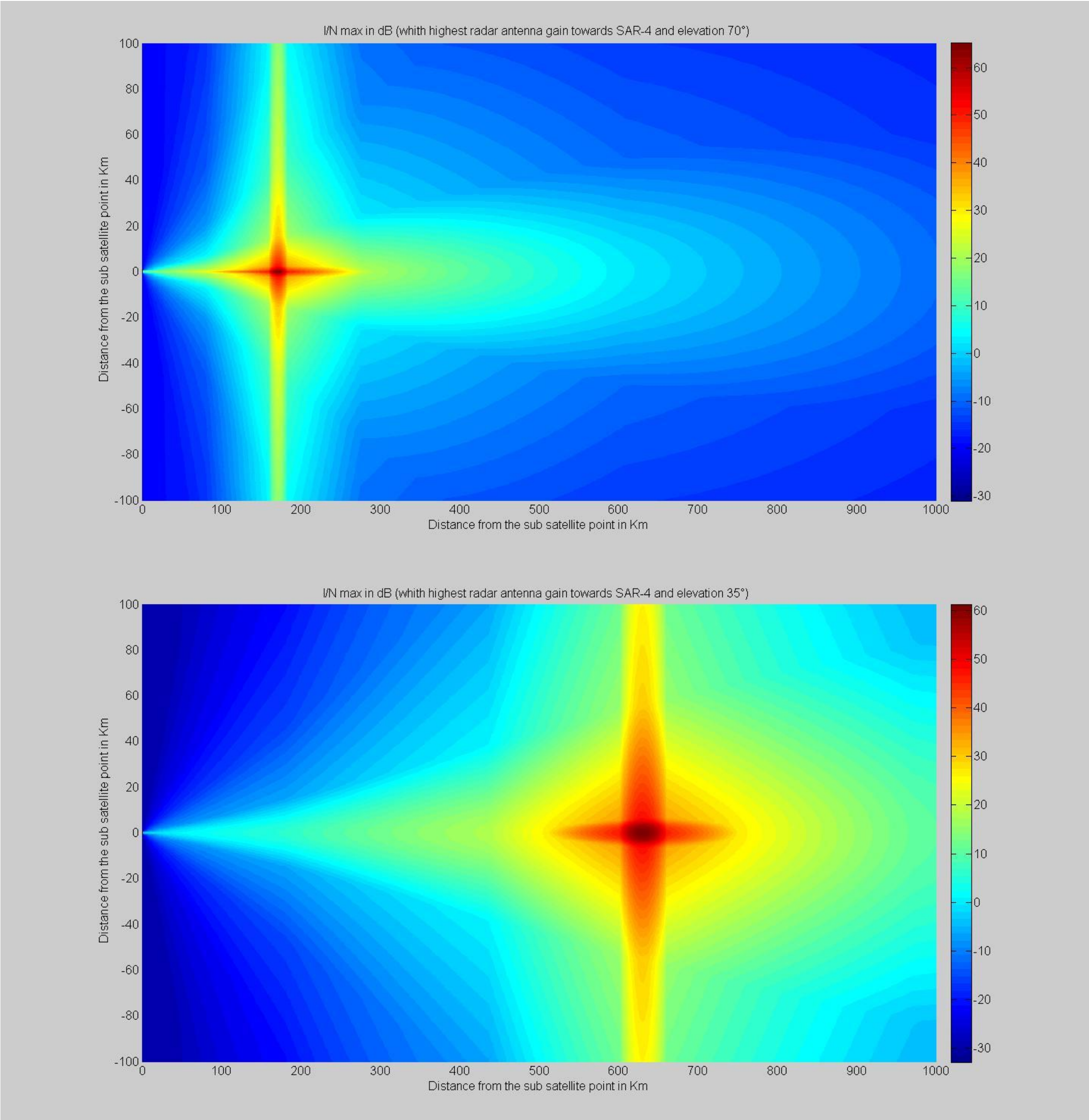

Figure 67 provides at two different beam positions the maximum average *I/N* level produced by EESS SAR-4 at the radar S2 receiver input (while radar S2 is pointing towards EESS SAR-4) assuming a processing gain, P_G, of 0 dB for elevation angles of 70° and 35°, respectively.

FIGURE 67

Maximum average *I*/*N* for an elevation angle 70° and 35° for radar S2

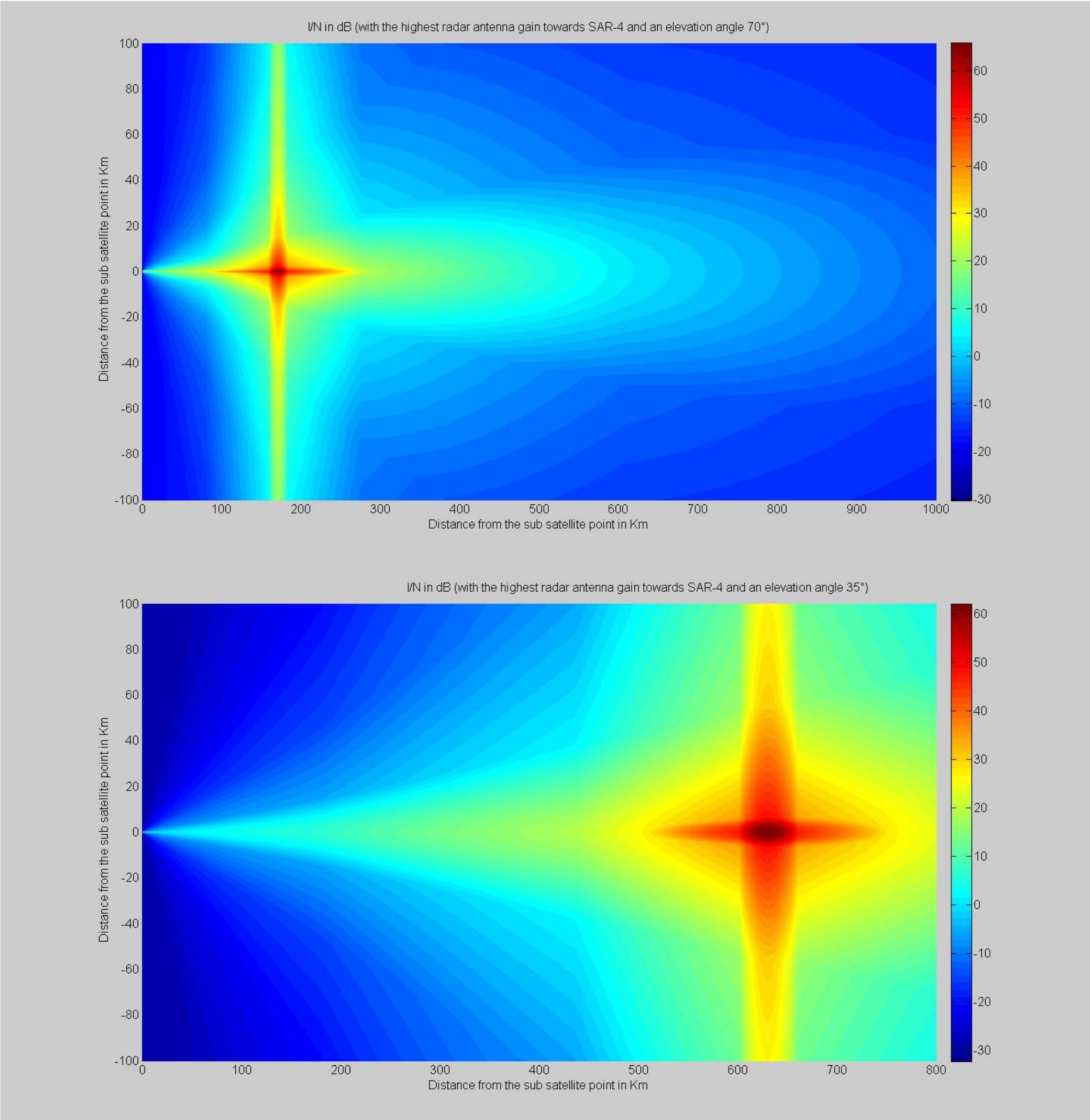

Using the values shown in the above Figures, the calculation results for maximum and minimum I/N ratio with a P_G of 0 dB are summarized in Tables 27 and 28 below.

TABLE 27

Estimation of I/N for terrestrial radars

(radar main beam pointing towards SAR satellite)

Radar	**Elevation (worst case)**	**A4**	**G4**	**S2**
Frequency band (GHz)		**10.0-10.5**	**10.0-10.5**	**10.0-10.5**
$I/N_{eff\ max}$ (0) (dB)	70°	58.2	65.1	65.8
$I/N_{eff\ max}$ (−1 & +1) (dB)	35°	26.8	33.7	34.4
$I/N_{eff\ max}$ (−2 & +2) (dB)	35°	19.9	26.8	27.5

TABLE 28

Estimation of minimum I/N for radiodetermination radars

(radar far side lobe pointing toward SAR satellite)

Radar	**A4**	**G4**	**S2**
Frequency band (GHz)	**10.0-10.5**	**10.0-10.5**	**10.0-10.5**
$I/N_{eff\ min}$ (0)	3.9	10.8	11.48
$I/N_{eff\ min}$ (−1 & +1)	–27.5	–20.6	–19.12
$I/N_{eff\ min}$ (−2 & +2)	–34.8	–27.5	–26.82

Probability of $I/N_{eff} \geq -6$dB

The probability of having an $I/N \geq -6$dB during the 5 s exposure time is computed using the following formula:

$$P_{\%} = \frac{2\pi(1-\cos\theta)}{2\pi} \times 100$$

where:

θ:	minimum radar off-axis angle needed for having I/N<–6dB
$2\pi(\cos\theta)$:	solid angle corresponding to I/N<=–6dB
$2\pi(1-\cos\theta)$:	solid angle corresponding to I/N >=–6dB
$2\pi = 2\pi(\cos\theta) + 2\pi(1-\cos\theta)$:	hemisphere solid angle

To compute the probability of having $I/N_{eff} \geq -6$dB the following steps are performed and are illustrated for the case of radar S2:

Step 1: Computation of the attenuation (dB) required to obtain an I/N_{eff} of –6 dB

FIGURE 68

Attenuation needed to meet an I/N_{eff} of −6 dB (Radar S2)

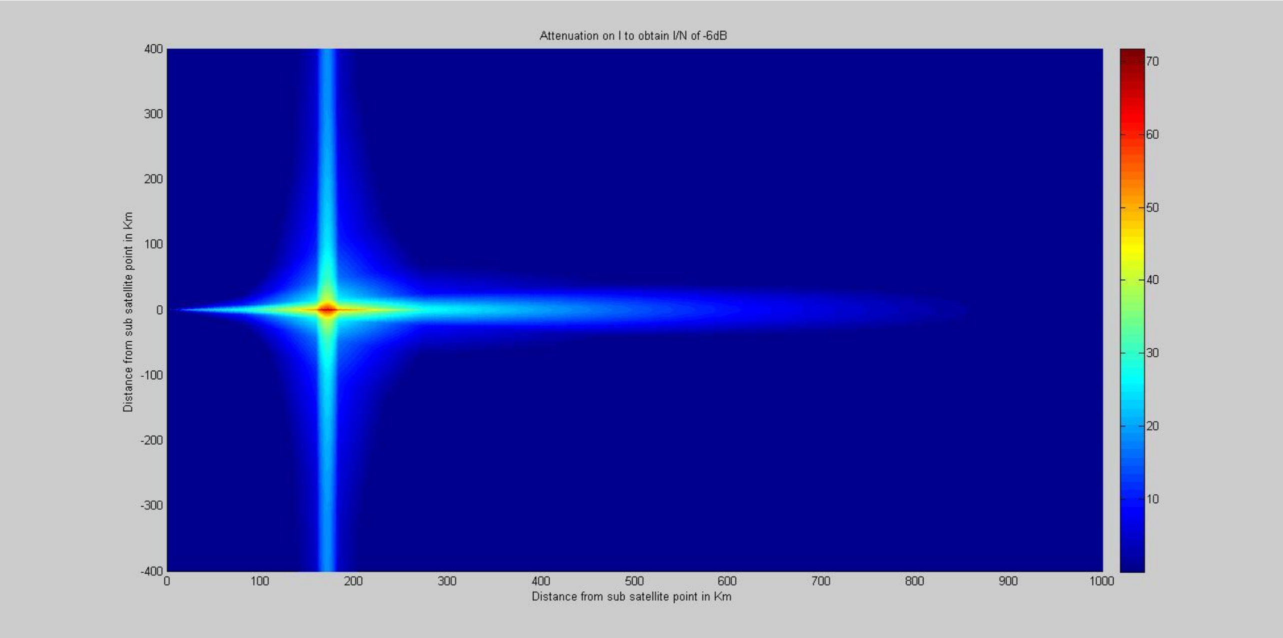

Step 2: Minimum radar S2 antenna off axis angle θ corresponding to Gr_{max}-Gr (θ) ≥ attenuation from step 1

The radar S2 antenna gain corresponding to an off axis angle higher or equal to 7.14° is equal to the antenna mask floor level. Therefore, in Fig. 69, an area with value of 7.14° corresponds to cases where *I*/*N* is above –6 dB in any case. The probability P is then 100%.

FIGURE 69

Off-axis angle needed to meet an I/N_{eff} of −6 dB (Radar S2)

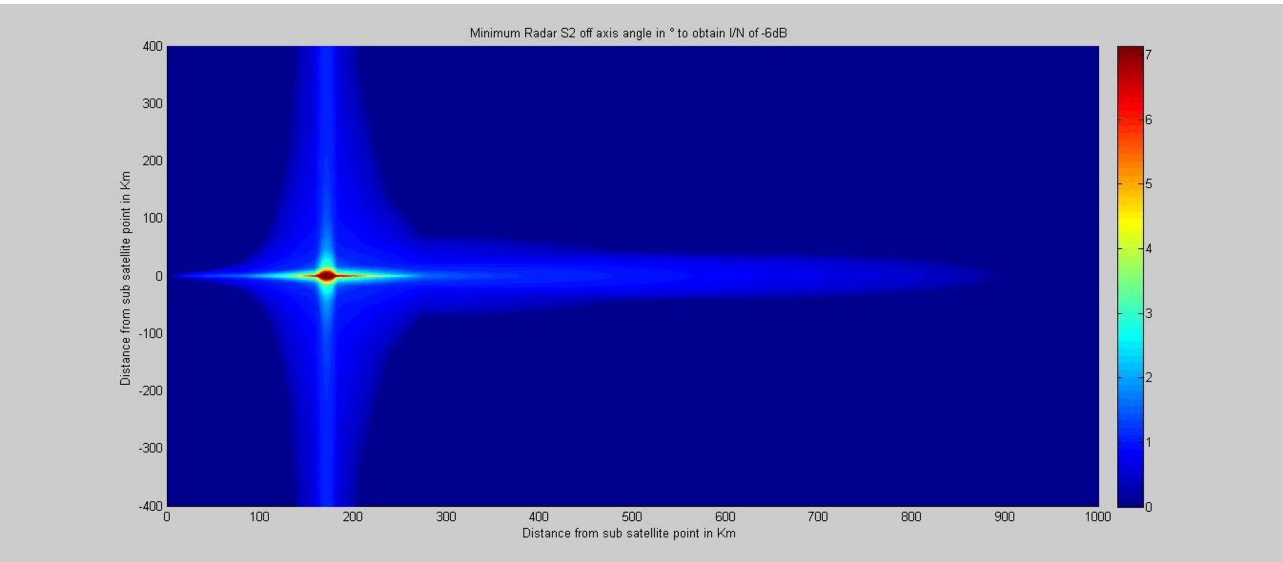

Step 3: Probability computation using θ from step 2

FIGURE 70

Probability of exceedance of an *I/N*

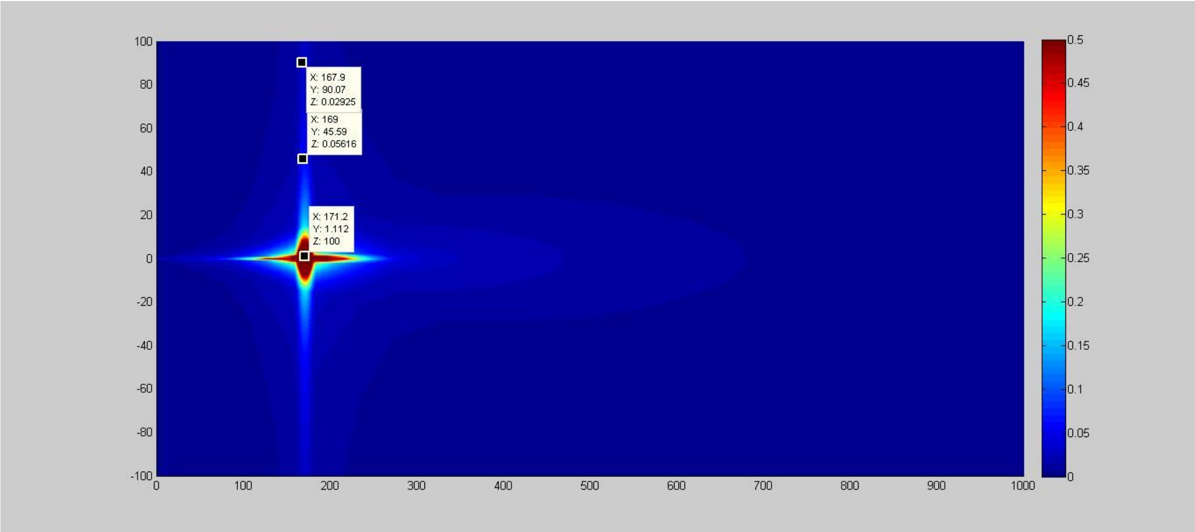

The steps 1 to 3 are repeated for each of the radars A4, G4, and S2. Table 29 summarizes the results.

TABLE 29

Estimation of the probability in % to have an *I/N* of −6 dB during the exposure time of EESS SAR-4 (5 s)

Radar	A4	G4	S2
Frequency band (GHz)	10.0-10.5	10.0-10.5	10.0-10.5
Probability $_{I/N\text{ exceed }-6\text{dB}}$ (0) (%)	100	100	100
Probability $_{I/N\text{ exceed }-6\text{dB}}$ (−1 & +1) (%) (radar location at 170 km from sub-satellite point)	0.15	0.054	0.059
Probability $_{I/N\text{ exceed }-6\text{dB}}$ (−2 & +2) (%) (radar location at 170 km from sub-satellite point)	0.1	0.03	0.032
Probability $_{I/N\text{ exceed }-6\text{dB}}$ (−1 & +1) (%) (at any other radar location)	Negligible	Negligible	Negligible
Probability $_{I/N\text{ exceed }-6\text{dB}}$ (−2 & +2) (%) (at any other radar location)	Negligible	Negligible	Negligible

Average time when $I/N_{eff} \geq -6$ dB (for an exposure time of 5 s)

The average time for which the effective *I/N* is higher than –6 dB is computed by multiplying the 5 s exposure time by the probability given in Table 30.

TABLE 30

Estimation of the average time for which the *I*/*N eff* is higher than −6 dB during the 5 s exposure time

Radar	A4	G4	S2
Frequency band (GHz)	10.0-10.5	10.0-10.5	10.0-10.5
Av time (*I*/*N*> −6dB) (0) (s)	5	5	5
Av time (*I*/*N*> −6dB) (−1 & +1) (ms) (radar location at 170 km from sub-satellite point)	7.5	2.7	2.9
Av time (*I*/*N*> −6dB) (−2 & +2) (ms) (radar location at 170 km from sub-satellite point)	5	1.5	1.6
Av time (*I*/*N*> −6dB) (−1 & +1) (at any other radar location)	Negligible	Negligible	Negligible
Av time (*I*/*N*> −6dB) (−2 & +2) (at any other radar location)	Negligible	Negligible	Negligible

In case the radar processing gain P_G is assumed as 0 dB then:

– EESS SAR-4 creates an *I*/*N* higher than –6dB into the radar receiver mainly when it is located in the exposure area of EESS SAR-4 in spotlight mode. The duration of such event is about 5s. However the probability that EESS SAR-4 takes a picture over an area where a radar site is located is very low.

– when the radar receiver is located outside the EESS SAR-4 exposure area but along the EESS SAR-4 satellite path the interference can be considered as negligible in terms of probability and average duration.

– when the radar receiver is located outside the EESS SAR-4 exposure area and not along the SAR-4 satellite path there is no interference at all.

Effect of the processing gain P_G

Table 31 provides the probability and average time computed using § 2.4.1 methodology with a radar processing gain P_G of 20 dB.

TABLE 31

Probability and average time with processing of 20 dB

Radar	A4		G4		S2	
Frequency band (MHz)	10.0-10.5		10.0-10.5		10.0-10.5	
	Proba	Av time	Proba	Av time	Proba	Av time
(0)	1.66%	83 ms	0.58%	30 ms	0.63%	31.5 ms
(−1 & +1) (radar location at 170 km from sub-satellite point)	0.027%	13 ms	0.011%	0.55 ms	0.012%	0.6 ms
(−2 & +2) (radar location at 170 km from sub-satellite point)	0%	0 s	0.006%	0.3 ms	0.007%	0.35 ms

The processing gain can therefore significantly mitigate the impact even when the radar receiver is located in the exposure area of an EESS SAR-4 operating in spotlight mode.

Results

Assuming a radar processing gain P_G of 20 dB:

1 the interference can be considered negligible in term of probability and average duration when the radar receiver is located outside or inside the EESS SAR-4 exposure area but along the EESS SAR-4 satellite path.

2 there is no interference when the radar receiver is located outside the EESS SAR-4 exposure area and not along the EESS SAR-4 satellite path.

4.3.3.2 Dynamic analysis (Study 2)

4.3.3.2.1 Methodology

In order to assess the potential interference conditions produced by an EESS SAR-4 system in spotlight mode, the same simulation model was used, with the same scenarios as in previous section.

The airborne radar A4 is considered fixed at 10 000 m, whereas in reality an aircraft would fly at high speed, during a limited time, at different altitudes and different directions. However, the duration of a SAR acquisition in spotlight mode is limited to 3 to 7 seconds depending on the incidence angle of the image area. An aircraft flying at 800 km/h during 7 seconds would fly 1.6 km, which is still within the 5 × 5 km spot illuminated by the EESS SAR-4 sensor, and simulating the movement of the aircraft would hence not modify the results for one acquisition. However, from one acquisition to another the aircraft would have disappeared from the target area.

4.3.3.2.2 Simulation results

4.3.3.2.2.1 Long-term scenario

Figure 71 gives the cdf of the averaged I/N values obtained. For each type of radar, the azimuth and elevation angles are selected randomly from one time step to the other within the limits defined in Table 27.

FIGURE 71

Average *I*/*N* values random pointing angles

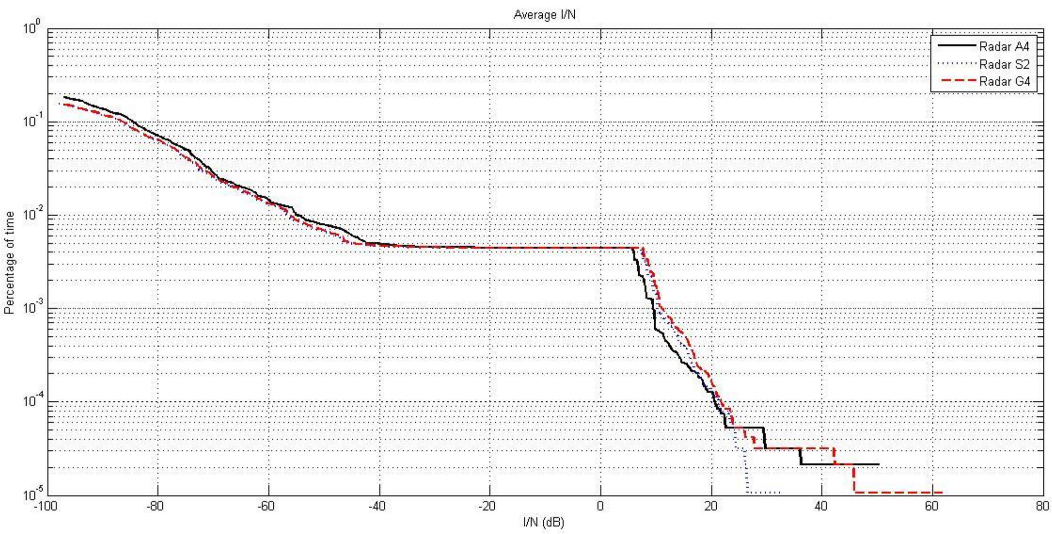

It can be seen that in case of main beam to main beam coupling the I/N can reach values as high as 60 dB. However these extremely high values are obtained for very low percentages of time in the order of 0.00001%, which is less than 100 ms over 11 days.

The *I*/*N* value of –6 dB would be exceeded less than 0.005% of the time, which is 47 seconds over 11 days. As shown in Fig. 72, this would not happen continuously, but would be spread amongst eight interference events of about 6 seconds each.

FIGURE 72

Average *I*/*N* values vs time

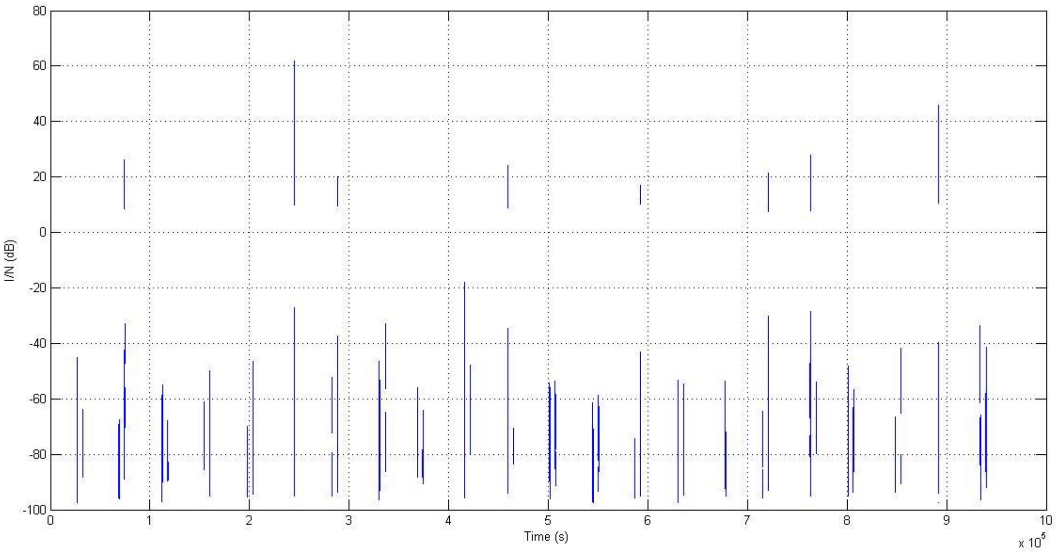

For radar A4, this assumes an aircraft being at a fixed position, whereas in reality from one acquisition to another the aircraft would have moved or even disappeared from the target area. In addition, during one month, the pointing angle of the radar would also change, thus decreasing the *I*/*N* values. The same stands for radar S2, although the ship movement would be much slower.

4.3.3.2.2.2 Short-term scenario

For each radar, the azimuth and elevation pointing angles are chosen randomly from one time step to the next within the limits given in Table 24. The results are given in terms of averaged *I*/*N* vs. time in Figs 73 to 75.

FIGURE 73

Average *I*/*N* values for radar A4

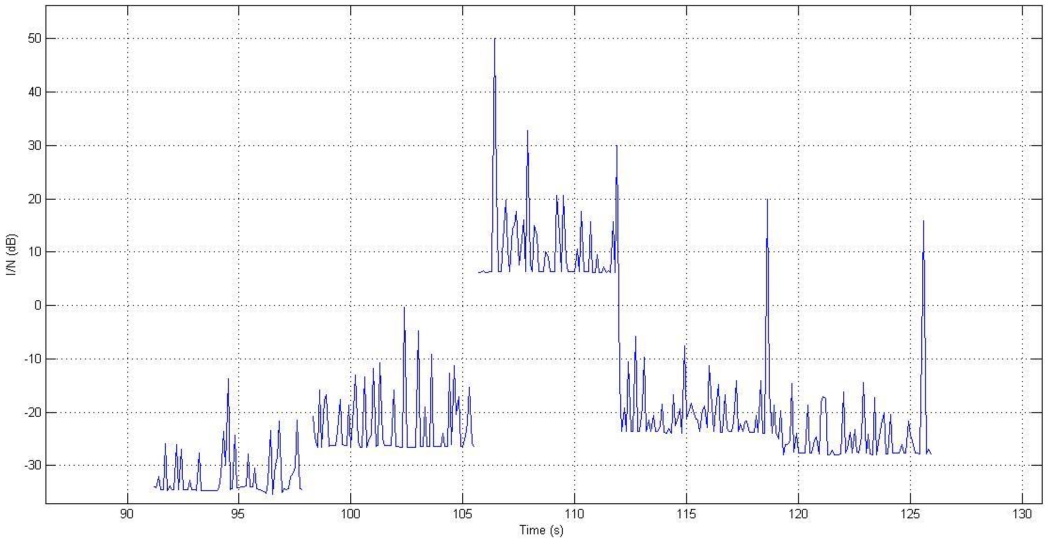

The five image acquisitions are clearly visible in Fig. 73. The effect of the radar main beam or first side lobes is visible here, and the radar protection criterion may be exceeded when the acquisition area is the same as, or closed to the radar location. For simplicity, the radar was pointed randomly at each time step. In a real situation it would track a target and the interference level would depend on the position of the target.

FIGURE 74

Average *I*/*N* values for radar S2

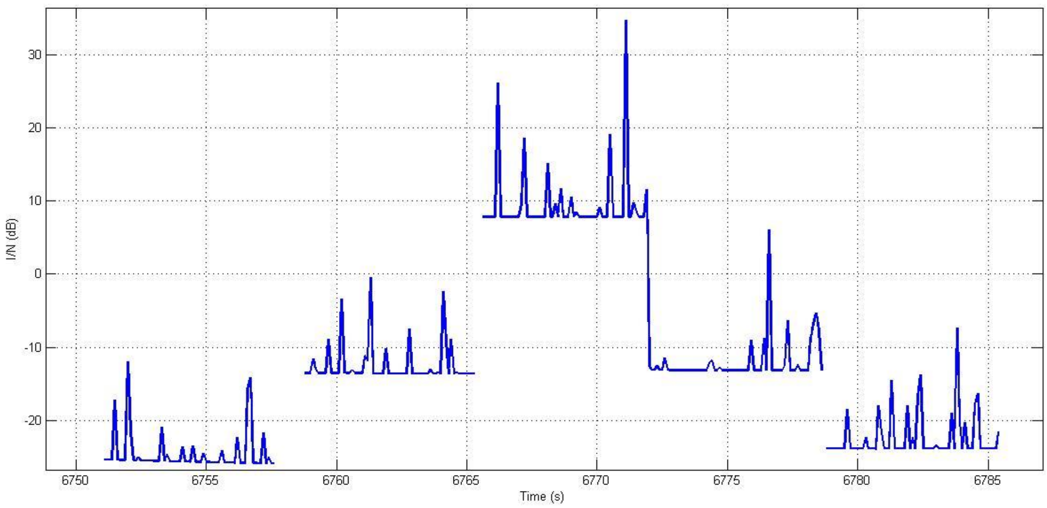

Also for radar S2 the five acquisitions are clearly visible. For simplicity of simulation the radar S2 which is normally shipborne has been located on land. The effect of the radar main beam or first side lobes is visible here, and the radar protection criterion may be exceeded when the acquisition area is the same as, or closed to the radar location.

For simplicity, the radar was pointed randomly at each time step. In a real situation it would track a target and the interference level would depend on the position of the target.

FIGURE 75

Average *I*/*N* values for radar G4

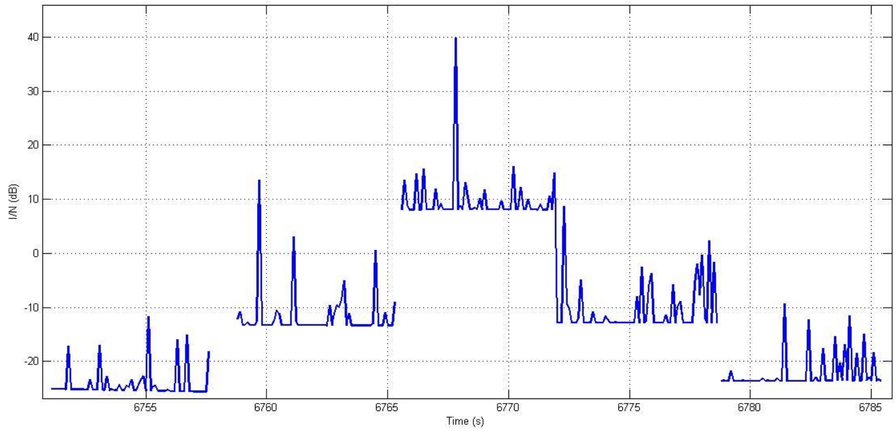

Here the effect of the radar first side lobes or main beam are also visible, with the *I*/*N* reaching 40 dB in one occasion. The same comment as for the shipborne case applies.

4.3.3.2.3 Mitigation technique: location of consecutive acquisitions

In the calculations performed for the short-term scenario, it has been assumed that the consecutive acquisitions of EESS SAR-4, separated by one second, systematically occur along the satellite pass, as shown in Fig. 76.

FIGURE 76

Worst case short-term scenario

In these conditions, all image target areas are aligned with the SAR antenna side lobes along track as depicted in Fig. 66. This would lead to a succession of worst case side SAR lobe levels illuminating the victim radar.

In reality, in spotlight mode, there would be no specific reason why these image target areas would be aligned, and even less why they would be aligned along the satellite path. On the contrary, in spotlight mode, the target areas may indeed be separated along track by the 45 km distance specified in Recommendation ITU-R RS.2043, but a further separation distance would exist across the satellite track, as shown in Fig. 77.

FIGURE 77

Example of realistic short-term scenario

As a result, the level of SAR sidelobes illuminating the victim radar is much lower, leading to more favourable results in terms of interference levels, as shown in Fig. 81.

FIGURE 78

Comparison of interference levels between the short-term scenarios for radar G4

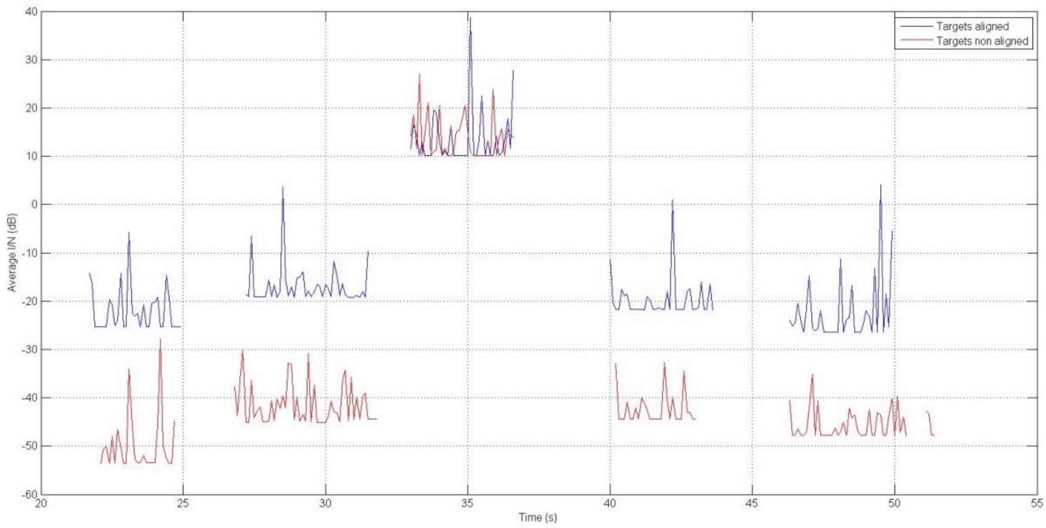

It can be seen that for the example of realistic case the interference levels obtained for the images which are not superimposed with the victim radar location are reduced by around 25 dB, falling below the *I/N* of –6 dB and limiting the duration of harmful interference into the victim radar.

4.3.3.3 Impact on EESS SAR pulsed interference into FMCW radars (Study 3)

4.3.3.3.1 Introduction

This section addresses the sharing performance simulation analyses between the EESS SAR-4 and RLS radars in the band 9 900-10 500 MHz based on the spectrum characteristic modelling method. The sharing effects are analyzed between the EESS SAR-4 and RLS radars including G4, A4, and

S2 in the band 9 900-10 500 MHz by simulating the different parameters of the EESS SAR-4 and radars.

Figure 79 (a)-(b) is the waveform/frequency spectra graph of wanted FMCW radar signal, EESS SAR-4 interference signal, and mixed signal with internal noise. Figure 82 (c)-(d) is the waveform/ frequency spectra graph of the processed mixed signal. Doppler frequency measurement is achieved by measuring the maximum amplitude of spectra graph, and then further calculates the object distance. It can be seen that although the power of interference signal is far greater than that of wanted signal, the amplitude of Doppler frequency amplitude is still greater than that of interference signal through the signal processing, by which the radar can detect the Doppler frequency correctly with no interference impact on the performance of the radar, which also validates the strong anti-interference capability of FMCW radar.

FIGURE 79

Interference simulation analyses from EESS SAR-4 to MFCW radar

(a) Waveform graph

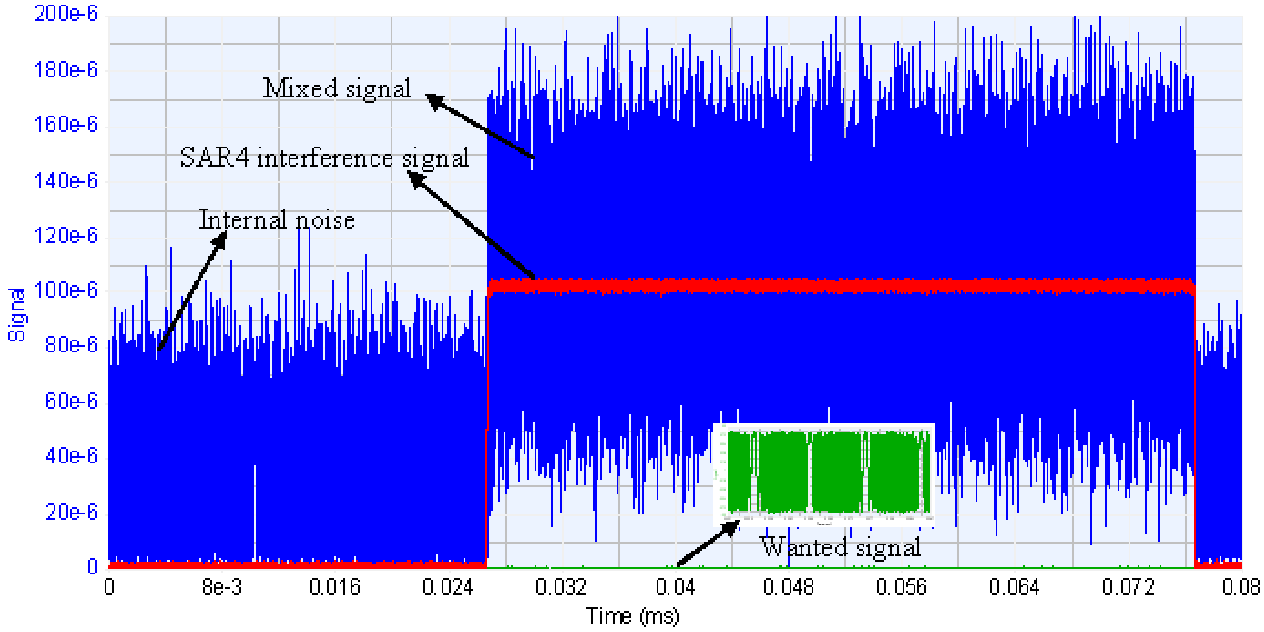

(b) Frequency spectra graph

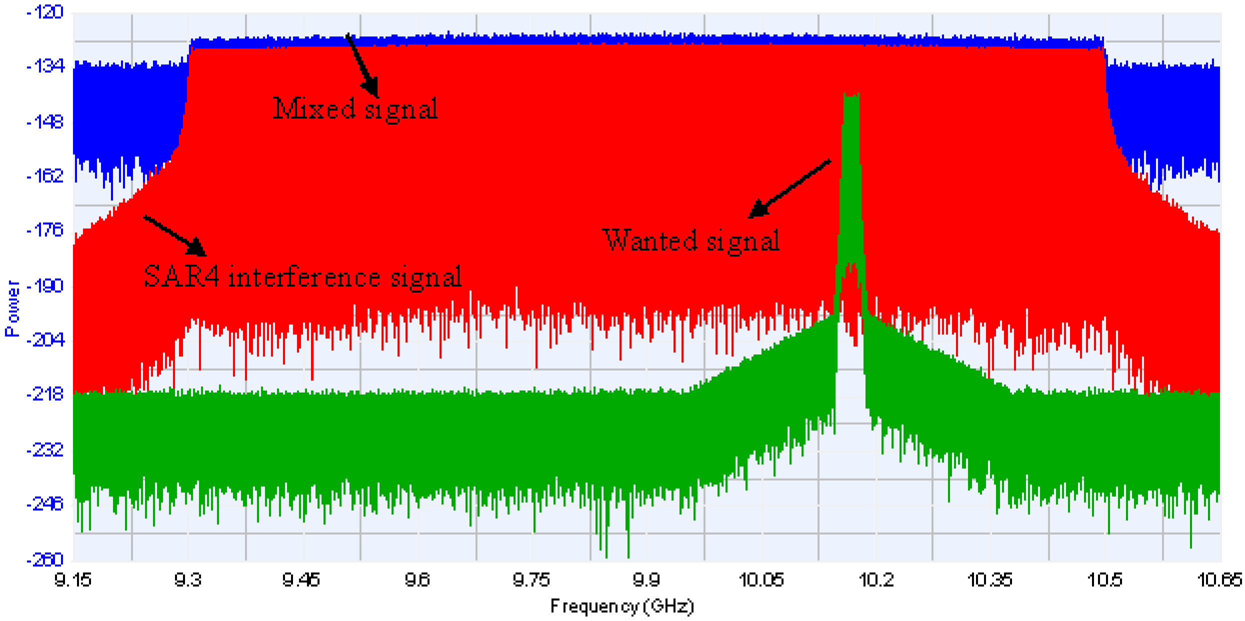

(c) Waveform graph

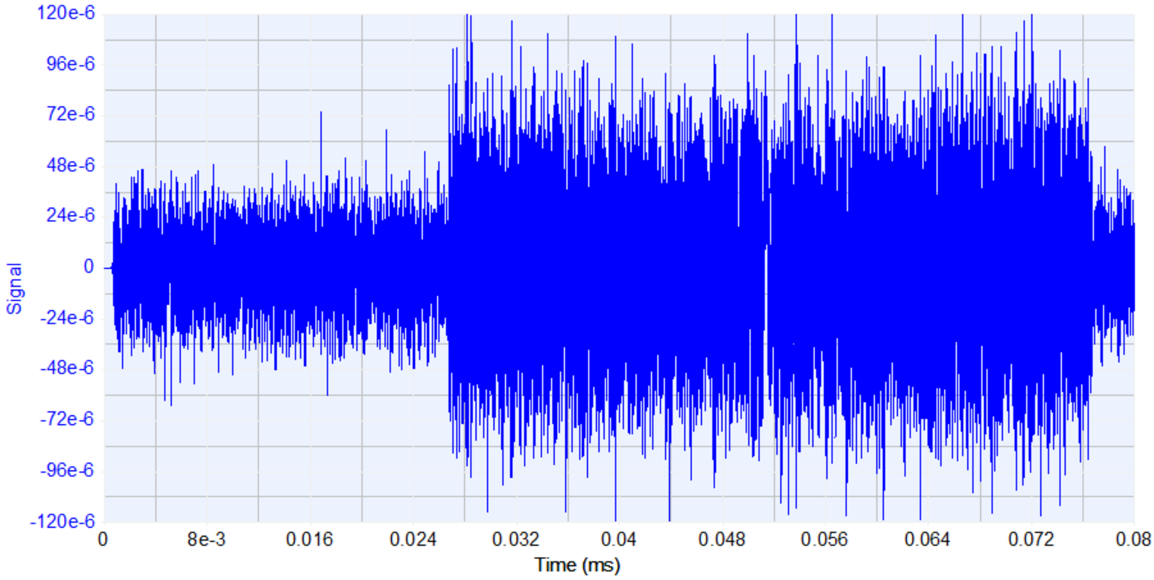

(d) Frequency spectra graph

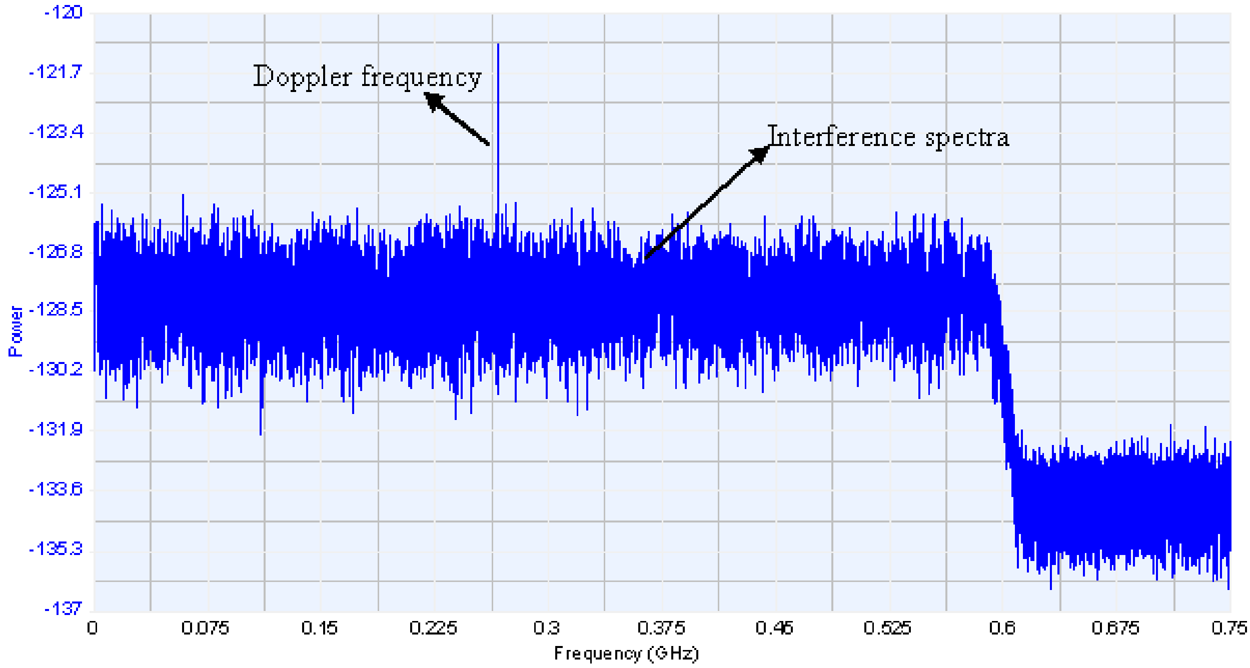

4.3.3.3.2 Interference simulation analyses from spaceborne EESS SAR-4 with adjustable parameters to FMCW radars

This section provides the interference simulation results from spaceborne EES SAR-4 with adjustable parameters as pulse width, repeat period and bandwidth to FMCW radars while keeping the same parameters of MFCW radars and the peak power of spaceborne SAR interference signals. The simulation results display the signal spectra by signal processing of MFCW radars.

(1) Interference effect under the condition of keeping the same parameters of pulse width and bandwidth of spaceborne SAR, with the repeat period adjustable.

The result of interference effect analysis from EESS SAR-4 interference signals under the condition of same pulse width and bandwidth and adjustable repeat period to FMCW radar is shown in Table 32 and Fig. 80.

TABLE 32

Interference effect analyses under the condition of same pulse width and bandwidth and adjustable repeat period

Number	Pulse width (μs)	Repeat period (μs)	Bandwidth (MHz)
1	50	100	1200
2	50	200	1200
3	50	400	1200
4	50	800	1200
Simulation result	When pulse width and bandwidth of SAR remain the same, the interference pulse into radar reduces in a setting time with the increase of repeat period, which manifests as the reduction of power spectral density (PSD) of SAR interference signals.		
Basic conclusion	When pulse width and bandwidth of SAR interference signal remain the same, the PSD of interference from SAR to FMCW radar will gradually reduce with the increase of repeat period of SAR, and the interference effect also falls.		

FIGURE 80

Interference effect analyses under the condition of same pulse width and bandwidth and adjustable repeat period

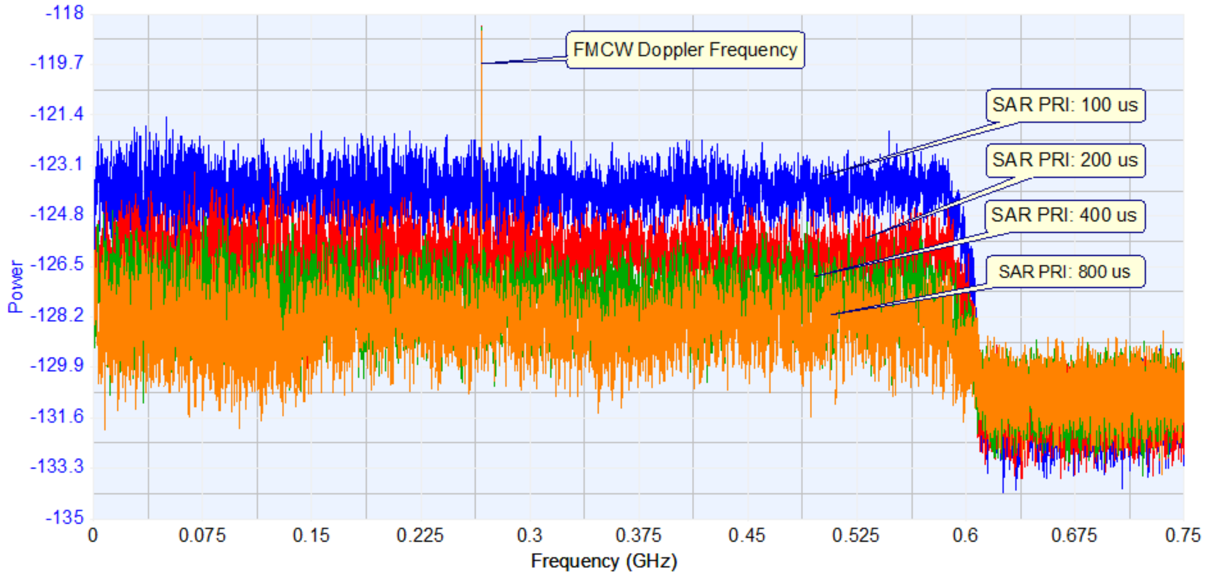

(2) Interference effect under the condition of keeping the same parameters of repeat period and bandwidth of spaceborne SAR, with the pulse width adjustable.

The result of interference effect analysis from EESS SAR-4 interference signals under the condition of same repeat period and bandwidth and adjustable pulse width to FMCW radar is shown in Table 33 and Fig. 81.

TABLE 33

Interference effect analyses under the condition of same repeat period and bandwidth and adjustable pulse width

Number	Pulse width (μs)	Repeat period (μs)	Bandwidth (MHz)
1	10	200	1200
2	20	200	1200
3	40	200	1200
4	80	200	1200
Simulation result	When repeat period and bandwidth of SAR-4 interference signal remain the same, the interference pulse in radar increases in a setting time with the increase of pulse width, which manifests as the increase of PSD of SAR-4 interference signals.		
Basic conclusion	When repeat period and bandwidth of SAR-4 interference signal remain the same, the PSD of interference from SAR-4 to FMCW radar will gradually increase with the increase of pulse width of SAR-4, and the interference effect also rises.		

FIGURE 81

Interference effect analyses under the condition of same repeat period and bandwidth and adjustable pulse width

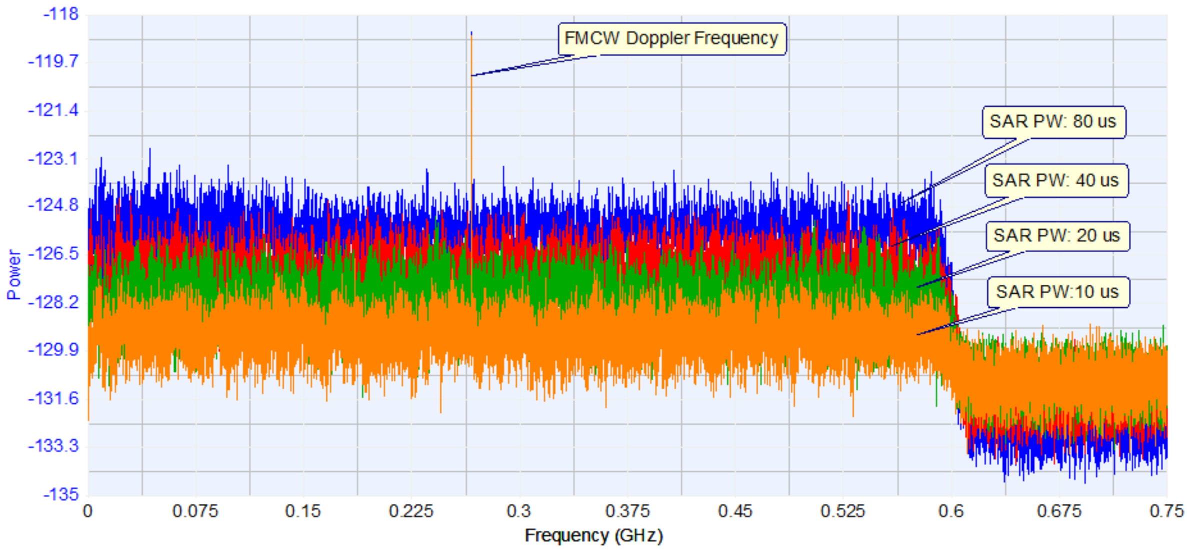

(3) Interference effect under the condition of keeping the same parameters of pulse width and repeat period of spaceborne SAR, with the bandwidth adjustable.

The result of interference effect analysis from EESS SAR-4 interference signals under the condition of same pulse width and repeat period and adjustable bandwidth to FMCW radar is shown in Table 34 and Fig. 85.

TABLE 34

Interference effect analyses under the condition of same pulse width and repeat period and adjustable bandwidth

Number	**Pulse width (μs)**	**Repeat period (μs)**	**Bandwidth (MHz)**
1	50	200	600
2	50	200	800
3	50	200	1000
4	50	200	1200
Simulation result	When pulse width and repeat period of SAR interference signal remain the same, with the increase of bandwidth, the spectra of SAR interference signal and the average power of signal reduces, and the interference effect gradually falls correspondingly.		
Basic conclusion	When pulse width and repeat period of SAR interference signal remain the same, the interference effect of SAR to FMCW radar will gradually decrease with the increase of bandwidth of SAR.		

FIGURE 82

Interference effect analyses under the condition of same pulse width and repeat period and adjustable bandwidth

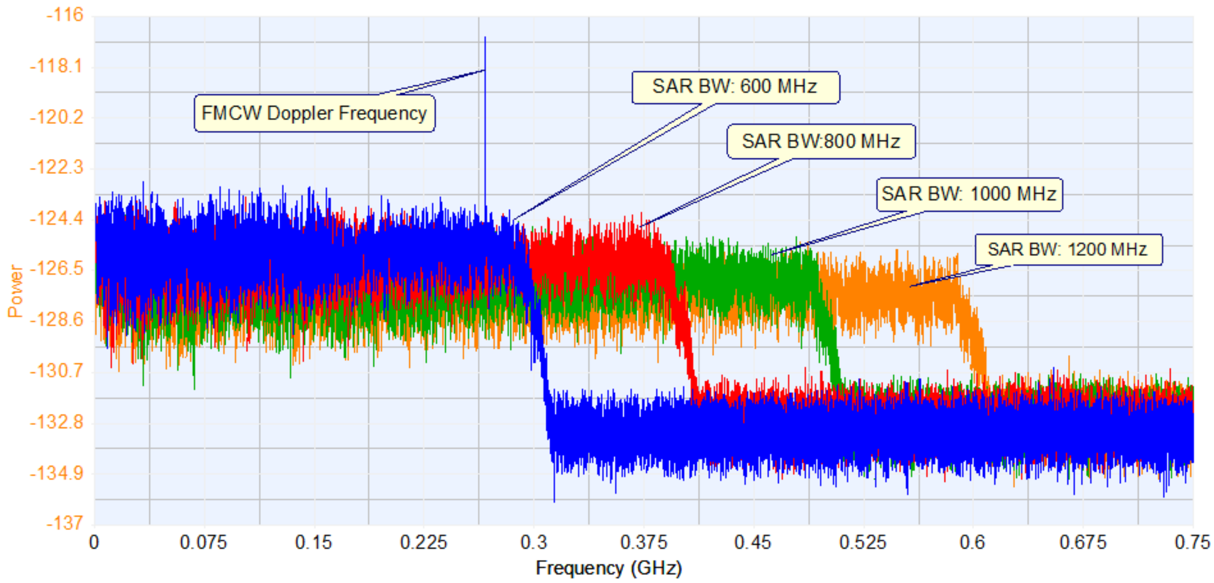

4.3.3.3.3 Interference simulation analyses from spaceborne EESS SAR-4 to FMCW radars with adjustable parameters

This section provides the interference simulation results from spaceborne EESS SAR-4 to FMCW radars with adjustable parameters as FM cycle, FM bandwidth and ranging time (signal time needed in FFT transform when measuring Doppler frequency).

(1) Interference effect under the condition of keeping the same parameters of FM cycle and bandwidth of FMCW radar, with the ranging time adjustable.

The result of interference effect analysis from spaceborne EESS SAR-4 under the condition of same FM cycle and FM bandwidth and adjustable test time or ranging time is shown in Table 35 and Fig. 83.

TABLE 35

Interference effect analyses under the condition of same FM cycle and FM bandwidth and adjustable ranging time

Number	**FM cycle (μs)**	**FM bandwidth (MHz)**	**Ranging time (ms)**
1	10	20	2
2	10	20	4
3	10	20	8
4	10	20	12
Simulation result	As the increase of ranging time, the number of FM cycle included and the FFT transform points in Doppler frequency measurement also rises, and then the equivalent coherent accumulation and the amplitude of Doppler frequency become greater, which correspondingly results in the enhancement of anti-interference capability.		
Basic conclusion	The compression of FMCW radar towards interference enhanced with the increase of ranging time.		

FIGURE 83

Interference effect analyses under the condition of same FM cycle and FM bandwidth and adjustable ranging time

(2) Interference effect under the condition of keeping the same parameters of FM bandwidth and ranging time of FMCW radar, with the FM cycle adjustable.

The result of interference effect analysis from EESS SAR-4 under the condition of same FM bandwidth and ranging time and adjustable FM cycle is shown in Table 36 and Fig. 84.

TABLE 36

Interference effect analyses under the condition of same FM bandwidth and ranging time and adjustable FM cycle

Number	FM cycle (μs)	FM bandwidth (MHz)	Ranging time (ms)
1	4	20	4
2	5	20	4
3	10	20	4
4	20	20	4
Simulation result	The amplitude of Doppler frequency(within or without the interference bandwidth) stays almost the same when the FM cycles are different, while the values of Doppler frequency are diverse; however, changes of FM cycle and Doppler frequency can be counteracted when calculating the distance with Doppler frequency, which will make the results of distance calculation generally the same.		
Basic conclusion	When FM bandwidth and ranging time remain the same, the change of FM cycle will not affect the interference to FMCW radar.		

FIGURE 84

Interference effect analyses under the condition of same FM bandwidth and ranging time and adjustable FM cycle

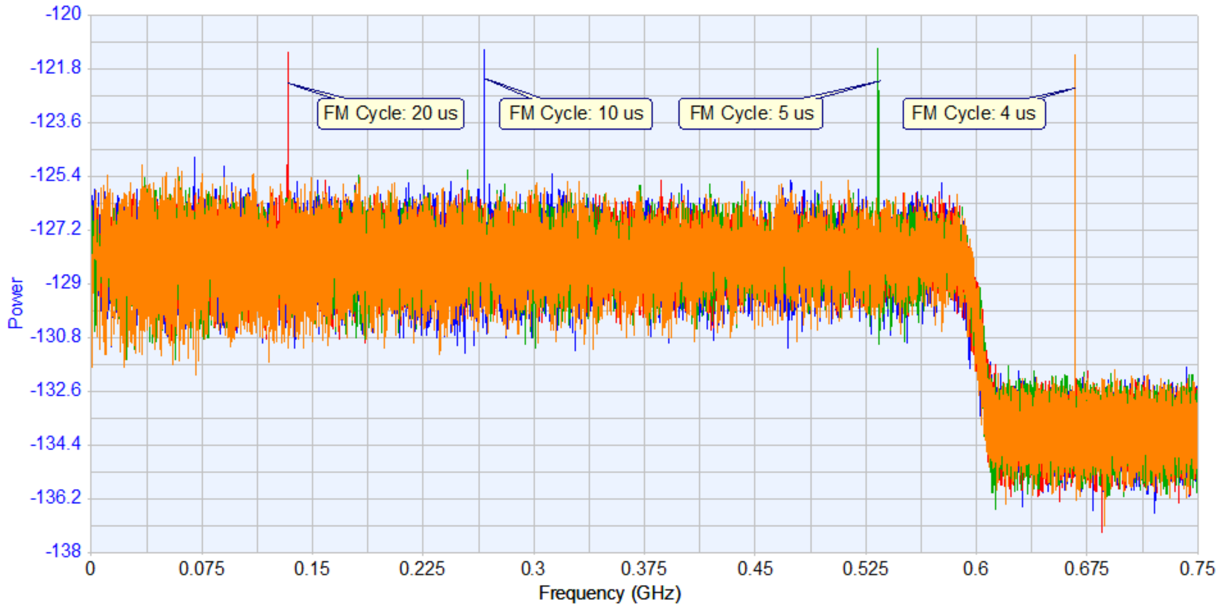

(3) Interference effect under the condition of keeping the same parameters of FM cycle and ranging time of FMCW radar, with the FM bandwidth adjustable.

The result of interference effect analysis from spaceborne EESS SAR-4 under the condition of same FM cycle and ranging time and adjustable FM bandwidth is shown in Table 37 and Fig. 85.

TABLE 37

Interference effect analyses under the condition of same FM cycle and ranging time and adjustable FM bandwidth

Number	**FM cycle (μs)**	**FM bandwidth (MHz)**	**Ranging time (ms)**
1	10	5	4
2	10	20	4
3	10	40	4
4	10	50	4
Simulation result	The amplitude of Doppler frequency (within or without the interference bandwidth) stays almost the same when FM bandwidths are different, while the values of Doppler frequency are diverse; however, changes of FM bandwidth and Doppler frequency can be counteracted when calculating the distance with Doppler frequency, which will make the results of distance calculation generally the same.		
Basic conclusion	When FM cycle and ranging time remain the same, the change of FM bandwidth will not affect the interference to FMCW radar.		

FIGURE 85

Interference effect analyses under the condition of same FM cycle and ranging time and adjustable FM bandwidth

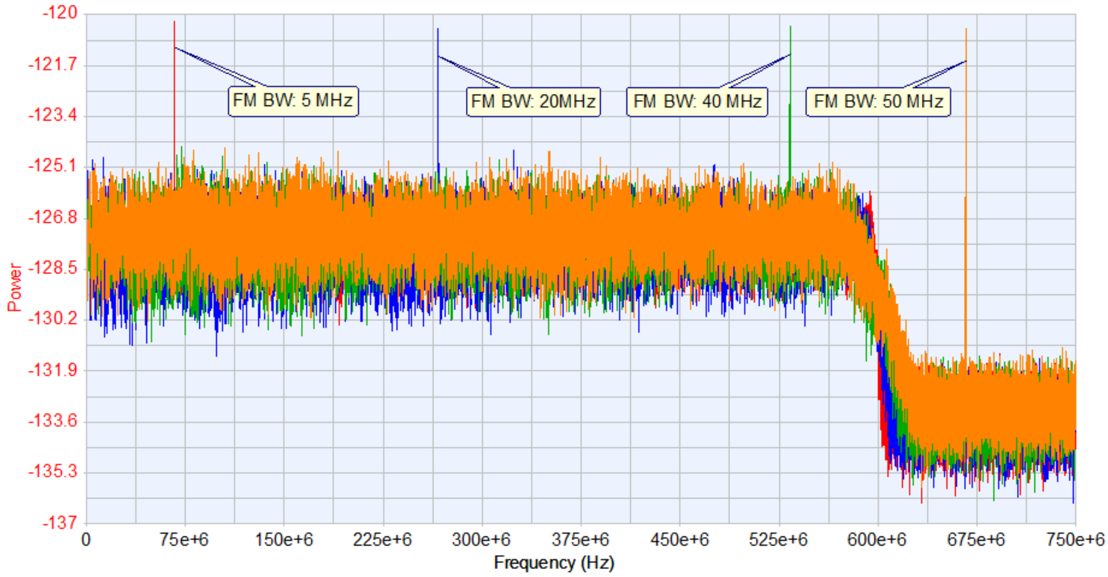

4.3.3.3.4 Protection criteria for FMCW radars sharing with spaceborne EESS SAR-4

FMCW radar will fail to perform Doppler measurement and distance calculation when the amplitude of Doppler frequency is completely suppressed by interference signals. Therefore, the interference power or the power ratio of interference to noise when the spectra amplitude of interference signals and the amplitude of Doppler frequency get equal can be used as interference criterion.

The significant parameters of A4, G4 and S2 FMCW radars as signal type, sensitivity, noise figure and 3 dB bandwidth are basically the same, on account of which it can be concluded that the three types of radar bear the same anti-jamming capability and the interference criterion or the power ratio of interference to noise is similar. The simulation analyses of interference criterion are mostly based on G4 radar and other types of radar can adopt the similar criterion.

The simulation results of interference criteria to FMCW radars are listed in Table 38. $P_{j\text{-}av}$ and $P_{j\text{-}peak}$ in Table 37 stand for the average power and peak power of EESS SAR-4 interference signals in the front-end of FMCW radar receiver, and the difference of which is 5.2 dB (viz. the duty ratio is 30%); N is the internal noise power of G4; I_{peak} is the peak power of EESS SAR-4 interference after the intermediate-frequency filter, the difference of the two parameters is –19.8 dB (viz. OTR value of intermediate-frequency filter in 0.5MHz); I_{av} is the average power of equivalent interference of I_{peak}, the difference of the two parameters is –19.2 dB (viz. duty ratio change of pulse width through filter).

TABLE 38

Simulation calculation results of interference criteria to FMCW radars

FM cycle (μs)	FM bandwidth (MHz)	Ranging time (ms)	$P_{j\text{-}av}$ (dBm)	$P_{j\text{-}peak}$ (dBm)	N (dBm)	$P_{j\text{-}peak/N}$	$I_{peak/N}$	$I_{av/N}$
10	20	1	–72.8	–67.6	–113.5	45.9	26.1	6.9
10	20	2	–70.4	–65.2		48.3	28.5	9.3
10	20	4	–67.3	–62.1		51.4	31.6	12.4

4.3.3.3.5 Summary of results of study 3

The analysis of interference from EESS SAR to FMCW radars indicate that :

– the PSD of interference from SAR to FMCW radar will gradually decrease with the increase of repeat period of SAR, and the interference effect also falls;

– the PSD of interference from SAR to FMCW radar will gradually increase with the increase of SAR pulse width, and the interference effect rises;

– the interference effect of SAR to FMCW radar will gradually decrease when the bandwidth of SAR reduces;

– the suppression to SAR interference enhanced with the increase of ranging time of FMCW radar, and interference effect reduced;

– the change of FM cycle and FM bandwidth will not affect the interference to FMCW radar.

According to the interference criterion of FMCW radar, and in case the ranging time was set as 1 ms, 2 ms and 4 ms, the allowable ratio of maximum average interference power to noise power is 6.9 dB, 9.3 dB and 12.4 dB, respectively, and the allowable ratio of maximum interference peak power to noise power is 26.1dB, 28.5 dB and 31.6 dB. This also applies to radars A4, G4, and S2.

It also can be seen that FMCW radars have strong interference mitigation capability.

4.3.4 Sharing studies on the impact of RLS emissions on SAR-4 receiver

4.3.4.1 Scenario

In Fig. 86, the black dots represent the location of 50 G4 radars transmitting in the band 10-10.5 GHz. This number is relatively low as this kind of tracking radars or tracking mode is not active 100% of the time. The blue dots represent the area where an image in high resolution mode may be taken by the SAR system. It has been assumed that 500 image areas were randomly positioned and not necessarily co-located with the radars.

FIGURE 86

Deployment of radars and image areas

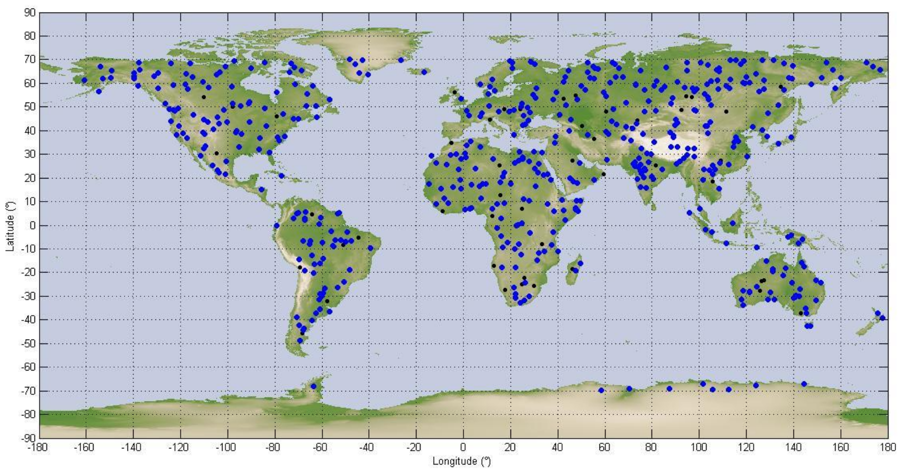

The simulation is run for 11 days with a time step of 1 second. Each time the satellite is within visibility of one area of interest (blue dot) within the relevant azimuth and incidence angles, this area is illuminated, for a duration which varies between 3 and 7 seconds. The EESS SAR-4 receiver will also be activated only during this portion of time. It is assumed that the rest of the time it is inactive. The aggregate interference from all radars in visibility during the acquisition is calculated and converted in *I*/*N*. The noise value is calculated in 500 MHz.

The EESS SAR-4 protection criterion is an *I*/*N* of −6 dB, not to be exceeded more than 5% of the time for random or non-systematic interference, which is the case here. Indeed, the radar systems operating in this band are tracking radars, which are active only for a fraction of time. In addition they are located on trailers, aircraft or ship and may be moved from one acquisition to the other. It is understood here that the reference time for this 5% allowance is the time when the EESS SAR-4 system is in operation (3% of the total time). When compared to the total simulation duration, the effective percentage of time of interference allowance should be in fact 5% times 3% which is 0.15% of the time.

4.3.4.2 Results

The results obtained for a deployment of 50 G4 radars are given in terms of cumulative distribution function of the *I*/*N* in Fig. 87.

FIGURE 87

***I*/N cdf for 50 radars in the band 10-10.5 GHz**

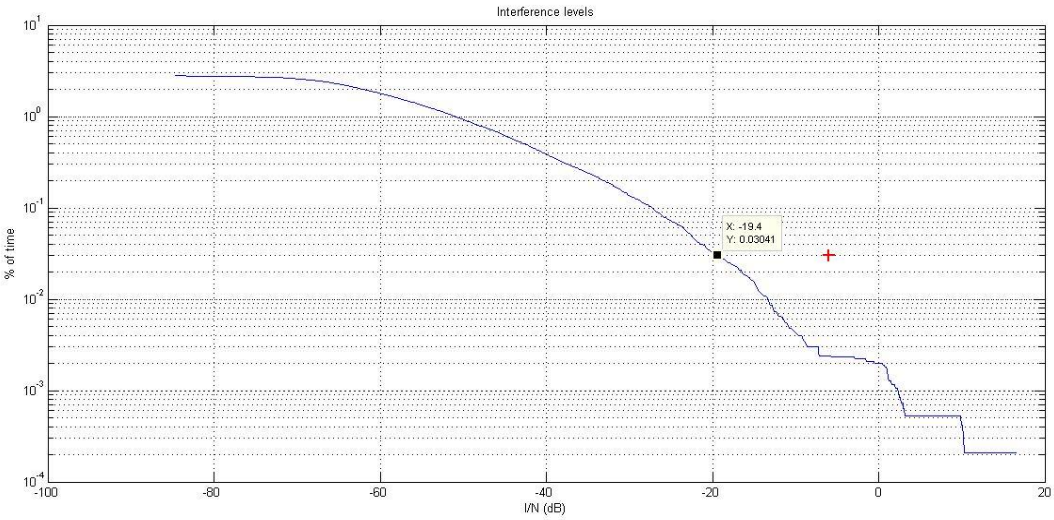

The maximum *I*/*N* is +18 dB and is obtained for 0.0001% of the total time. The *I*/*N* obtained for 1% of the time when the sensor is active is –19 dB, 13 dB below the protection criterion.

These results do not account for any EESS SAR-4 processing gain.

5 Summary

Studies showed that in the frequency band 9 000-9 200 MHz sharing would be difficult due to the safety aspects of the relevant services. Should the case the use of the band 9 000-9 200 MHz be totally excluded from consideration to satisfy the contiguous requirement for EESS SAR, the frequency range 8 700-9 000 MHz would not allow contiguous extension to the current EESS (active) allocation. Therefore this summary addresses the frequency band above 9 200 MHz only.

In case of multiple EESS SAR-4 systems (number *N*) operating in the frequency band 9 200-9 300 MHz and/or 10-10.5 GHz, the probabilities calculated in the studies have to be multiplied by *N* to obtain the aggregate probability as the probabilities corresponding to each SAR system are statistically uncorrelated.

Table 39 summarizes the overall results of the effects of EESS SAR-4 systems into RDS radar receivers.

TABLE 39

Summary of studies results

	9 200-9 300 MHz	**9.3-10 GHz**	**10-10.5 GHz**
Services affected	RNS	RNS/RLS	RLS
Maximum $I/N_{average}$	26.8 dB-PG	Sharing condition already studied before WRC-12 and conclusions still applicable to SAR systems with chirp bandwidth between 600 MHz and 1 200 MHz	68.6 dB-PG
% of time that maximum I/N average occurs (over 11 days)	0.00001 × N		0.00001 × N
% of time that $I/N_{av} - PG = -6$dB is exceeded (over 11 days)	0.00004 × N		0.005 × N
% of time that $I/N_{av} = -6$ dB is exceeded (over 11 days)	Never		Much lower than 0.005 × N (depending on PG)

PG : radar receiver processing gain in dB (the effect of pulsed interference is difficult to quantify and is strongly dependent on radar receiver-processor design and mode of system operation. In general, numerous features of radars can be expected to help suppress low duty-cycle pulsed interference. Techniques for suppression of low-duty-cycle pulsed interference are contained in Recommendation ITU-R M.1372 (see also Recommendation ITU-R M.1461 and Report ITU-R M.2081). Report ITU-R RS.2094 shows that such processing gain can be significant.

N : number of wideband EESS SAR-4 satellite systems operating in the considered band.

6 Supporting documents

ITU-R Recommendations

ITU-R Recommendations are cited with their current state of validity unless mentioned otherwise.

ITU-R M.1372 Efficient use of the radio spectrum by radar stations in the radiodetermination service

ITU-R M.1461 Procedures for determining the potential for interference between radars operating in the radiodetermination service and systems in other services

ITU-R M.1796-2 Characteristics of and protection criteria for terrestrial radars operating in the radiodetermination service in the frequency band 8 500-10 680 MHz

ITU-R M.1851 Mathematical models for radiodetermination radar systems antenna patterns for use in interference analyses

ITU-R RS.1280 Selection of active spaceborne sensor emission characteristics to mitigate the potential for interference to terrestrial radars operating in frequency band 1-10 GHz

ITU-R RS.2043 Characteristics of synthetic aperture radars operating in the Earth exploration-satellite service (active) around 9 600 MHz

ITU-R Reports

ITU-R Reports are cited with their current state of validity unless mentioned otherwise.

ITU-R M.2081 Test results illustrating compatibility between representative radionavigation systems and radiolocation and EESS systems in the band 8.5-10 GHz

ITU-R RS.2274 Spectrum requirements for spaceborne synthetic aperture radar applications planned in an extended allocation to the Earth exploration-satellite service around 9 600 MHz.

ICAO Documents

Document 9718 ICAO RF Handbook

Annex A

List of acronyms and abbreviations

ARNS	Aeronautical radionavigation service
ASDE	Airport surface detection equipment
EESS	Earth explotation-satellite service
GCA	Ground control approach
FFT	Fast Fourier Transformation
FM	Frequency Modulation
IF	Intermediate Frequency
LoS	Line-of-sight
NBF	Narrow band filter
NLFM	Non-linear Frequency modulation
OTR	On-tune-rejection
PAR	Precision approach radar
PRF	Pulse repetition frequency
PSD	Power spectral density
RDS	Radio determination service
RLS	Radio location service
RNS	Radio navigation service
SAR	Synthetic aperture radar